^{1}H-NMR spectra of the synthesized dithiocarbamato ligands

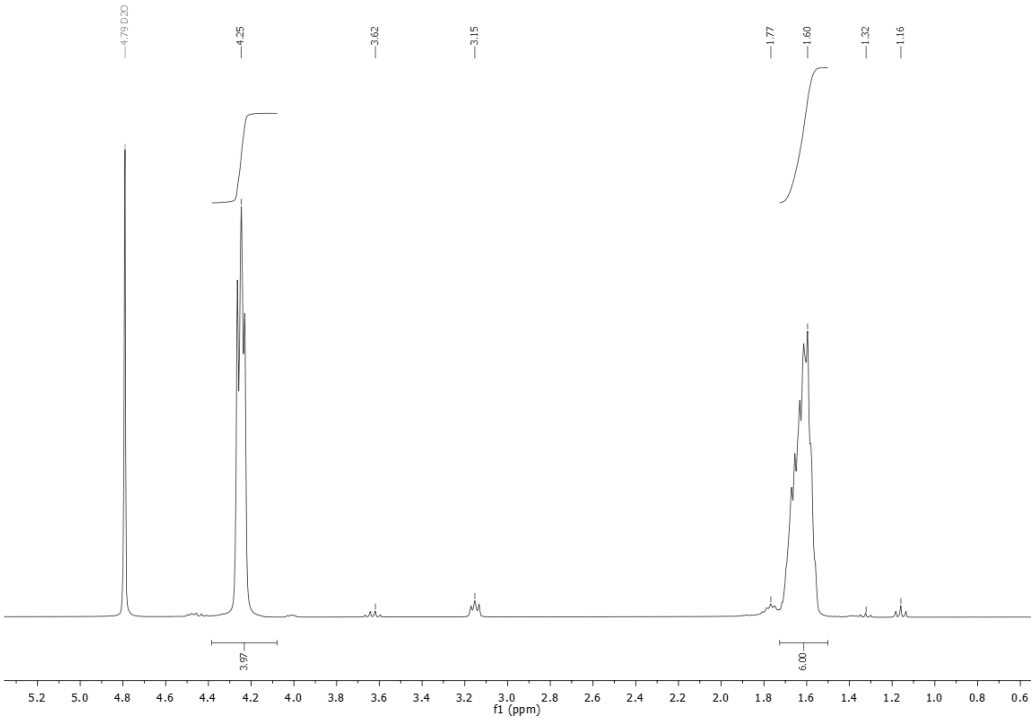

Figure S1: ^{1}H-NMR (D_2O, 300.13 MHz, 298 K) spectrum of piperidine dithiocarbamate potassium salt (K(pipeDTC)).

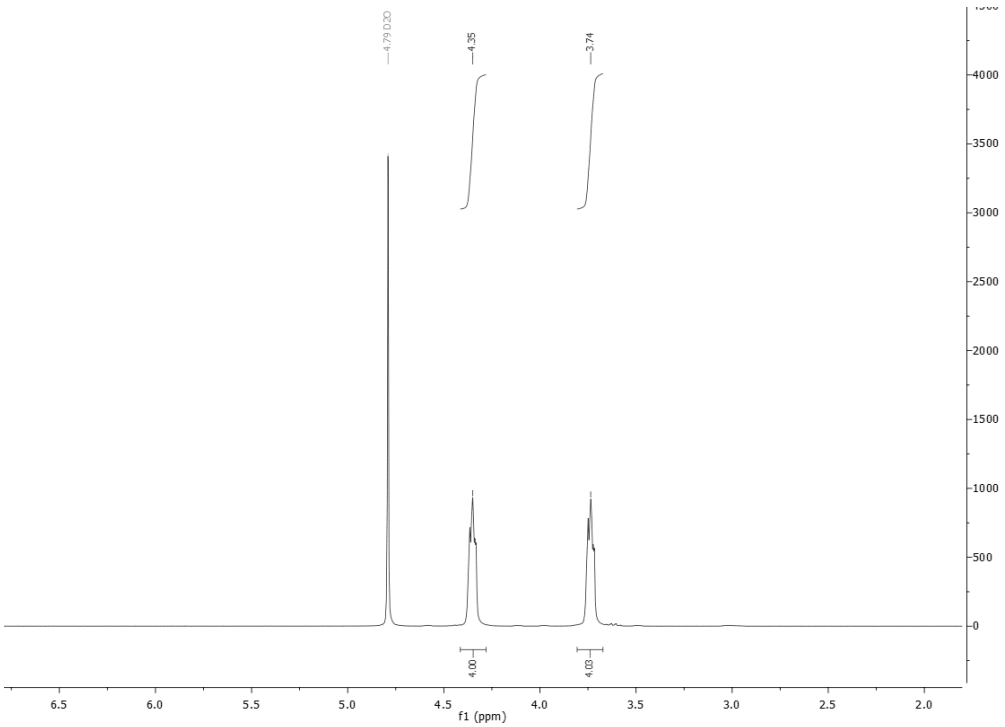

Figure S2: ^{1}H-NMR (D_2O, 300.13 MHz, 298 K) spectrum of morpholine dithiocarbamate potassium salt (K(morphDTC)).

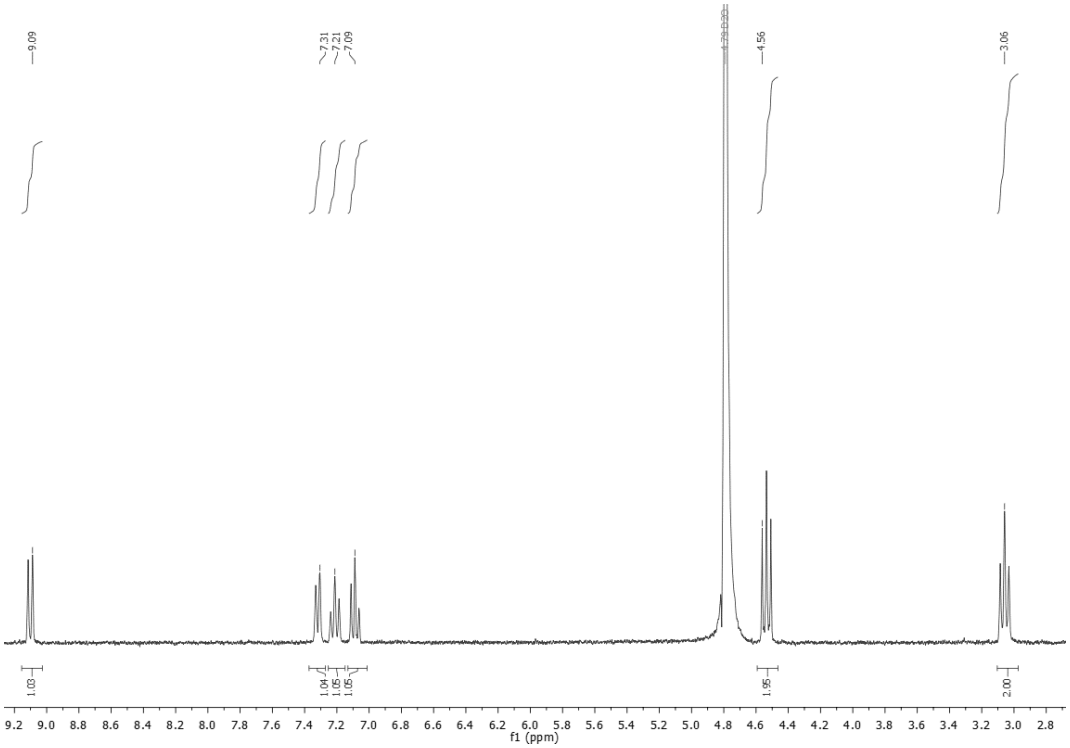

Figure S3: ^{1}H-NMR (D_2O, 300.13 MHz, 298 K) spectrum of indoline dithiocarbamate sodium salt (K(indolineDTC)).

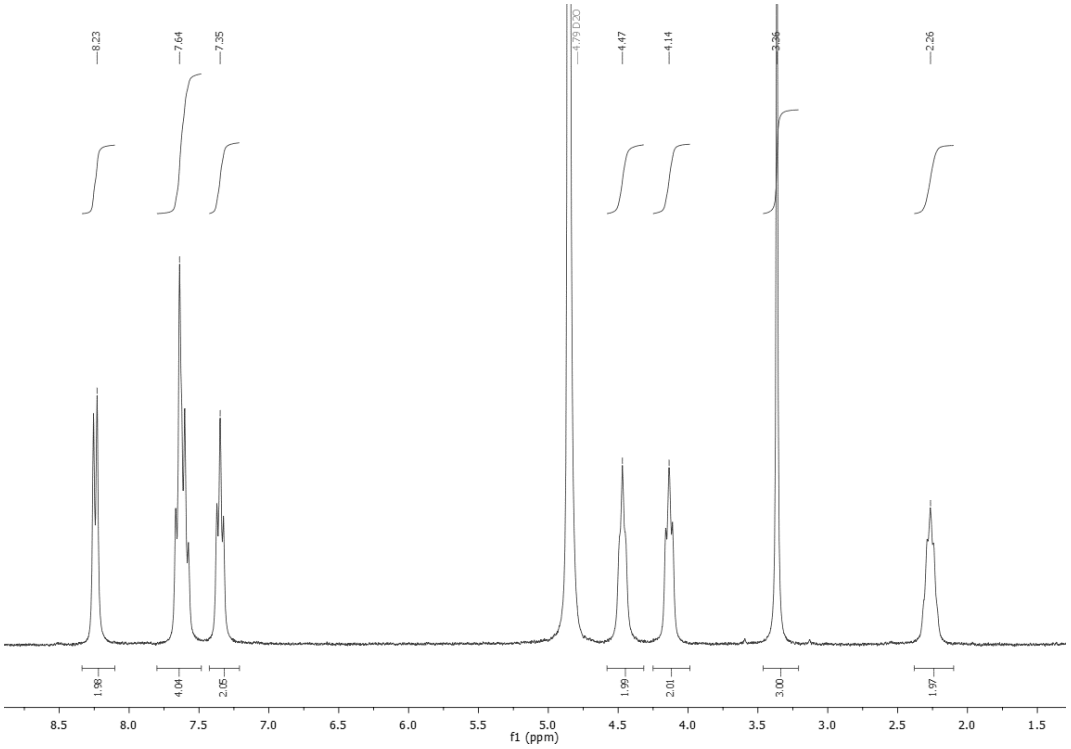

Figure S4: ^{1}H-NMR (D_2O, 300.13 MHz, 298 K) spectrum of *N*-methyl-*N*-propyl-carbazole dithiocarbamate sodium salt (Na(Carbz-pr-*N*(Me)-DTC)).

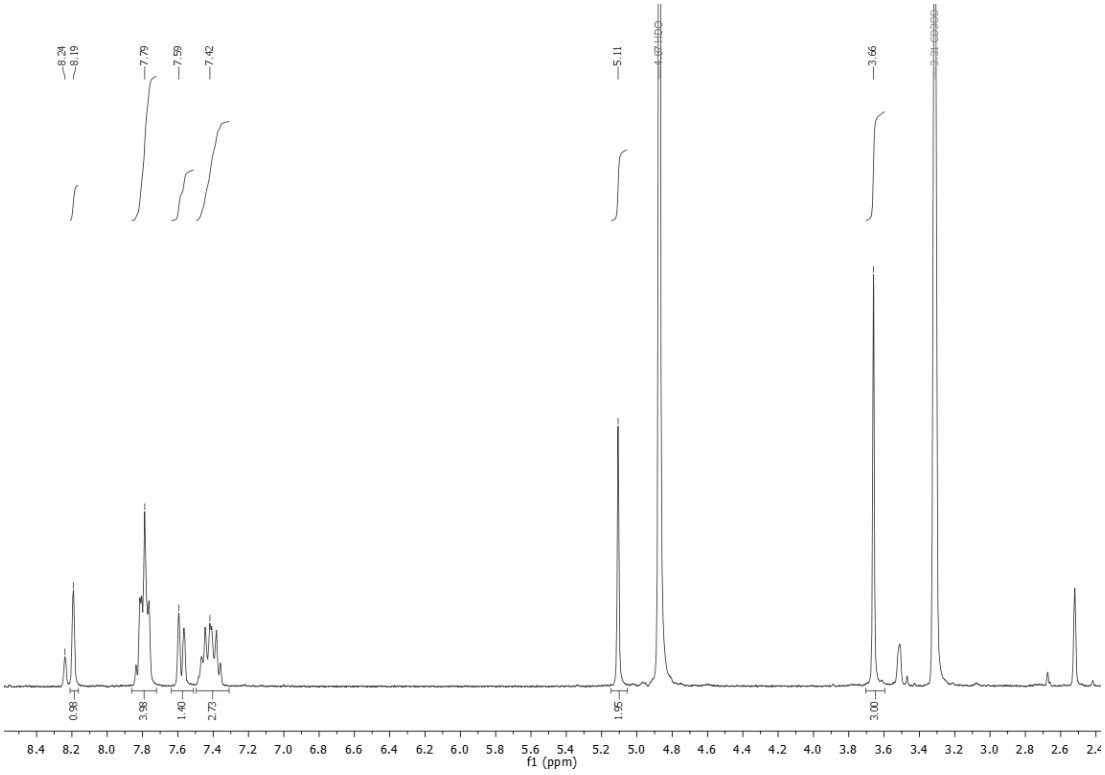

Figure S5: ^{1}H-NMR (MeOH-d_4, 300.13 MHz, 298 K) spectrum of Methyl(2-(naphtalen-2-ylamino)-2-oxoethyl)dithiocarbamate potassium salt (K(*β*-Napht-Sar-DTC)).

^{1}H-NMR spectra of the synthesized [$Ru_2(DTC)_x(DTC')_{(5-x)}$]Br complexes

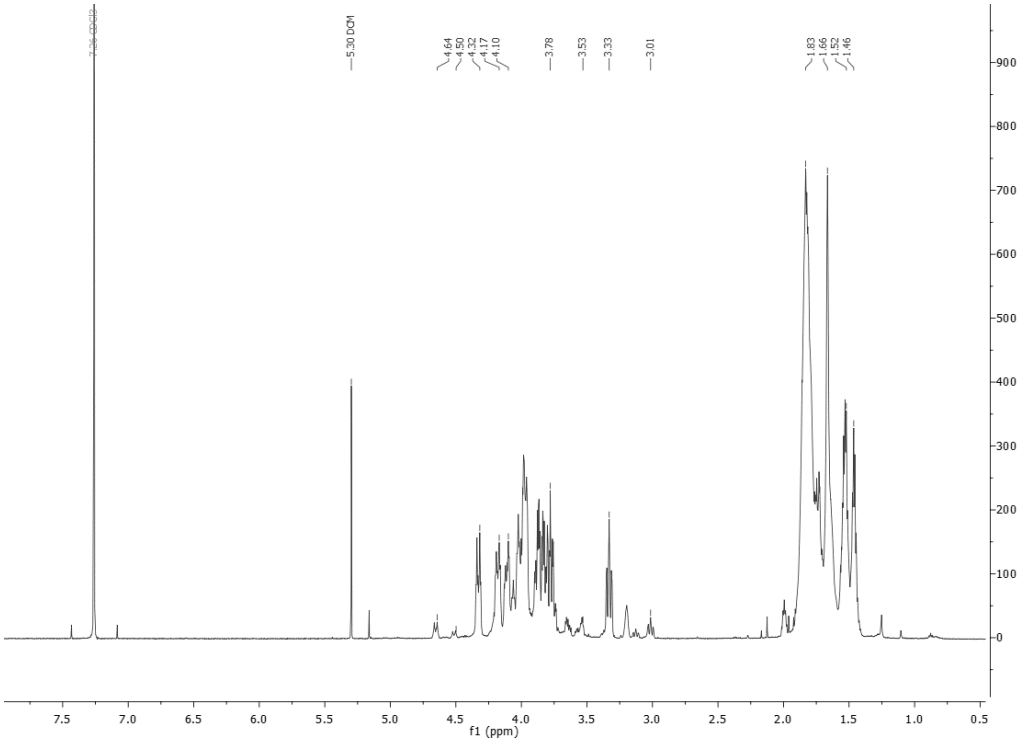

Figure S6: ^{1}H-NMR spectrum ($CDCl_3$, 599.90 MHz, 298 K) of pentakis(piperidine dithiocarbamate)diruthenium(III) bromide, [Ru_2(pipeDTC)$_5$]Br.

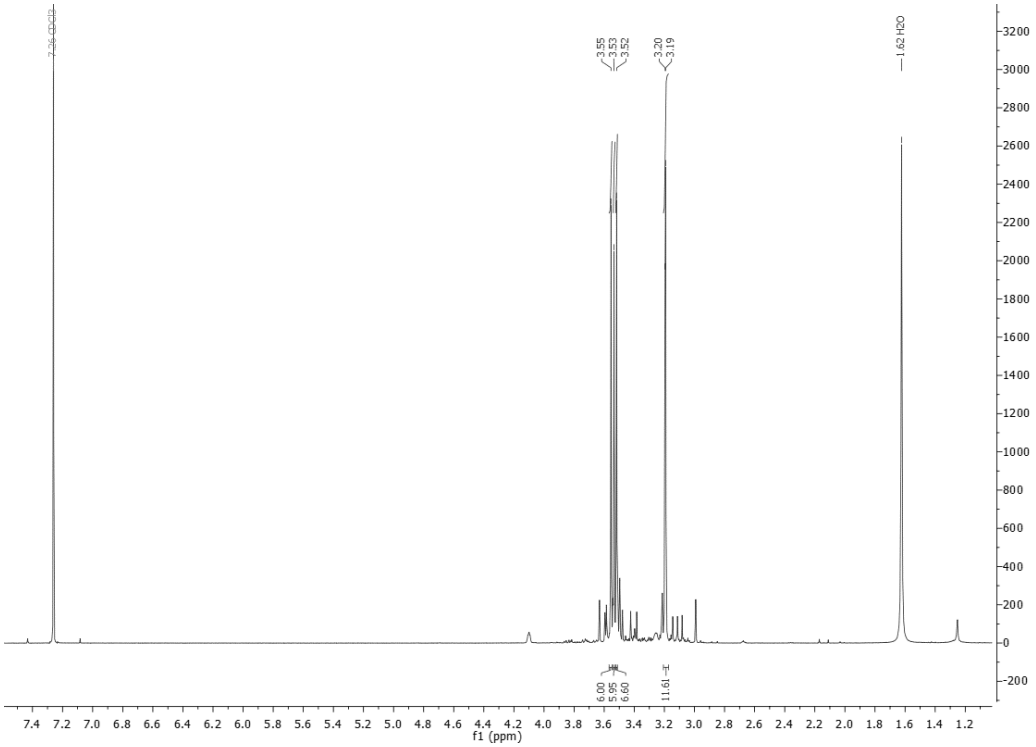

Figure S7: ^{1}H-NMR spectrum ($CDCl_3$, 599.90 MHz, 298 K) of pentakis(dimethyl dithiocarbamate)diruthenium(III) bromide, $[Ru_2(DMDT)_5]Br$.

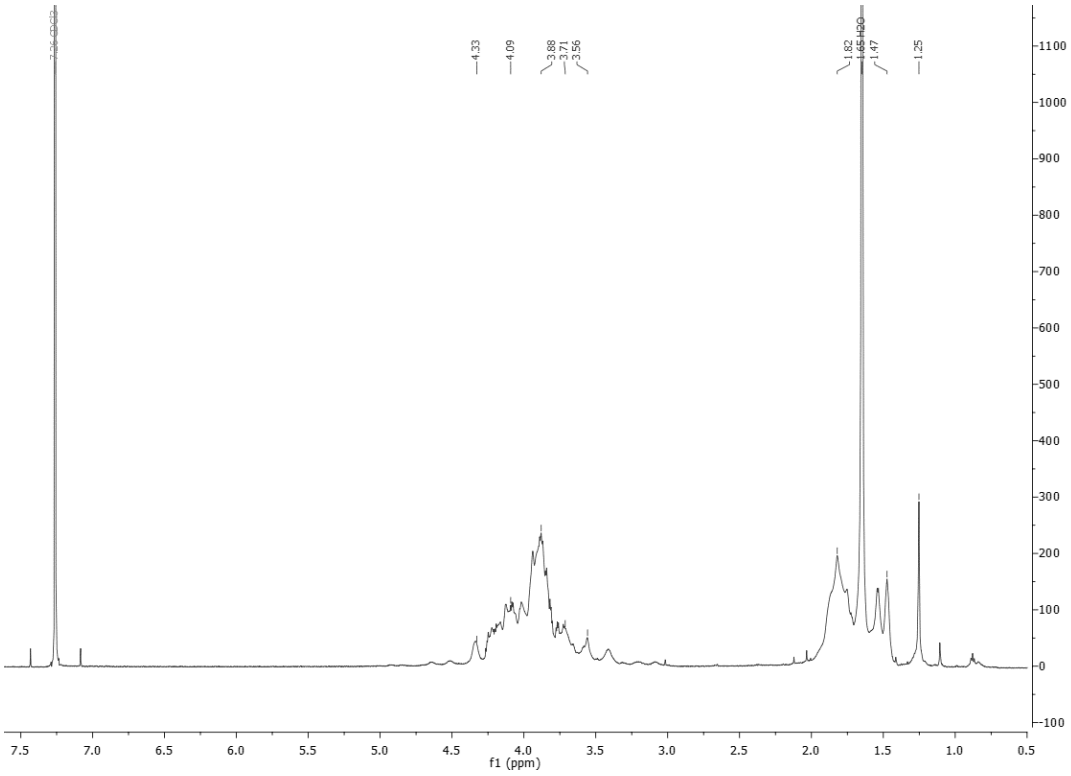

Figure S8: ^{1}H-NMR spectrum ($CDCl_3$, 599.90 MHz, 298 K) of tris(piperidine dithiocarbamate)-bis(morpholine dithiocarbamate)diruthenium(III) bromide, $[Ru_2(pipeDTC)_3(morphDTC)_2]Br$.

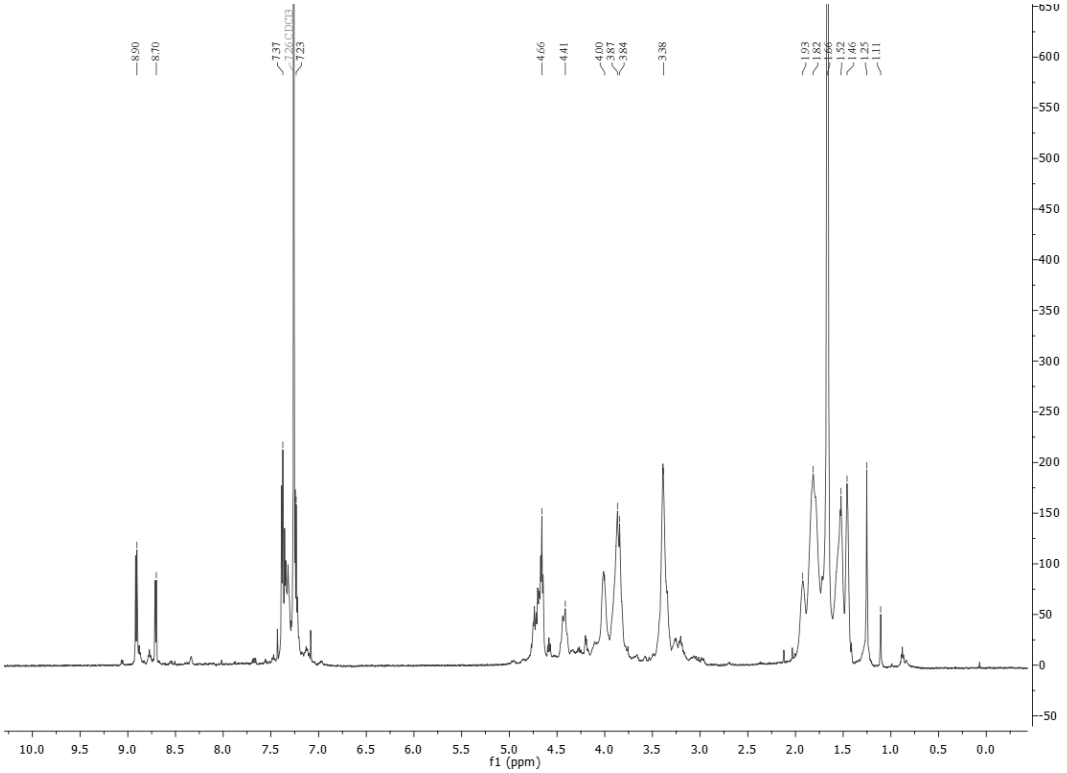

Figure S9: ^{1}H-NMR spectrum ($CDCl_3$, 599.90 MHz, 298 K) of $[Ru_2(pipeDTC)_x(indolineDTC)_y]Br$.

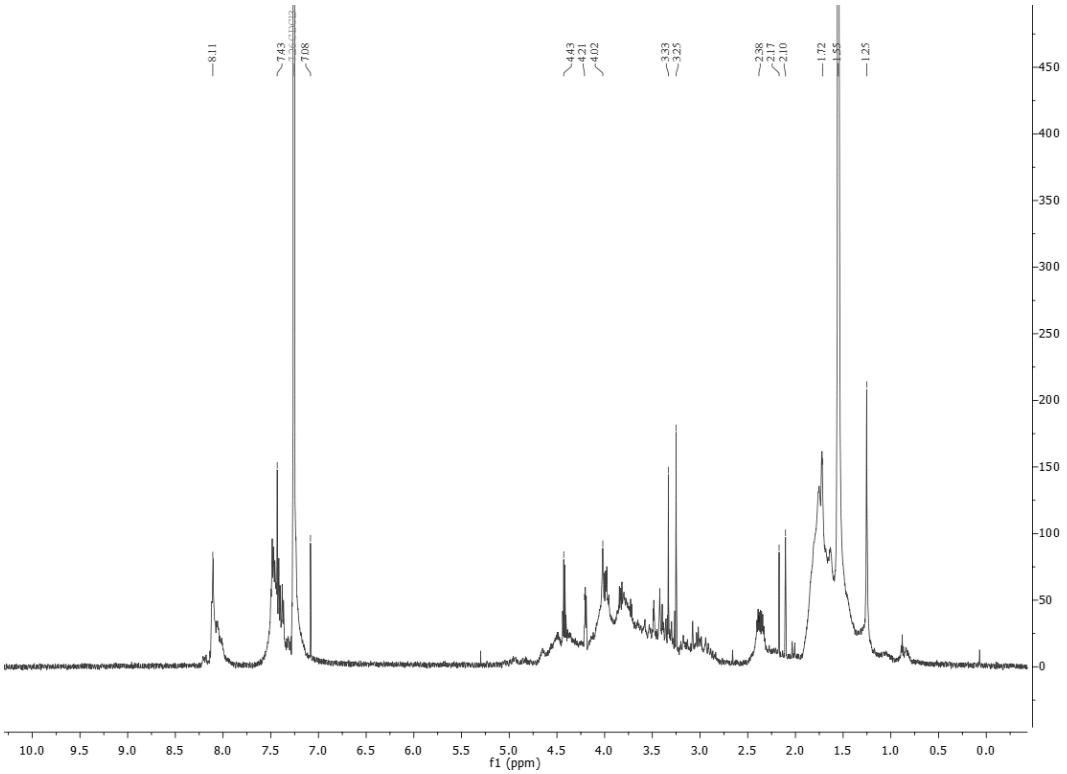

Figure S10: ^{1}H-NMR spectrum ($CDCl_3$, 599.90 MHz, 298 K) of $[Ru_2(pipeDTC)_x(Carbz\text{-}pr\text{-}N(Me)\text{-}DTC)_y]Br$.

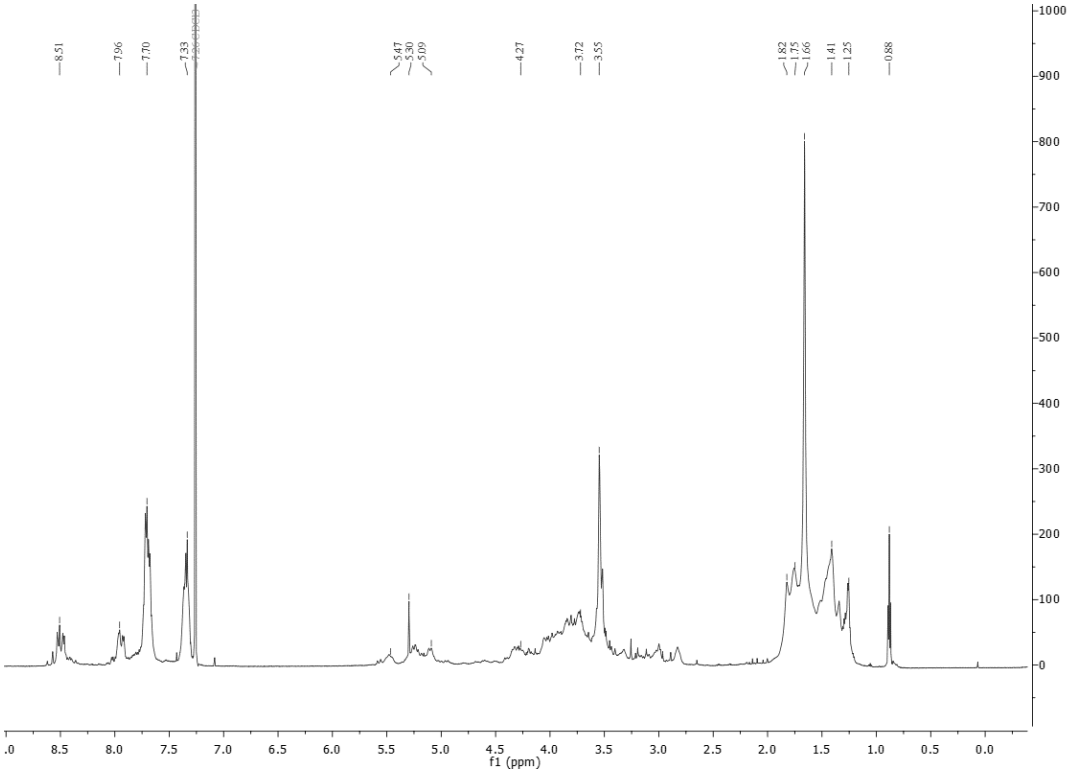

Figure S11: ^{1}H-NMR spectrum ($CDCl_3$, 599.90 MHz, 298 K) of $[Ru_2(pipeDTC)_x(\beta\text{-Napht-Sar-DTC})_y]Br$.

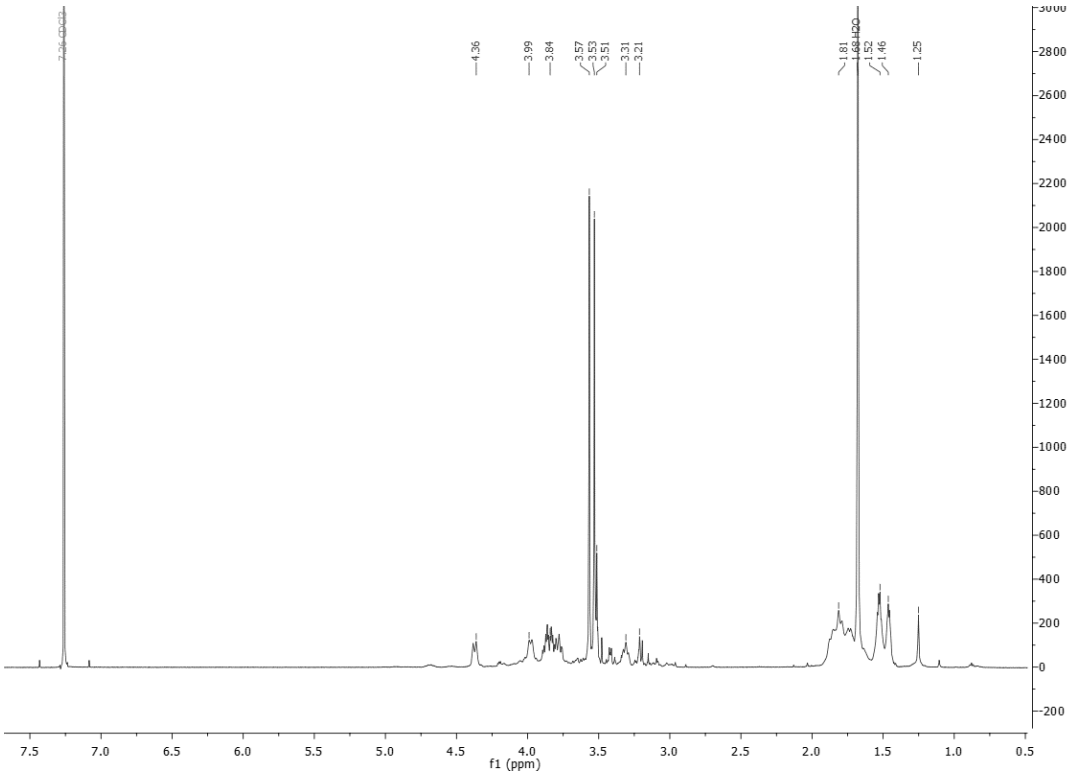

Figure S12: ^{1}H-NMR spectrum ($CDCl_3$, 599.90 MHz, 298 K) of $[Ru_2(pipeDTC)_x(DMDT)_y]Br$

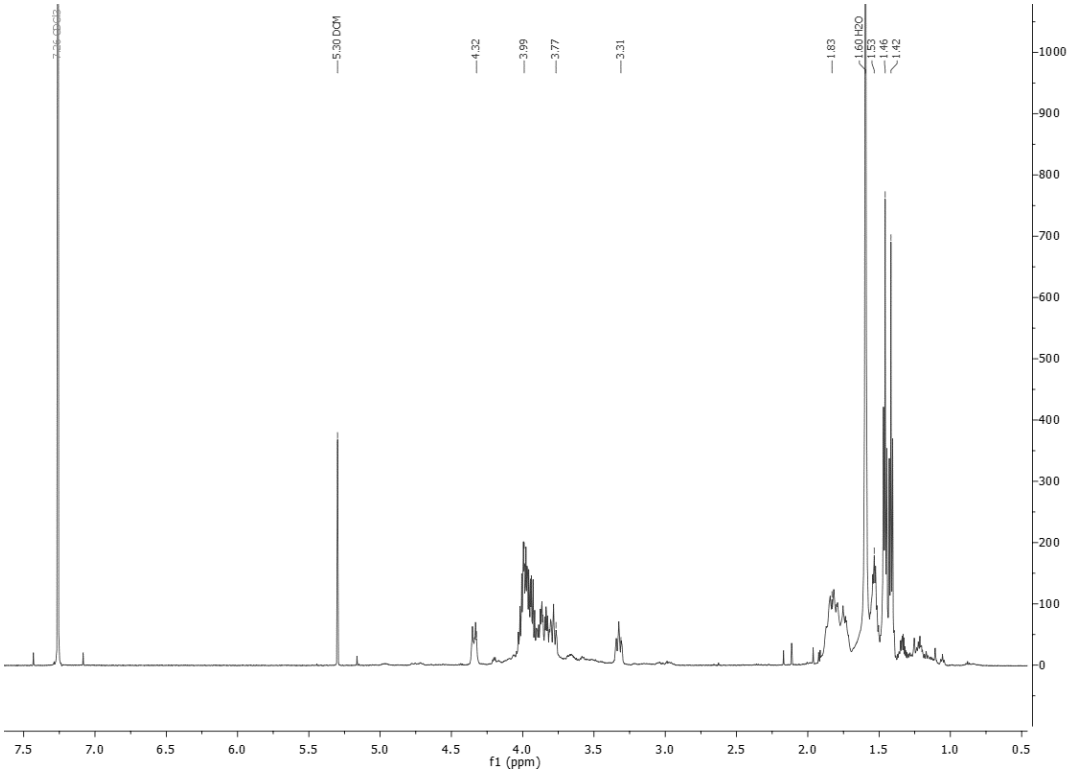

Figure S13: ^{1}H-NMR spectrum ($CDCl_3$, 599.90 MHz, 298 K) of $[Ru_2(pipeDTC)_x(DEDT)_y]Br$.

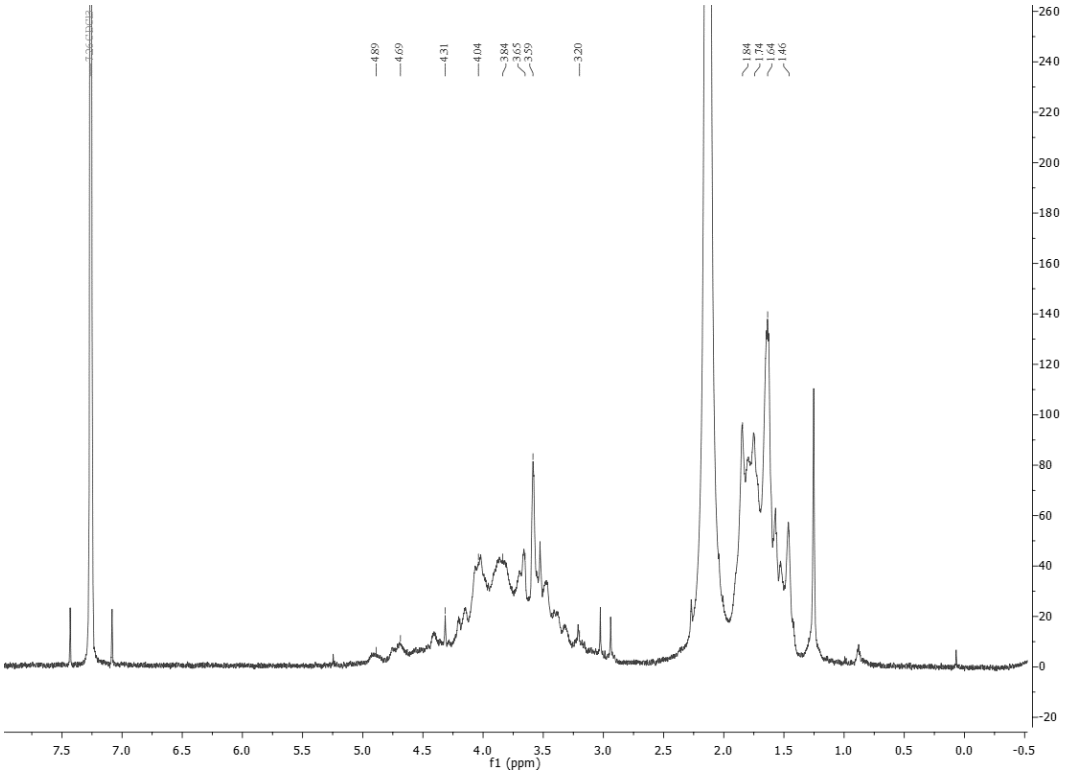

Figure S14: ^{1}H-NMR spectrum ($CDCl_3$, 599.90 MHz, 298 K) of tetrakis(piperidine dithiocarbamato)-(β-glucoside methyl amino ethyl dithiocarbamato)diruthenium(III) bromide $[Ru_2(pipeDTC)_4(gluc\text{-}MAE\text{-}DTC)]Br$.

FT-IR spectra of the synthesized $[Ru_2(DTC)_x(DTC')_{(5-x)}]Br$ complexes

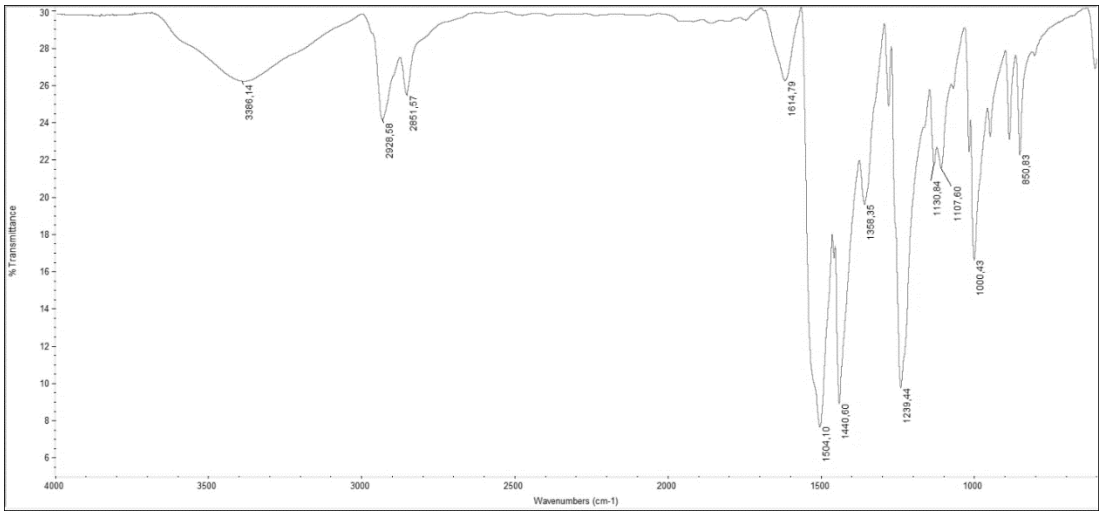

Figure S15: Medium FT-IR (4000-600 cm^{-1}, KBr) spectrum of *pentakis*(piperidineDTC) diruthenium(III) bromide, $[Ru_2(pipeDTC)_5]Br$.

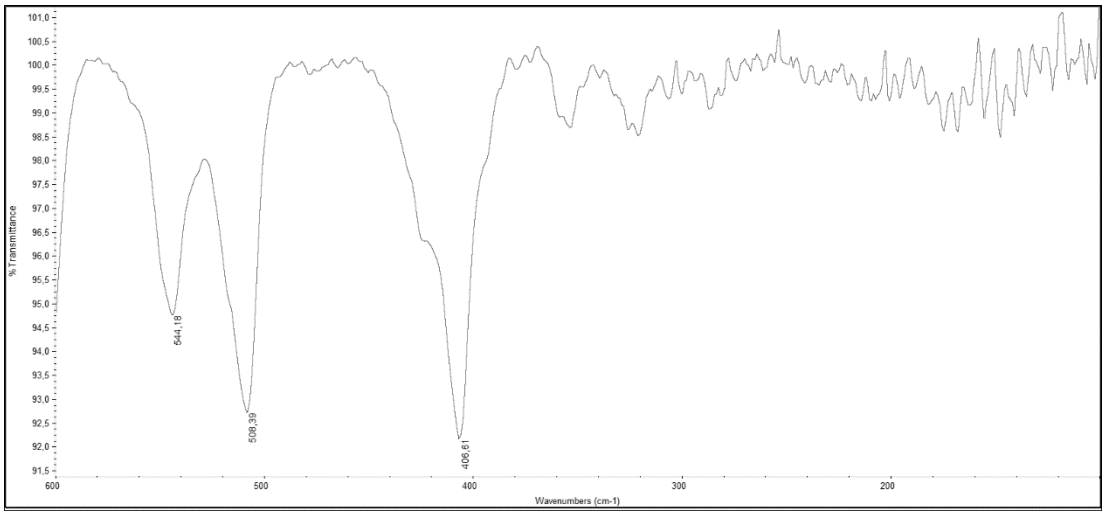

Figure S16: Far FT-IR (600-200 cm^{-1}, nujol) spectrum of *pentakis*(piperidine dithiocarbamate)diruthenium(III) bromide, $[Ru_2(pipeDTC)_5]Br$.

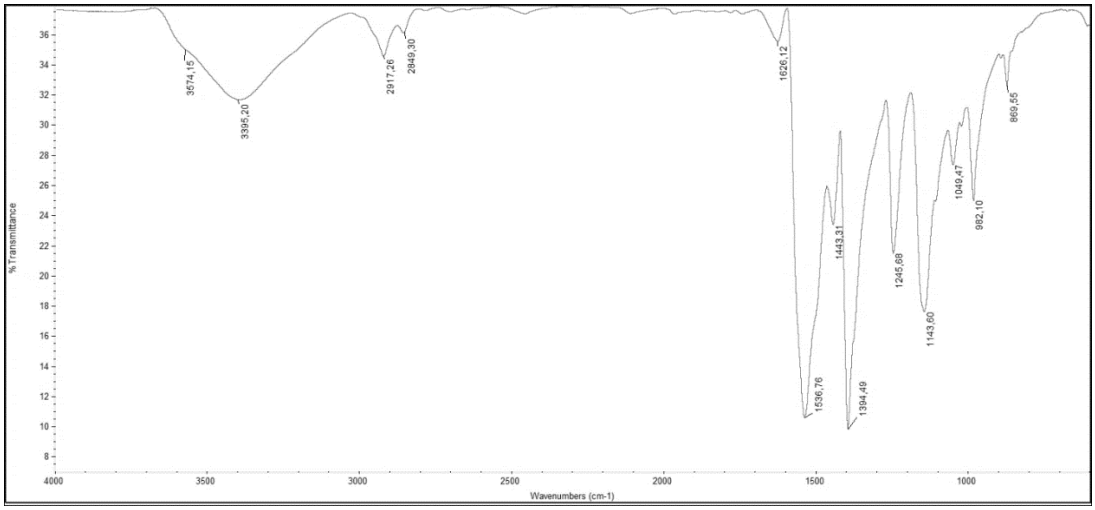

Figure S17: Medium FT-IR (4000-600 cm^{-1}, KBr) spectrum of *pentakis*(dimethyl dithiocarbamate)diruthenium(III) bromide, $[Ru_2(DMDT)_5]Br$.

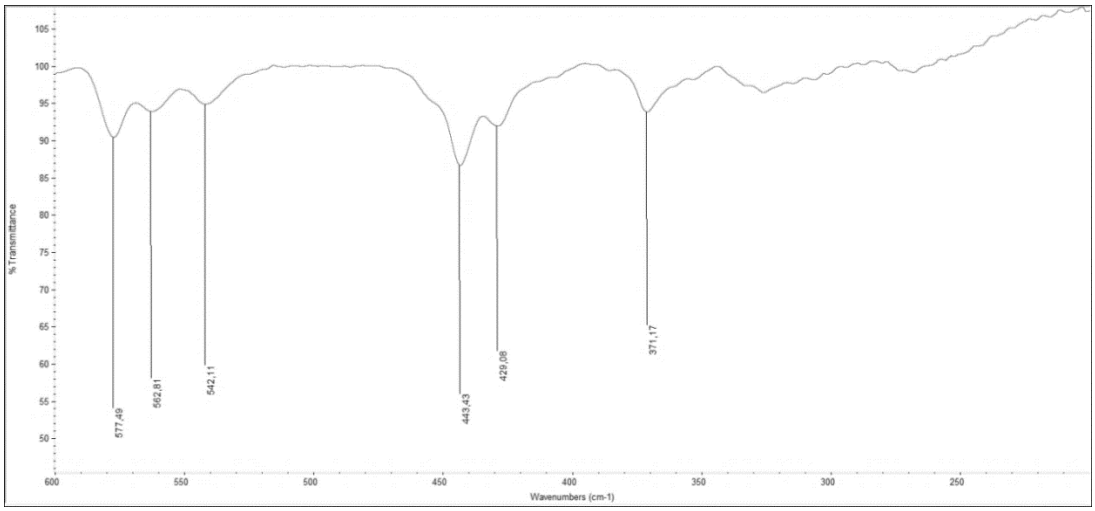

Figure S18: Far FT-IR (4000-600 cm^{-1}, KBr) spectrum of *pentakis*(dimethyl dithiocarbamate)diruthenium(III) bromide, $[Ru_2(DMDT)_5]Br$.

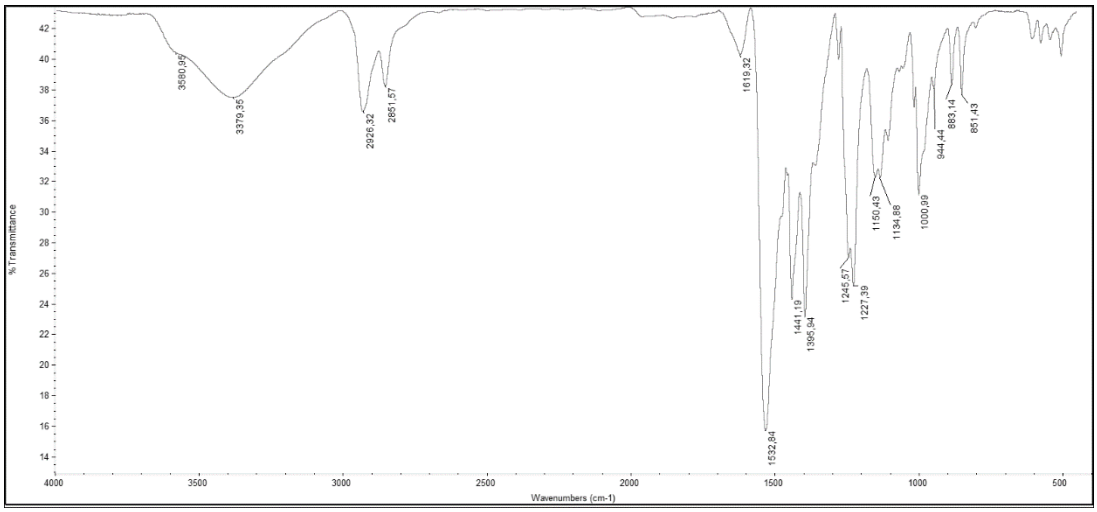

Figure S19: Medium FT-IR (4000-600 cm^{-1}, KBr) spectrum of $[Ru_2(pipeDTC)_x(DMDT)_y]Br$.

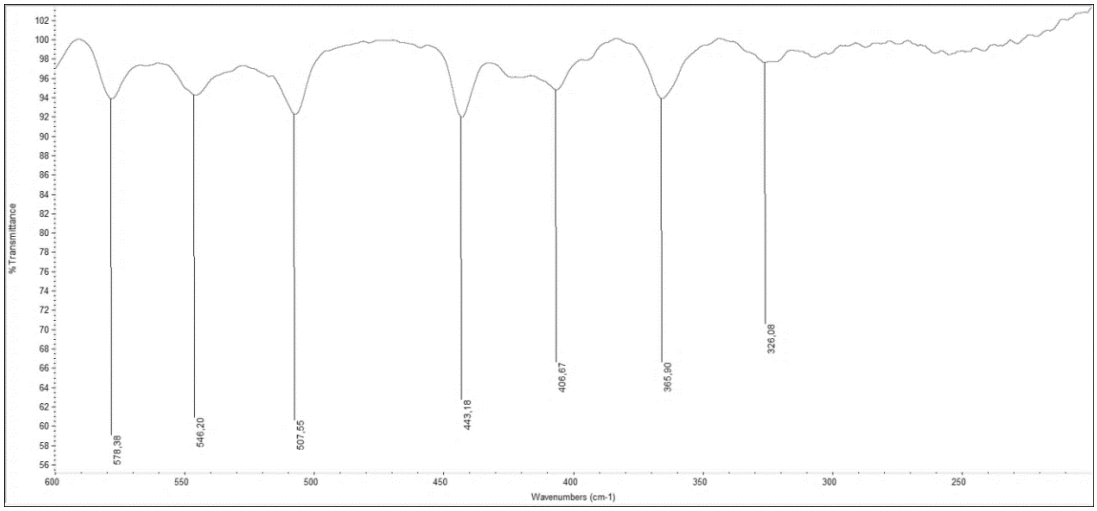

Figure S20: Far FT-IR (600-200 cm^{-1}, nujol) spectrum of $[Ru_2(pipeDTC)_x(DMDT)_y]Br$.

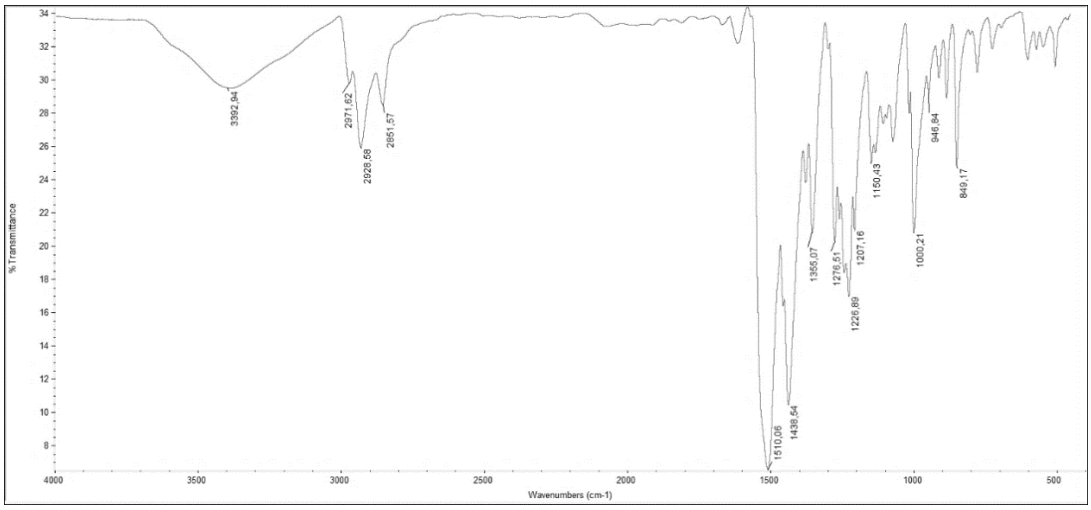

Figure S21: Medium FT-IR (4000-600 cm^{-1}, KBr) spectrum of $[Ru_2(pipeDTC)_x(DEDT)_y]Br$.

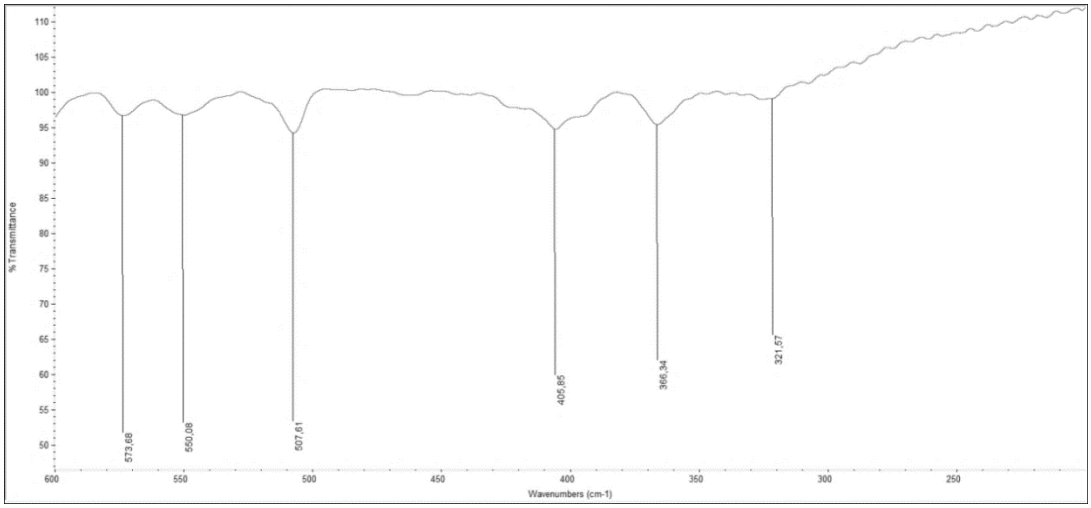

Figure S22: Far FT-IR (600-400 cm^{-1}, nujol) spectrum of $[Ru_2(pipeDTC)_x(DEDT)_y]Br$.

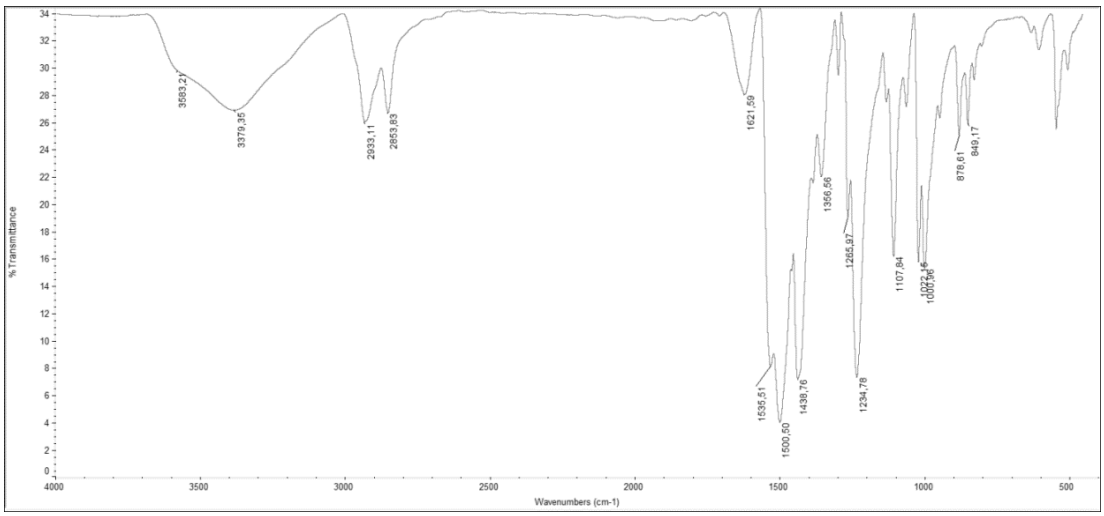

Figure S23: Medium FT-IR (4000-600 cm^{-1}, KBr) spectrum of *tris*(piperidine dithiocarbamate)-*bis*(morpholine dithiocarbamate)*di*ruthenium(III) bromide, $[Ru_2(pipeDTC)_3(morphDTC)_2]Br$.

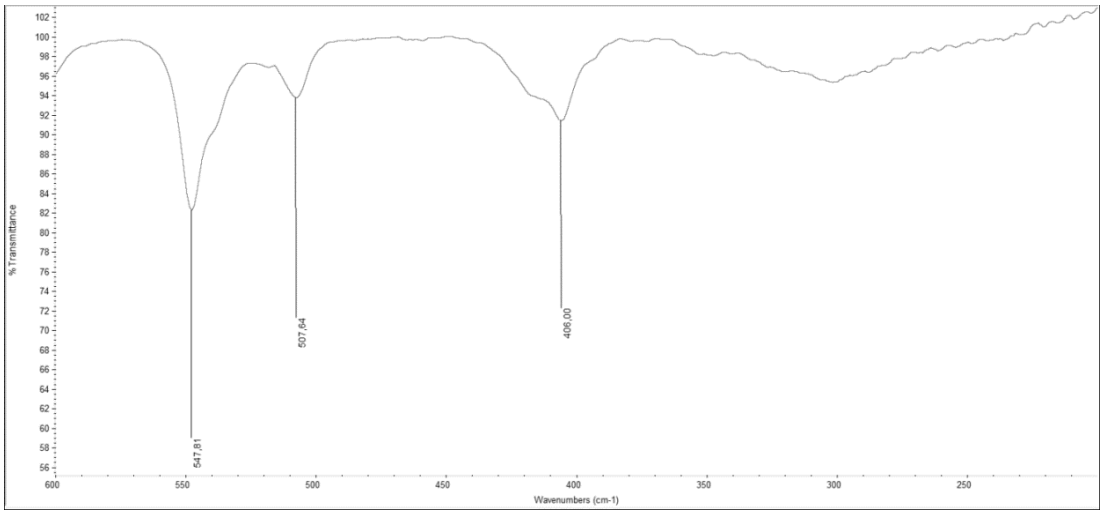

Figure S24: Far FT-IR (600-200 cm^{-1}, nujol) spectrum of *tris*(piperidine dithiocarbamate)-*bis*(morpholine dithiocarbamate)*di*ruthenium(III) bromide, $[Ru_2(pipeDTC)_3(morphDTC)_2]Br$.

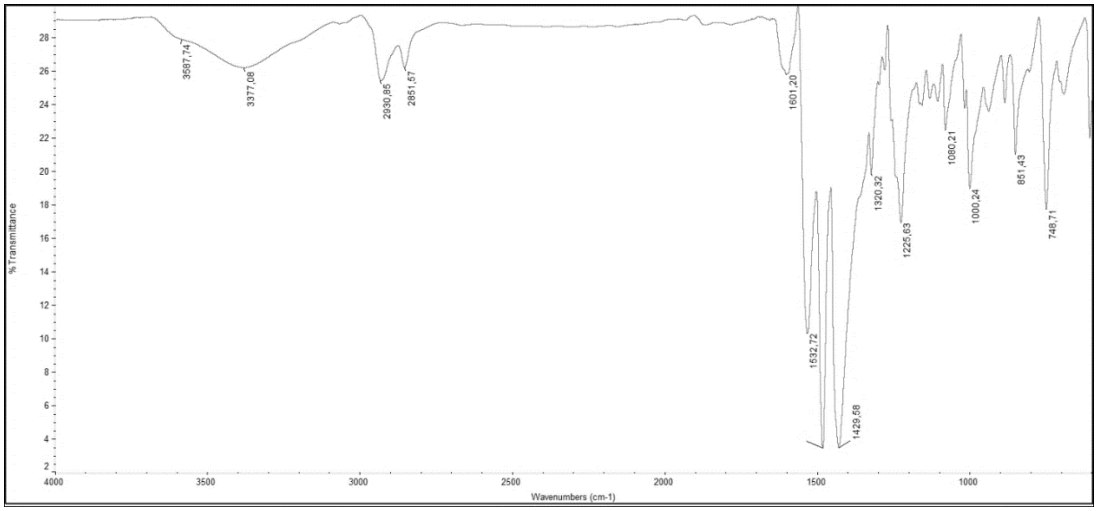

Figure S25: Medium FT-IR (4000-600 cm^{-1}, KBr) spectrum of $[Ru_2(pipeDTC)_x(indolineDTC)_y]Br$.

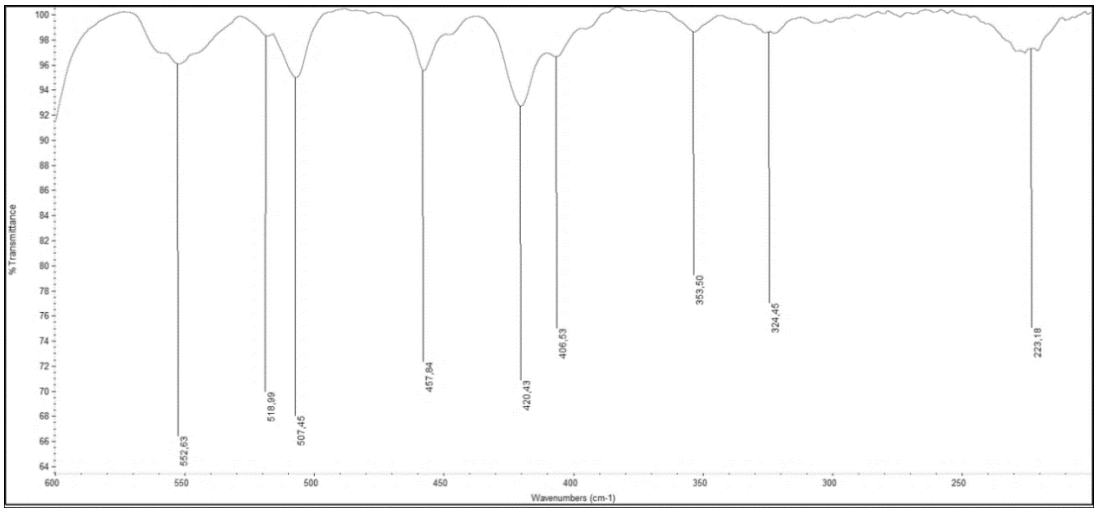

Figure S26: Far FT-IR (600-200 cm^{-1}, nujol) spectrum of $[Ru_2(pipeDTC)_x(indolineDTC)_y]Br$.

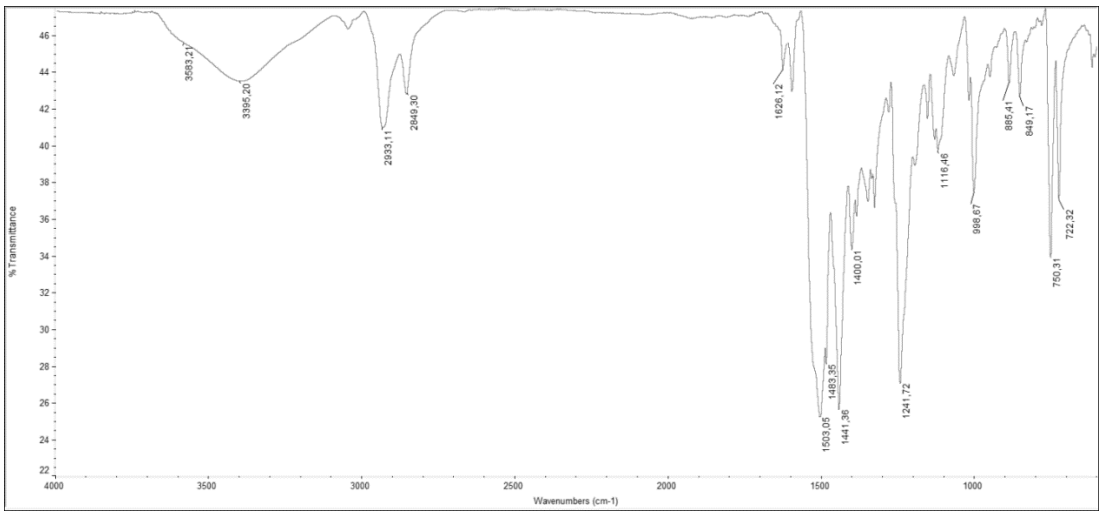

Figure S27: Medium FT-IR (4000-600 cm^{-1}, KBr) spectrum of [Ru_2(pipeDTC)$_x$(Carbz-pr-*N*Me-DTC)$_y$]Br.

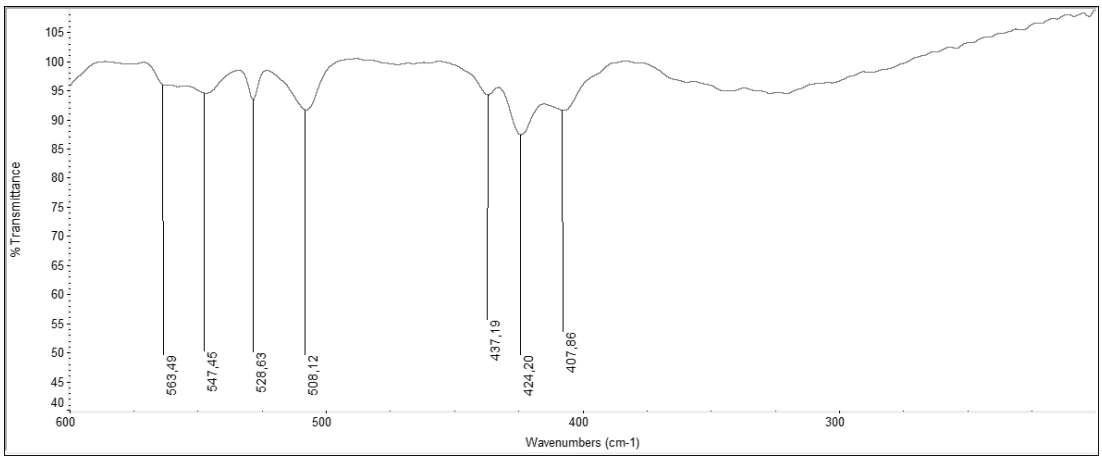

Figure S28: Far FT-IR (600-400 cm^{-1}, KBr) spectrum of [Ru_2(pipeDTC)$_x$(Carbz-pr-*N*Me-DTC)$_y$]Br.

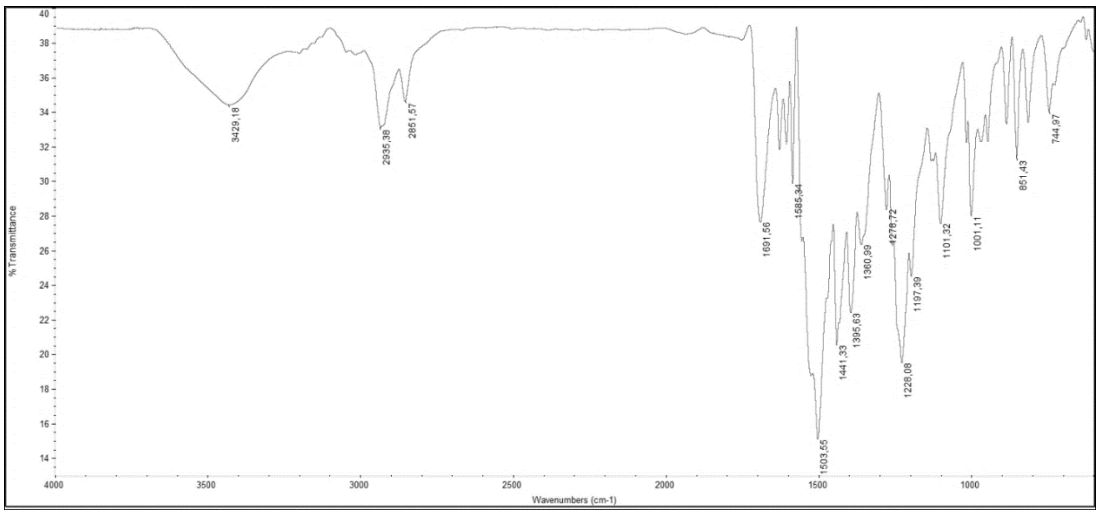

Figure S29: Medium FT-IR (4000-600 cm^{-1}, KBr) spectrum of [Ru_2(pipeDTC)$_x$(β-Napht-Sar-DTC)$_y$]Br.

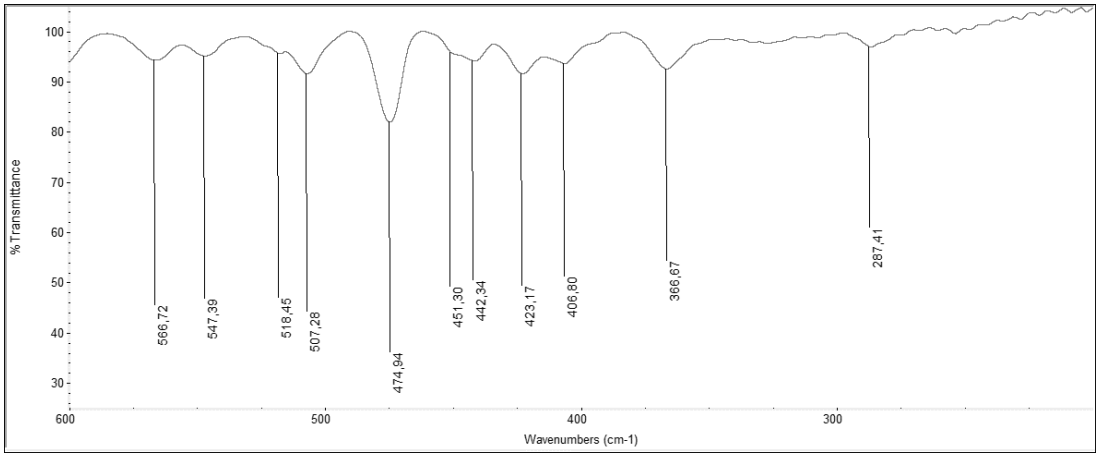

Figure S30: Far FT-IR (600-200 cm^{-1}, nujol) spectrum of [Ru_2(pipeDTC)$_x$(β-Napht-Sar-DTC)$_y$]Br.

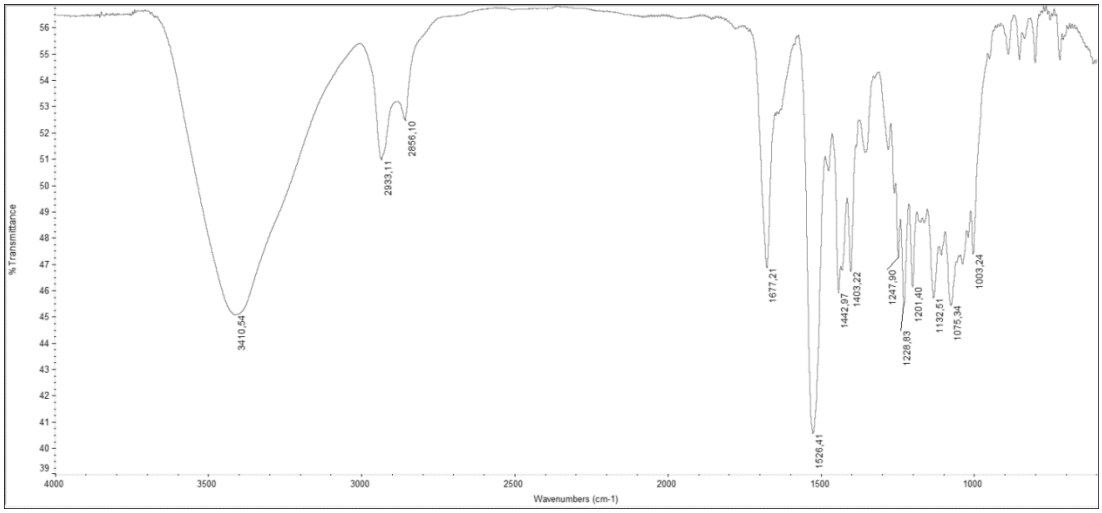

Figure S31: Medium FT-IR (4000-600 cm^{-1}, KBr) spectrum of *tris*-(piperidine dithiocarbamate) *bis*-(glucMAEdithiocarbamate)*di*ruthenium(III) bromide, $[Ru_2(pipeDTC)_3(glucMAE\text{-}DTC)_2]Br$.

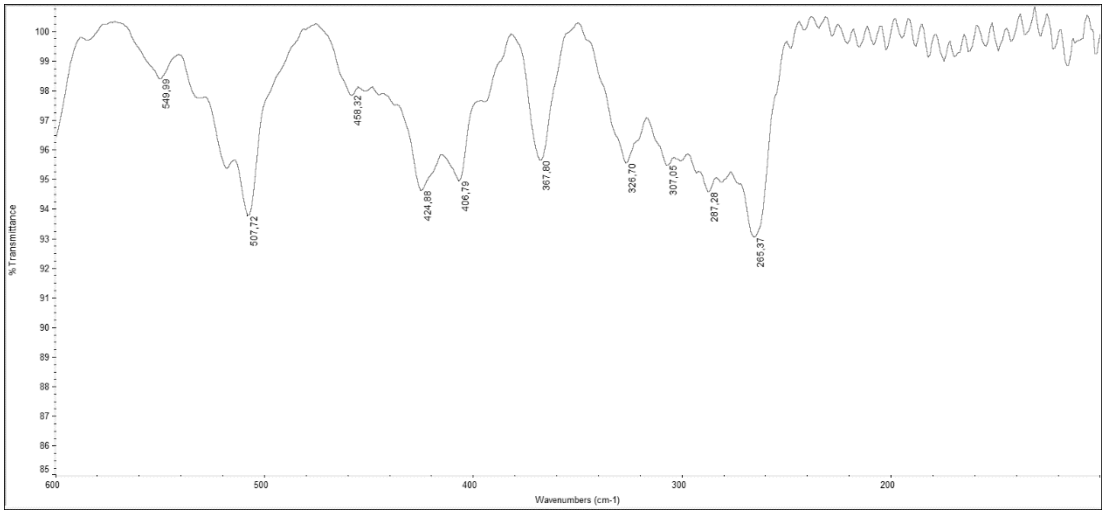

Figure S32. Far FT-IR (600-200 cm^{-1}, KBr) spectrum of *tris*-(piperidine dithiocarbamate) *bis*-(glucMAEdithiocarbamate)*di*ruthenium(III) bromide, $[Ru_2(pipeDTC)_3(glucMAE\text{-}DTC)_2]Br$.

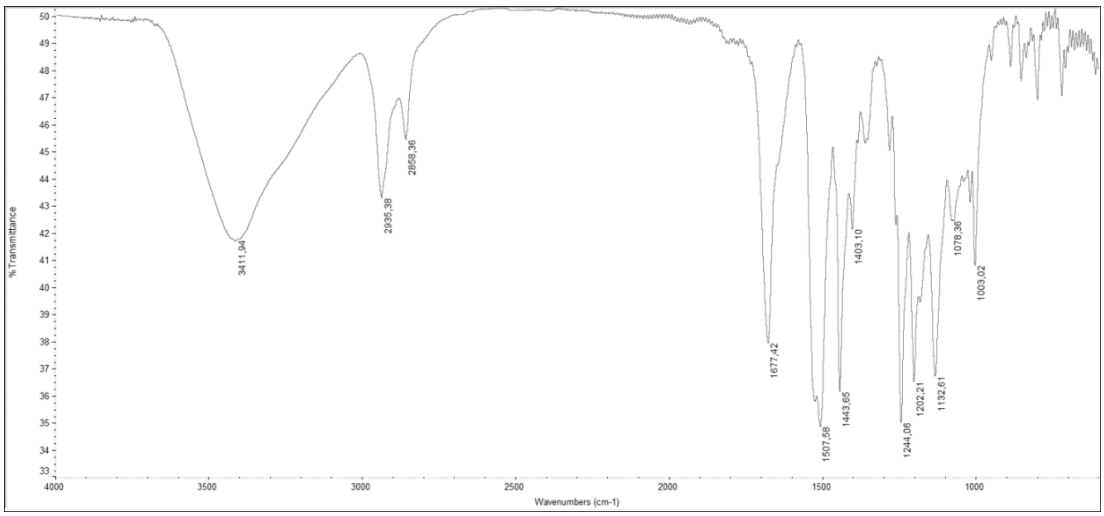

Figure S33: Medium FT-IR (4000-600 cm^{-1}, KBr) spectrum of *tetrakis*-(piperidine dithiocarbamateglucMAEdithiocarbamate)*di*ruthenium(III) bromide, $[Ru_2(pipeDTC)_4(glucMAE\text{-}DTC)]Br$.

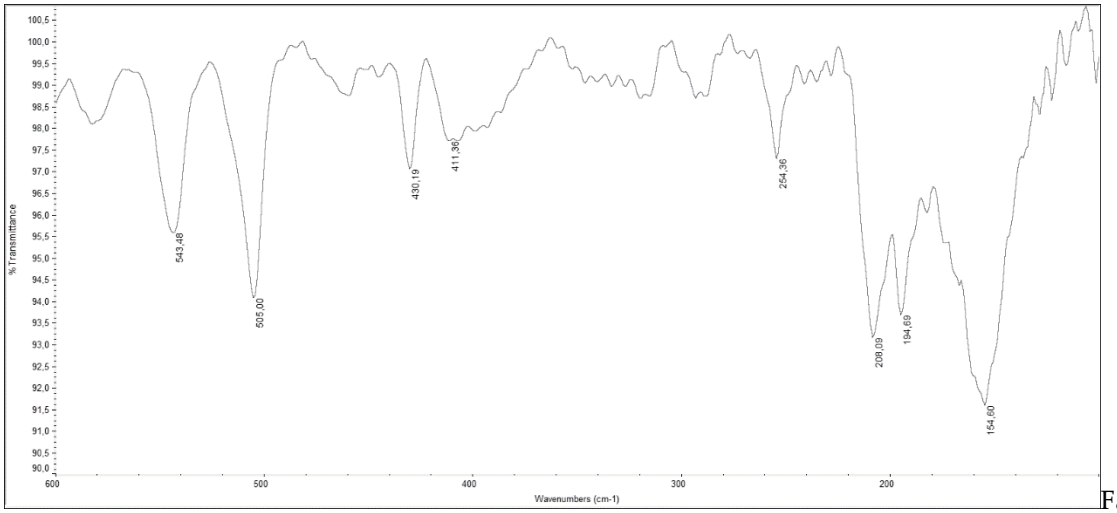

Figure S34: Far FT-IR (600-200 cm^{-1}, KBr) spectrum of the oxidized of the bimetallic oxidized precursor.

UV-Vis spectra of the synthesized $[Ru_2(DTC)_x(DTC')_{(5-x)}]Br$ complexes

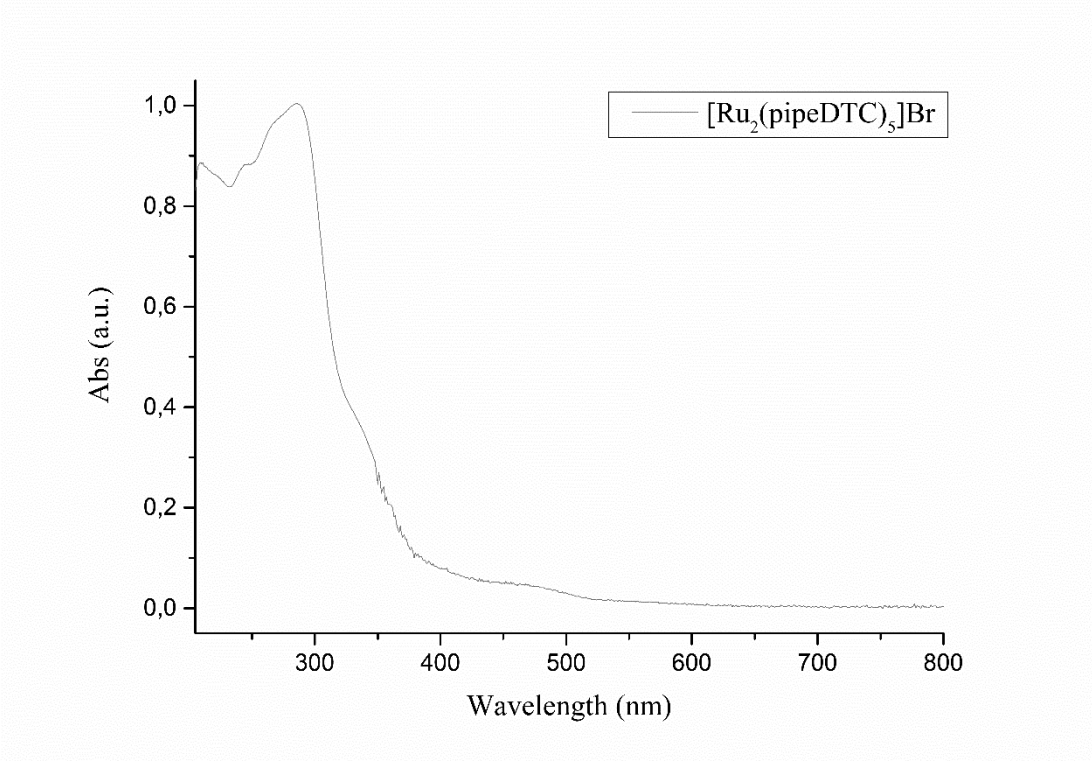

Figure S35: UV-Vis spectrum of $[Ru_2(pipeDTC)_5]Br$ recorded in MeOH (800-205 nm).

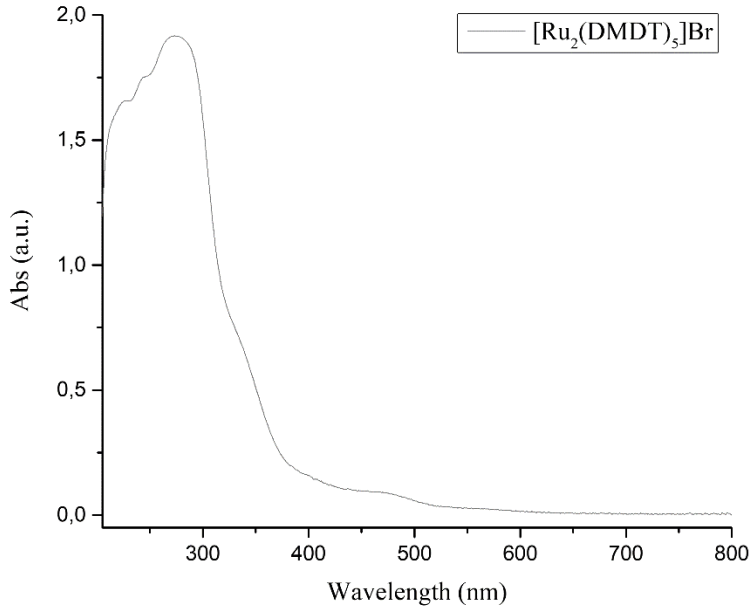

Figure S36: UV-Vis spectrum of $[Ru_2(DMDT)_5]Br$ recorded in MeOH (800-205 nm).

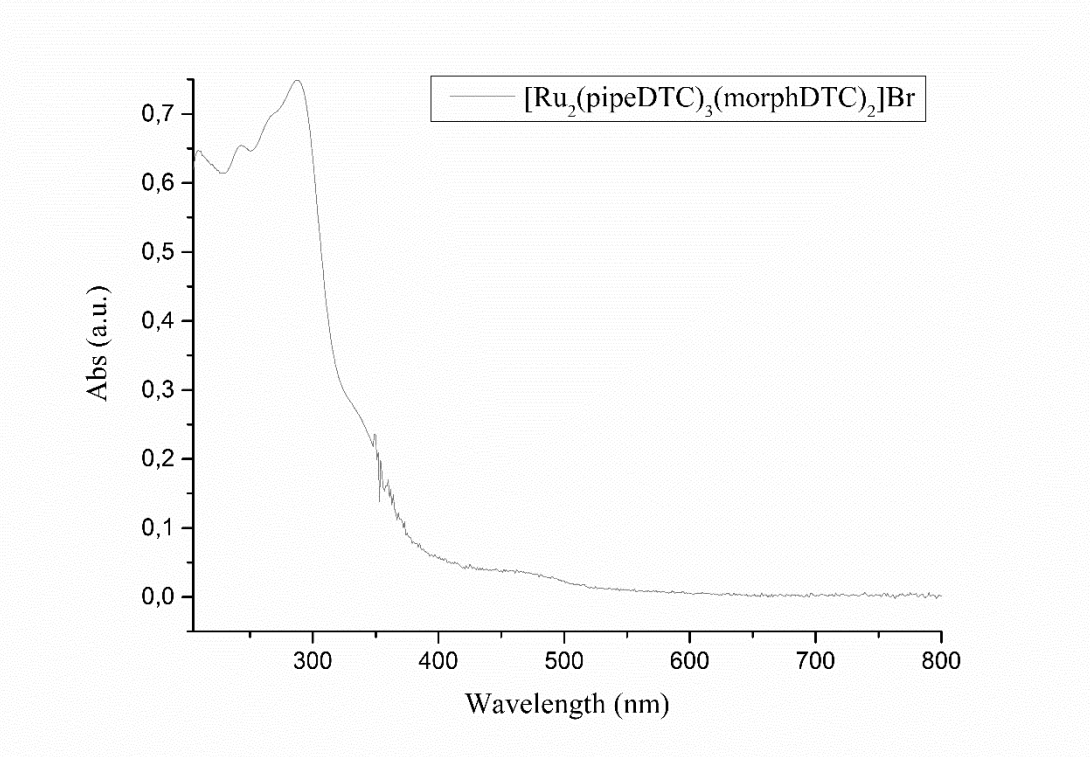

Figure S37: UV-Vis spectrum of [Ru2(pipeDTC)3(morphDTC)2]Br recorded in MeOH (800-205 nm).

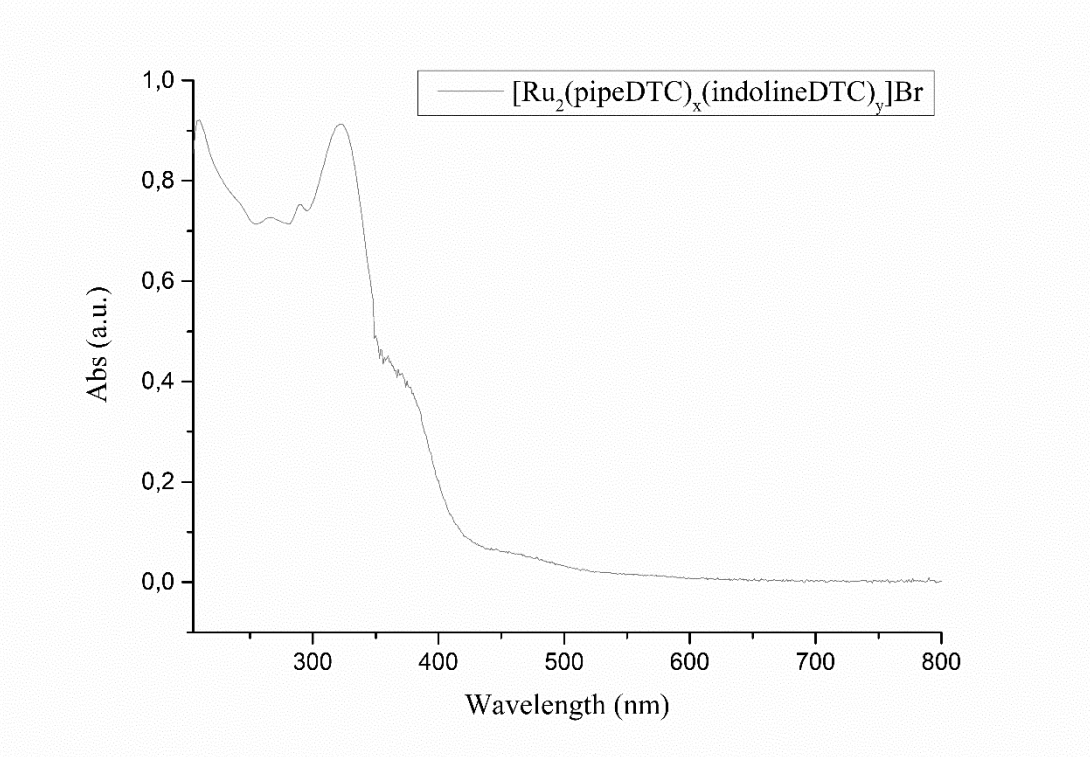

Figure S38: UV-Vis spectrum of [Ru2(pipeDTC)x(indolineDTC)y]Br recorded in MeOH (800-205 nm).

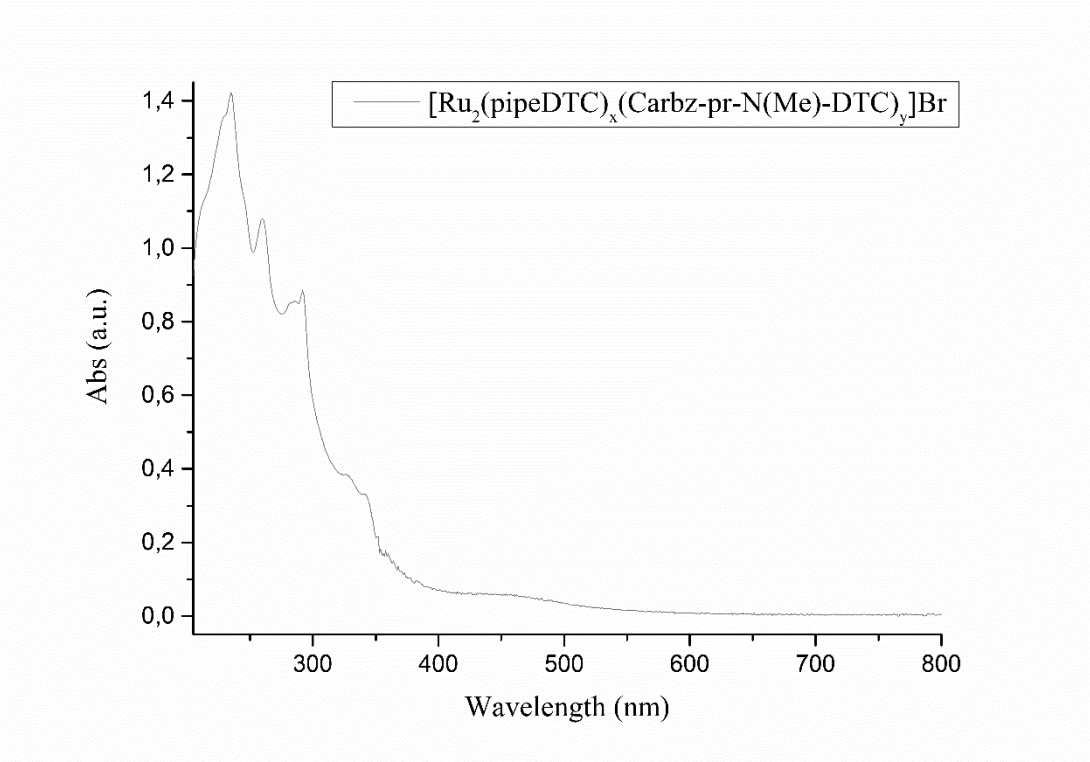

Figure S39: UV-Vis spectrum of [Ru2(pipeDTC)x(Carbz-pr-*N*(Me)-DTC)y]Br recorded in MeOH (800-205 nm).

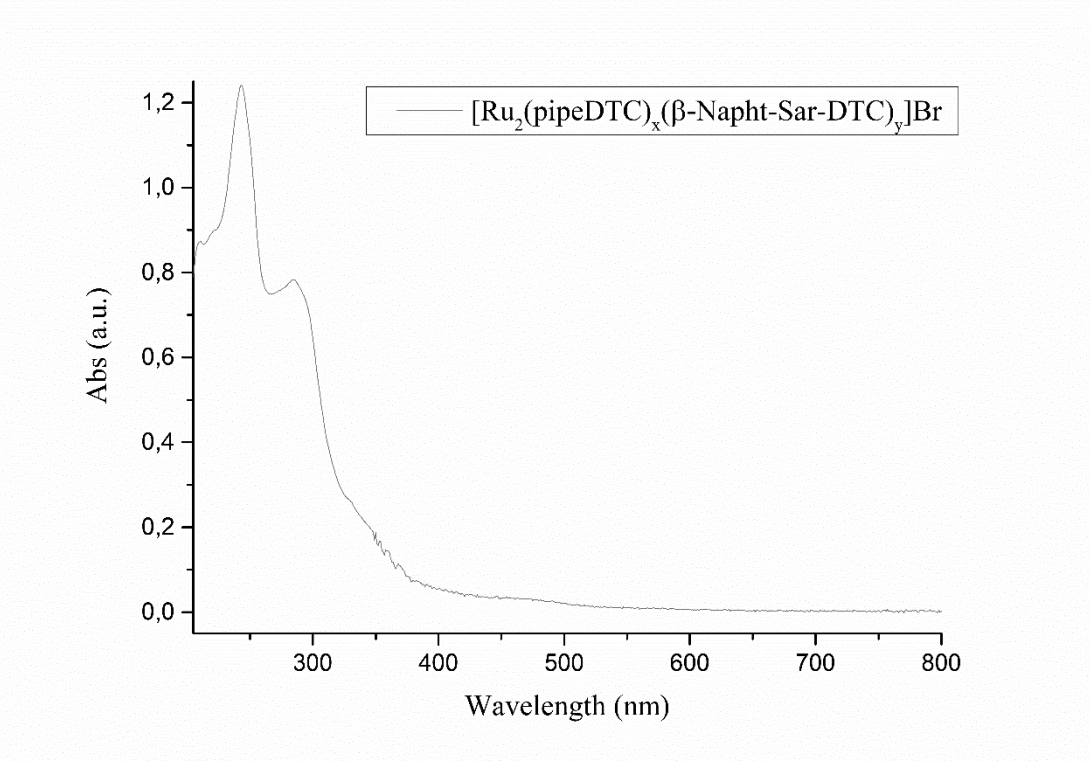

Figure S40: UV-Vis spectrum of [Ru2(pipeDTC)x(β-Napht-Sar-DTC)y]Br recorded in MeOH (800-205 nm).

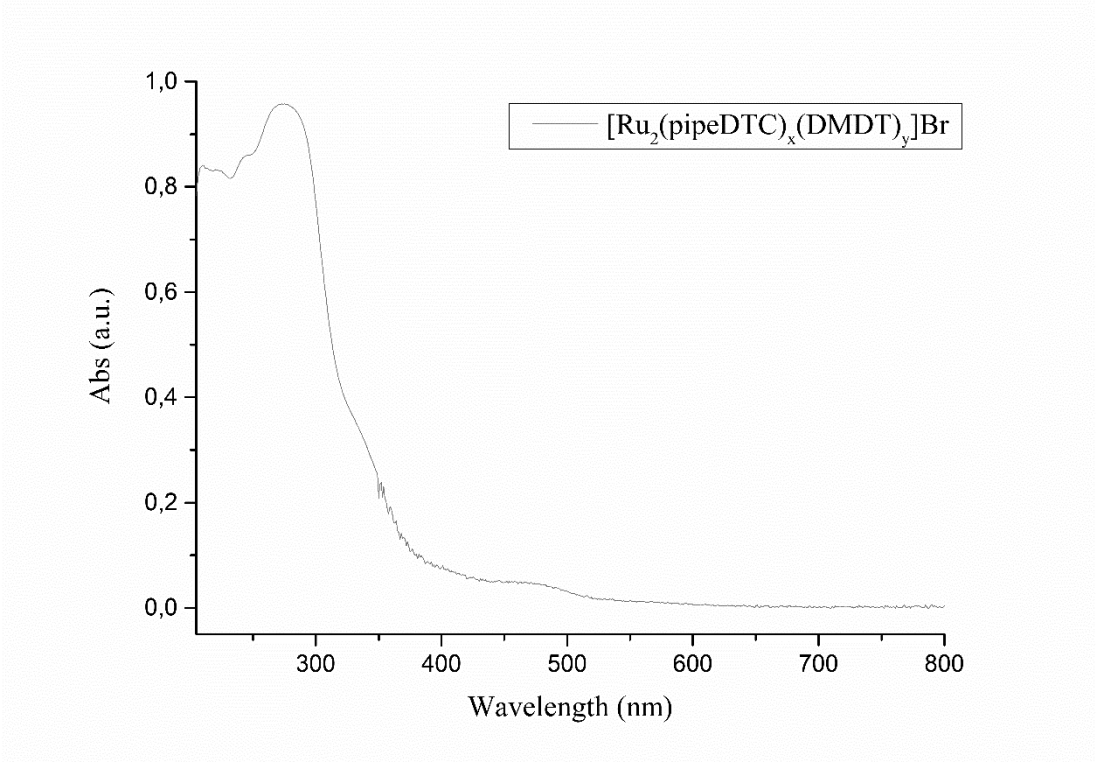

Figure S41: UV-Vis spectrum of [Ru2(pipeDTC)x(DMDT)y]Br recorded in MeOH (800-205 nm).

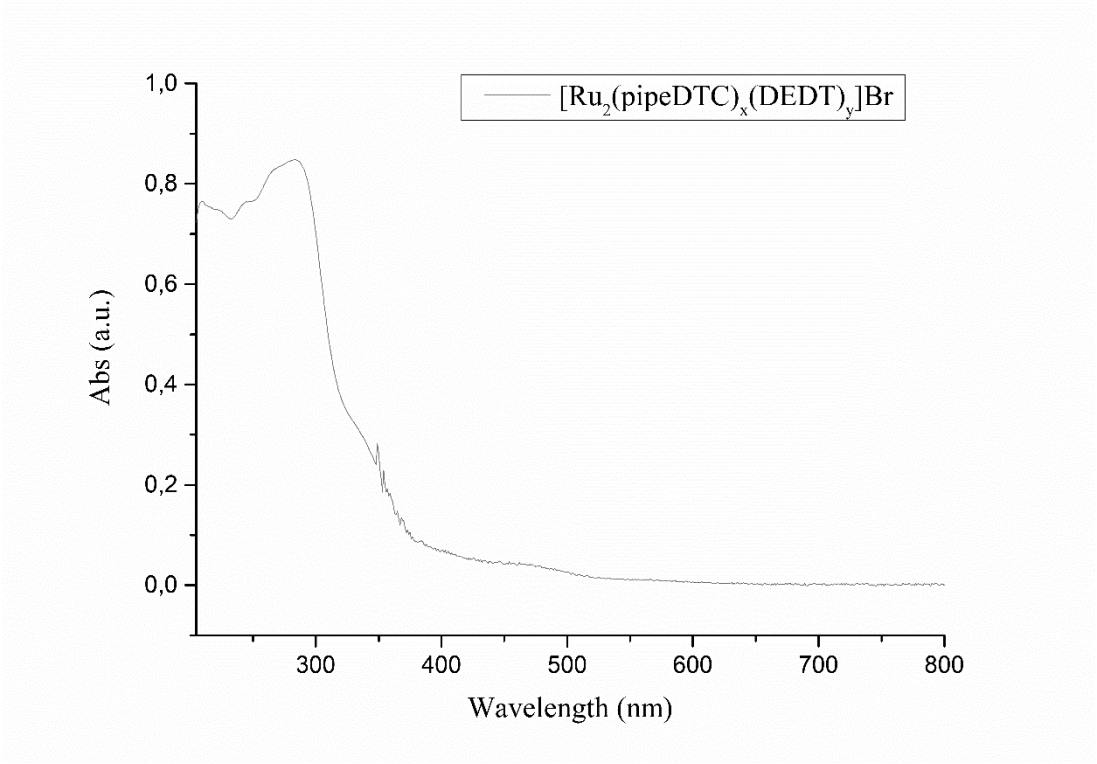

Figure S42: UV-Vis spectrum of [Ru2(pipeDTC)x(DEDT)y]Br recorded in MeOH (800-205 nm).

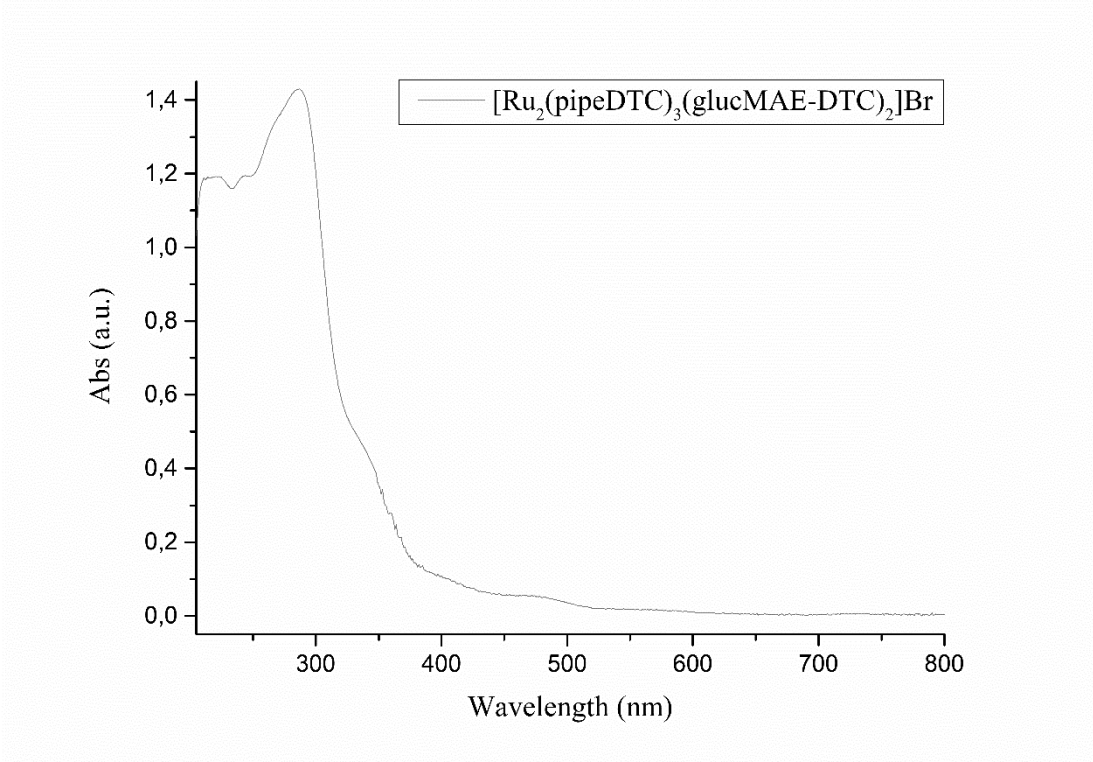

Figure S43: UV-Vis spectrum of [Ru2(pipeDTC)3(glucMAE-DTC)2]Br recorded in MeOH (800-205 nm).

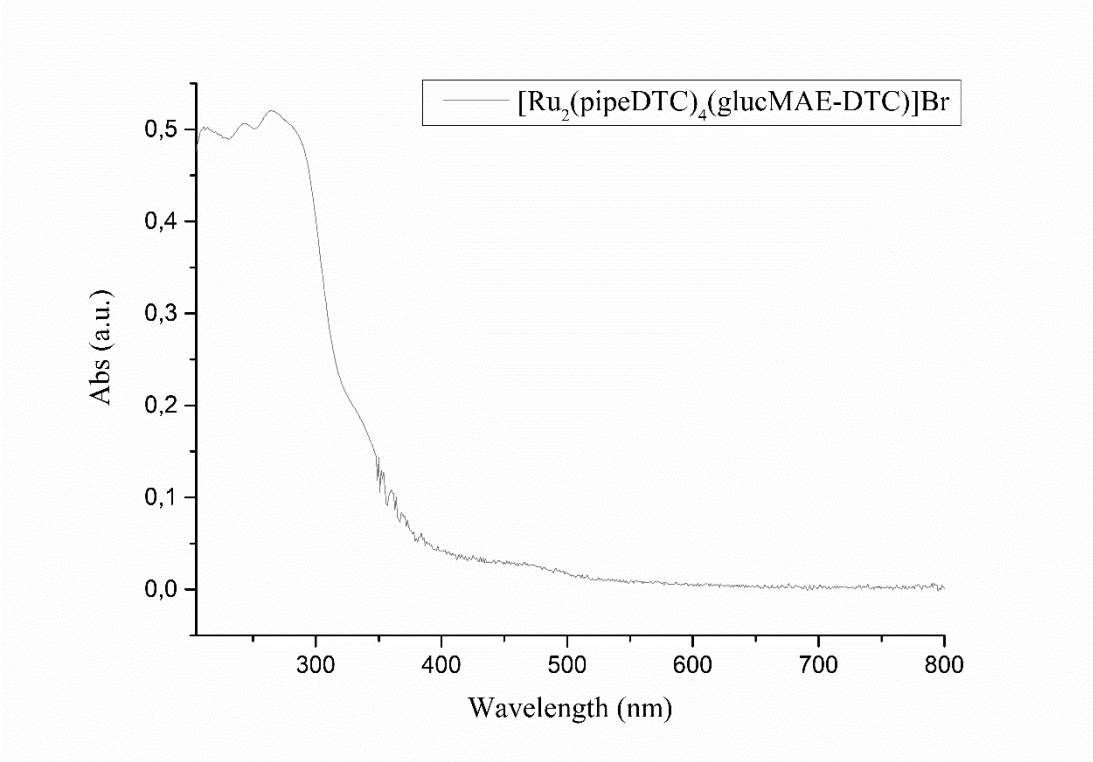

Figure S44: UV-Vis spectrum of [Ru2(pipeDTC)4(glucMAE-DTC)]Br recorded in MeOH (800-205 nm).

Antiproliferative activity

MDA-MB-231 and PC3 cells were separately cultured in 75 cm^2 cell culture flasks in complete medium (DMEM high glucose), with addition of FBS (10%), L-glutamine (4 mM), and incubated at 37 °C in a 5% carbon dioxide-controlled atmosphere.

This was followed by treatment for 24 and 48 hours with vehicle (control; namely DMSO) or each compound (dissolved in the vehicle) in fresh medium at the defined concentrations. Compounds were weighed in sterile test tubes of 1 ml and pre-dissolved in DMSO. The final concentrations of the tested compounds were 0.05, 0.1, 1. 5 and 10 μM.

Cell count with Trypan Blue exclusion test

24 and 48 hours after treatment with each compound, the medium was removed from the flask, and the cells washed with 6 mL of PBS, and then shacked in presence of 1 mL of trypsin, followed by 3-min incubation. MEM was then added, and the obtained cellular suspension seeded in 96-well microplates ($10 \cdot 10^3$ cells/well) in the proper growth medium (200 μL), and incubated at 37 °C in a 5% CO_2 atmosphere for 24 h to allow cell adhesion. This was followed by treatment for 24 and 48 hours with vehicle (control; namely DMSO) or each compound (dissolved in the vehicle) in fresh medium at the defined concentrations (i.e., 10 μM, 5 μM, 2 μM, 1 μM, 0.5 μM).

Cells were counted with a Burker cell-counting chamber using the Trypan blue. This dye selectively stains dead cells. The values resulting from the cell counts of both cell lines (in triplicate). From the analysis of the test results, it was calculated the value of the concentration at which the test substance, compared to the untreated control, can reduce the population of viable cells by 50% (IC50).

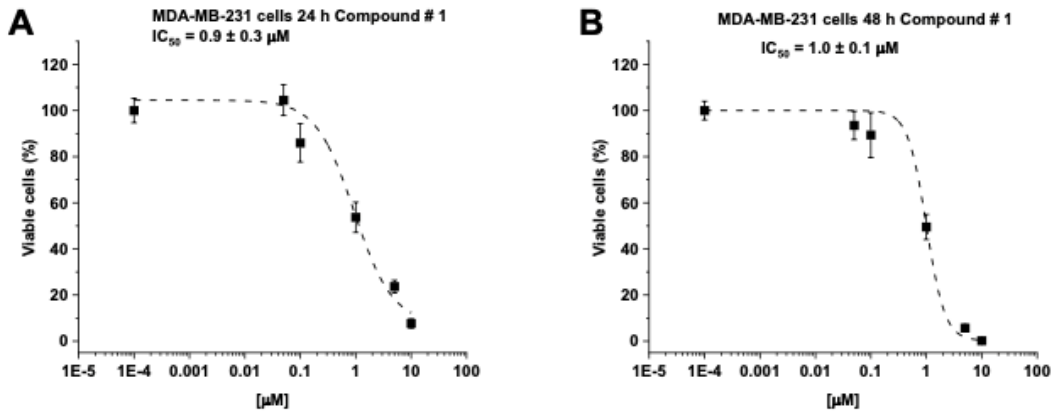

Figure S46: IC50 determination for the treatment with compound #1 of MDA-MB-231 for 24 (A) and 48 (B) hours

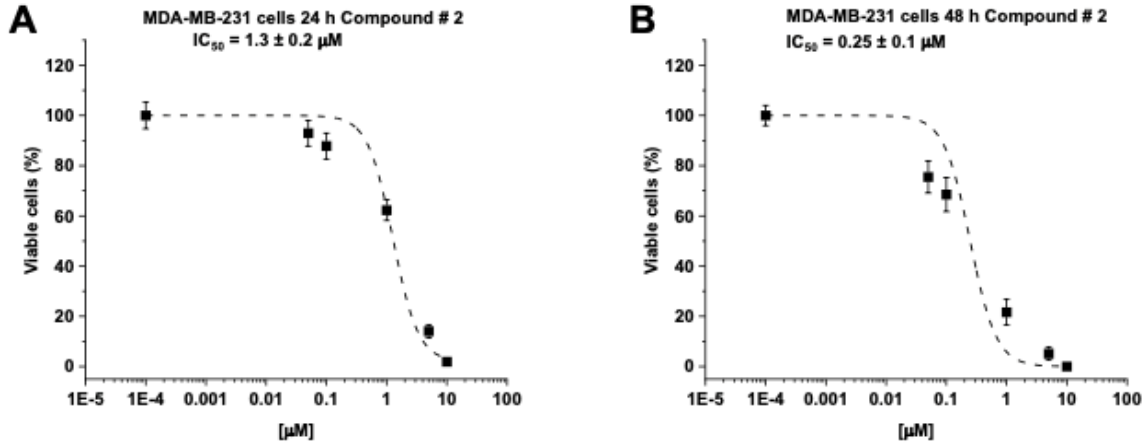

Figure S47: IC50 determination for the treatment with compound #2 of MDA-MB-231 for 24 (A) and 48 (B) hours

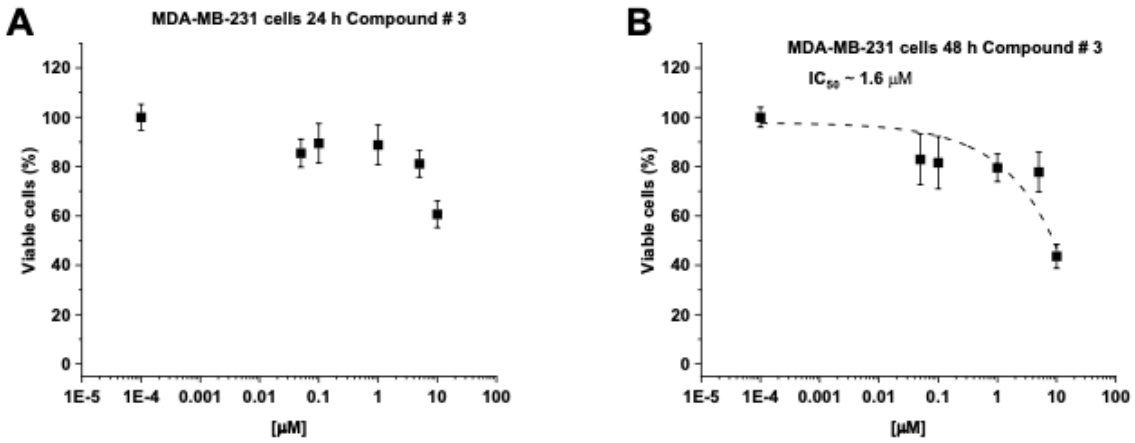

Figure S48: IC50 determination for the treatment with compound #3 of MDA-MB-231 for 24 (A) and 48 (B) hours

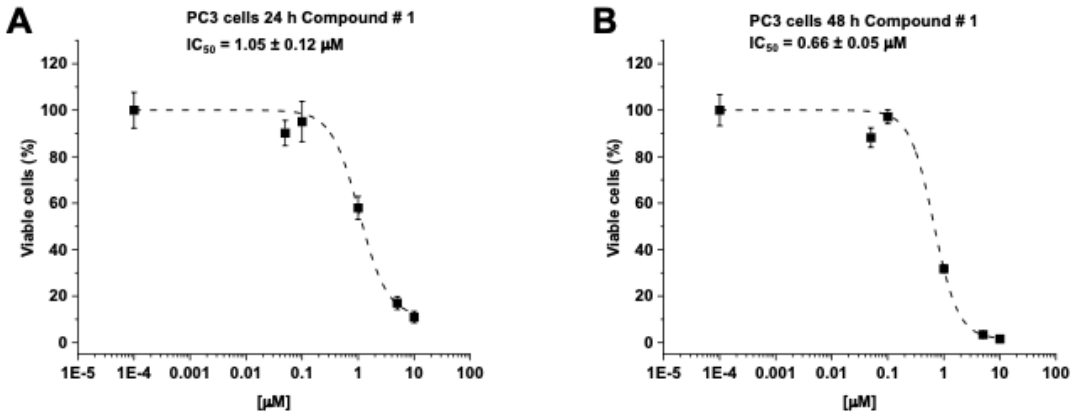

Figure S49: IC50 determination for the treatment with compound #1 of PC3 for 24 (A) and 48 (B) hours

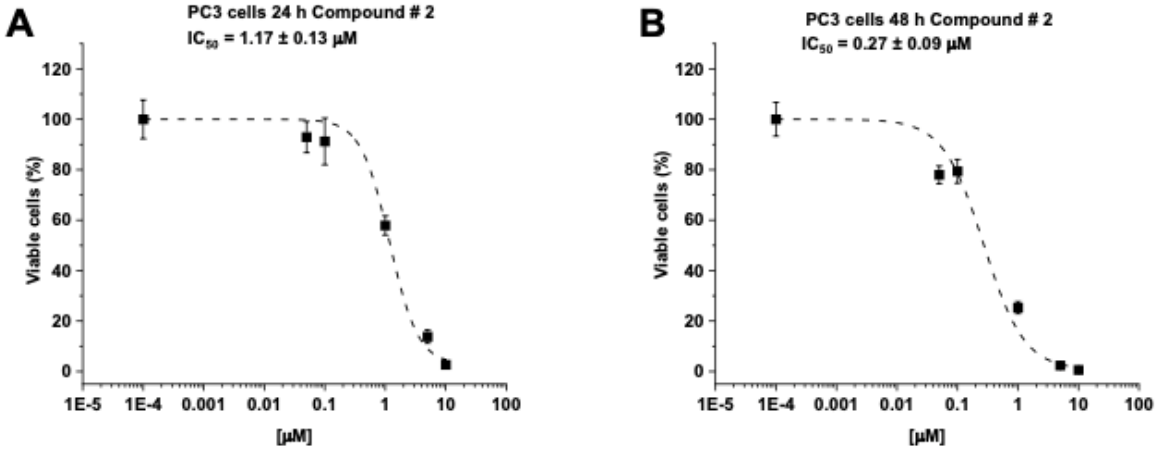

Figure S50: IC50 determination for the treatment with compound #2 of PC3 for 24 (A) and 48 (B) hours

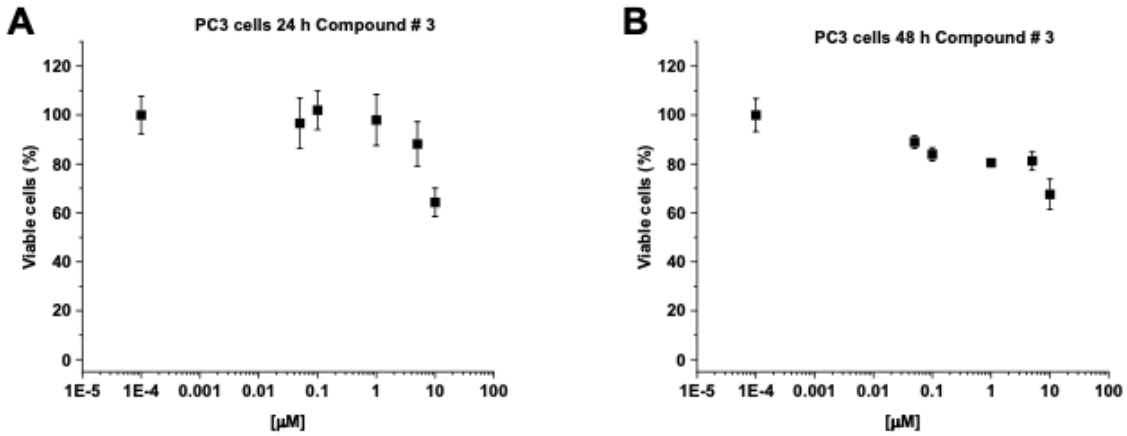

Figure S51: IC50 determination for the treatment with compound #3 of PC3 for 24 (A) and 48 (B) hours

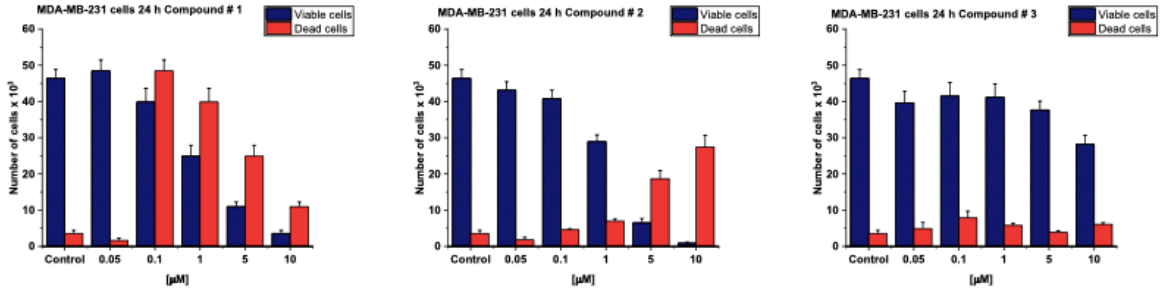

Figure S52: Bar charts reporting viable and dead MDA-MB-231 cells 24 hours post-treatment with compound #1, #2, and #3 respectively.

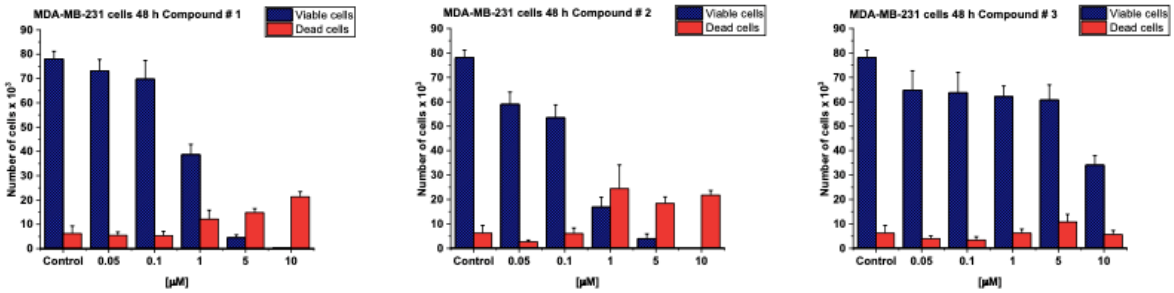

Figure S53: Bar charts reporting viable and dead MDA-MB-231 cells 48 hours post-treatment with compound #1, #2, and #3 respectively.

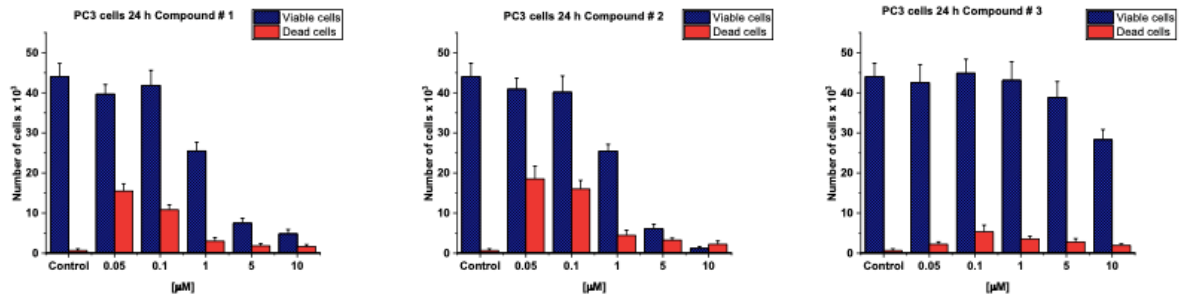

Figure S54: Bar charts reporting viable and dead PC3 cells 24 hours post-treatment with compound #1, #2, and #3 respectively.

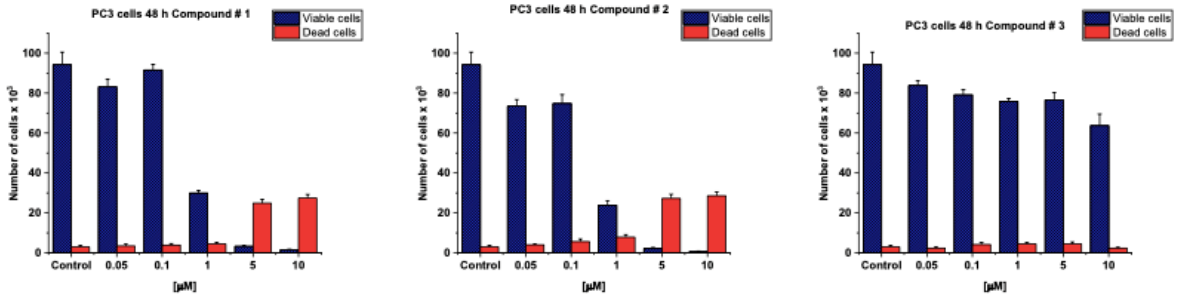

Figure S55: Bar charts reporting viable and dead PC3 cells 48 hours post-treatment with compound #1, #2, and #3 respectively.

Evaluation of cell viability by the WST-1 assay.

To evaluate the vitality and the cell proliferation the cell proliferation assay called WST-1 was also used or 4- [3- (4-iodophenyl) -2- (4-nitrophenyl) -2H-5-tetrazolium] -1,3-benzene disulfonate (Roche Diagnostics, Mannheim, Germany). This is a colorimetric assay for quantification spectrophotometric of cell proliferation, viability and cytotoxicity, carried out in a 96-well plate. At the time of determination, the cells were incubated with the WST-1 reagent, ready for use, for 0.5-3 hours, in a humidified atmosphere (37 ° C, 5% CO2). During that period of incubation, the formazan dye was quantified with a multi-well spectrophotometer (ELISA reader), using a wavelength of 450 nm. The absorbance measure directly correlates with the number of viable cells. The absorbance of the complete medium only (white) was subtracted from the absorbance measured in the samples.

From the analysis of the test it was calculated the value of the concentration at which the substance in examination, compared to the untreated control, reduces the proliferation of cell populations by 50% (IC50).

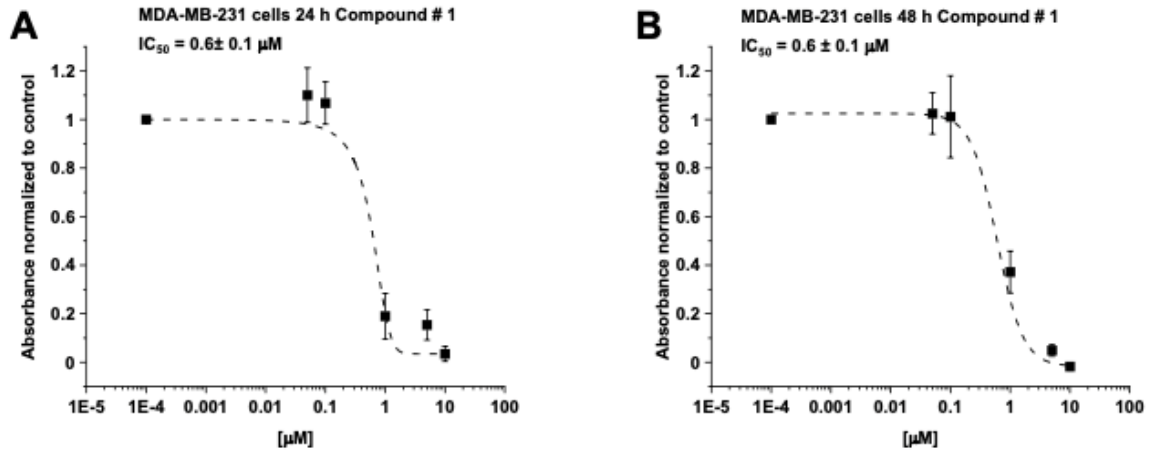

Figure S56: IC50 determination for the treatment with compound #1 of MDA-MB-231 for 24 (A) and 48 (B) hours.

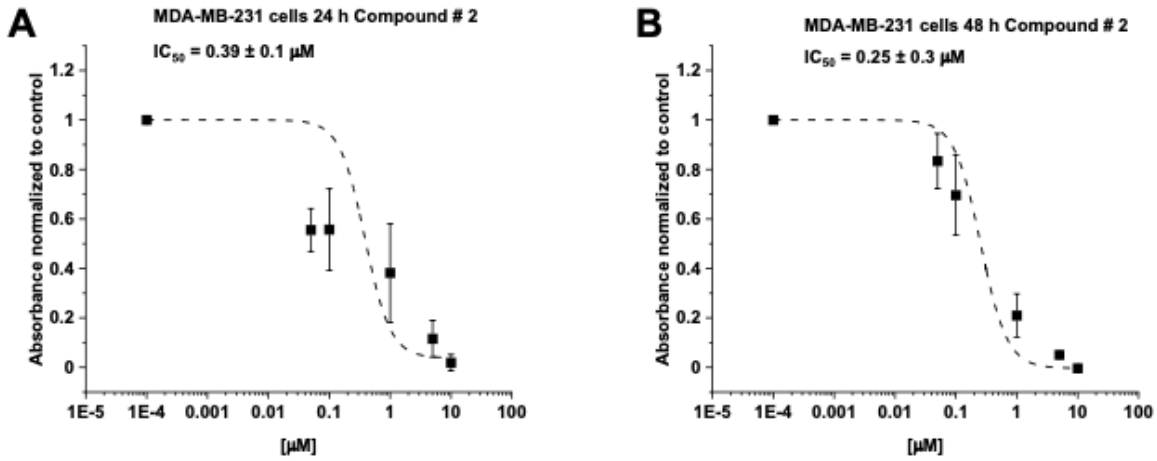

Figure S57: IC50 determination for the treatment with compound #2 of MDA-MB-231 for 24 (A) and 48 (B) hours.

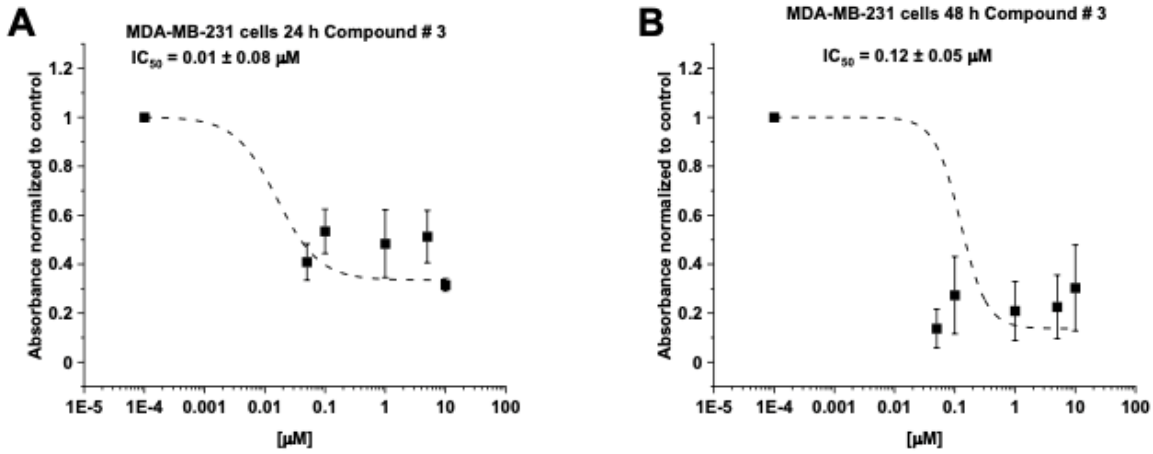

Figure S58: IC50 determination for the treatment with compound #3 of MDA-MB-231 for 24 (A) and 48 (B) hours.

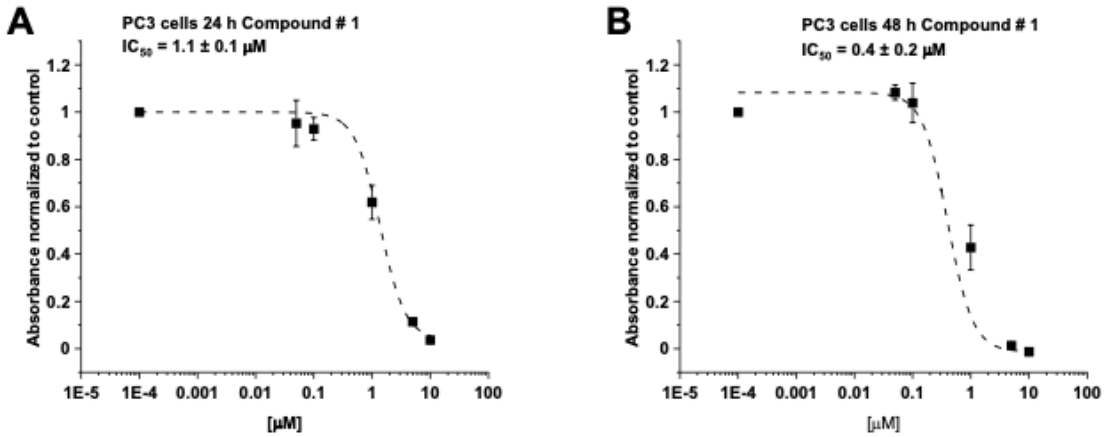

Figure S59: IC50 determination for the treatment with compound #1 of PC3 for 24 (A) and 48 (B) hours.

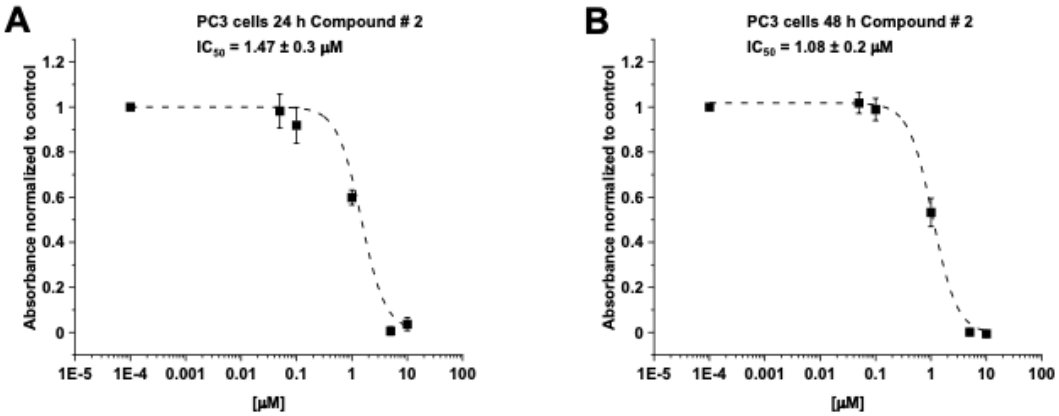

Figure S60: IC50 determination for the treatment with compound #2 of PC3 for 24 (A) and 48 (B) hours.

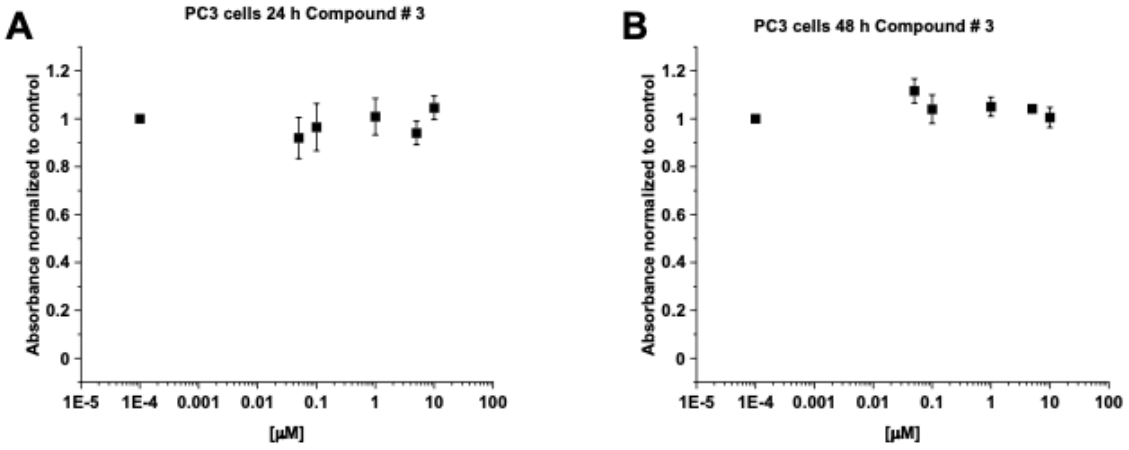

Figure S61: IC50 determination for the treatment with compound #3 of PC3 for 24 (A) and 48 (B) hours.

Flow cytometric evaluation of the cell cycle.

$60x10^3$ of MDA-MB-231 and PC3 cell were respectively seeded in a 24-well plate with 1 mL of complete medium per well in duplicate. The two cell lines were treated with the compounds under examination at the concentrations resulting from the IC50 for the 24- and 48-hours treatment obtained by the Trypan blue test (Table 5). At the beginning of the treatment (time 0) and after 24 and 48 hours respectively, the cells were detached and incubated on ice for 20 minutes with a solution of Propidium Iodide. Such dye, intercalating between the DNA bases, allows the evaluation of the cellular DNA content. At the end of the incubation time, the cells were analysed on a flow cytometer. At least $10x10^3$ were analysed for each sample events. All histograms reported in Appendix A.

Statistical Analysis

Values reported in Table 5, in the IC50 curves and in the column, charts correspond to the means ± ESM (Standard Error of Mean) of the 3 experiments conducted separately in triplicate. Statistical analysis was performed using the software

OriginLab 2020b. Column charts IC50 curves were obtained using the same software package. IC50 curves were fitted with the Hill equation. The reported cell cycle values in Table 6 and Table 7 are the mean ± SD (Standard deviation) of two wells. Cell cycle analysis was performed using the FlowJo V10.7 software.

Appendix A

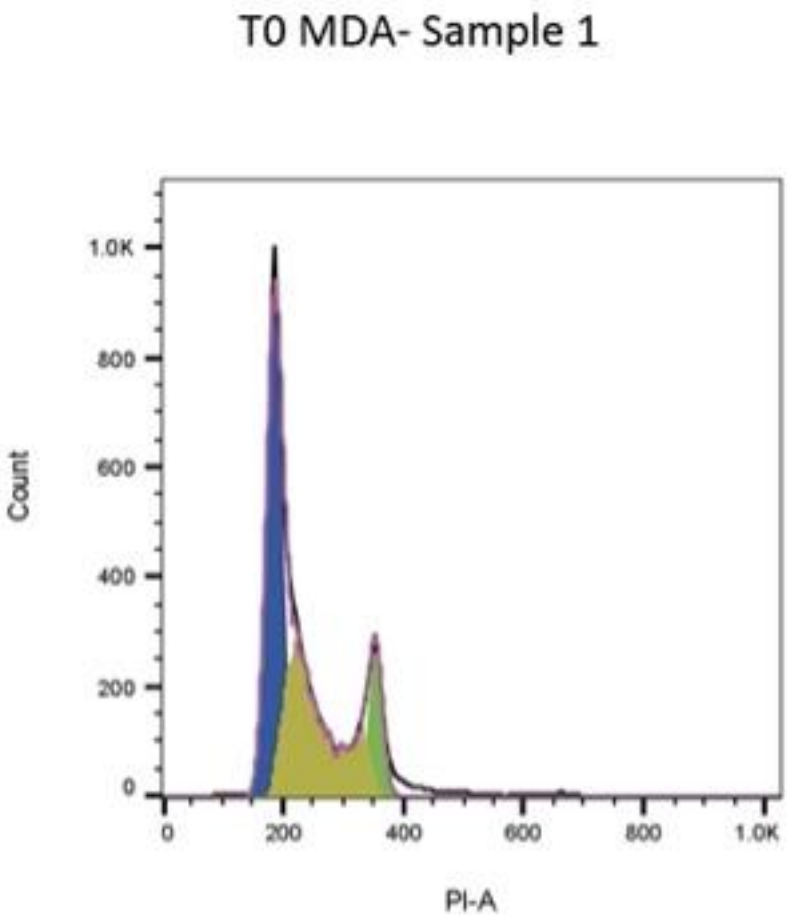

T0_MDA1_001.fcs
Cell Cycle
16052

RMSD : 8.97
%G1 : 47.8
%S : 39.8
%G2 : 12.3
G1 Mean : 187
G2 Mean : 356
G1 CV : 10.0
G2 CV : 4.49
% less G1 : -5.12
% greater G2 : 6.15

T0 MDA- Sample 2

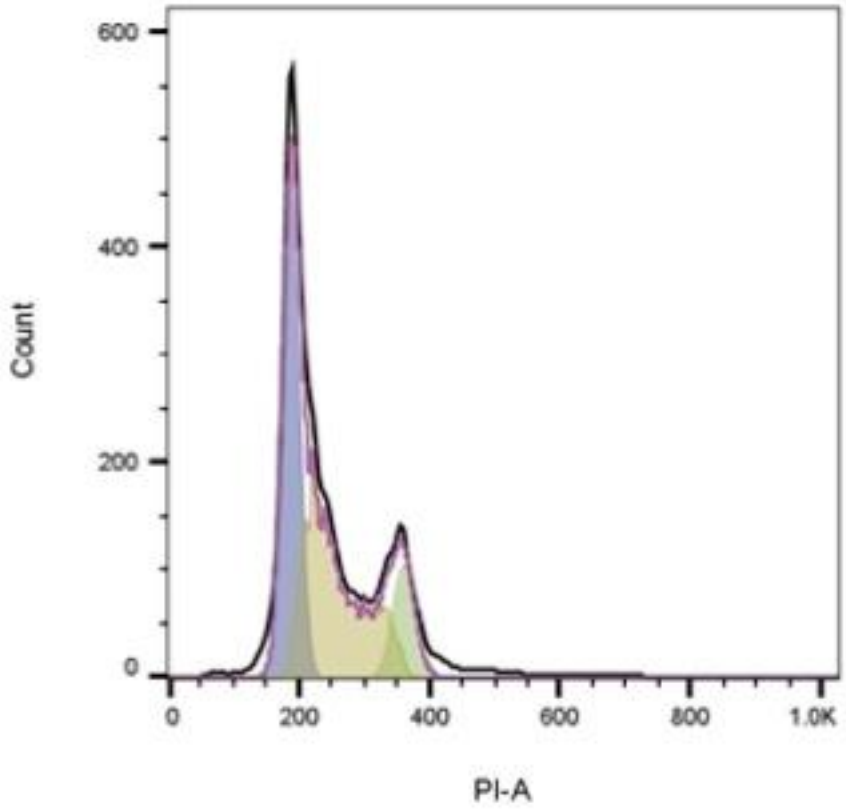

T0_MDA1.fcs
Cell Cycle
11455

RMSD : 3.63
%G1 : 41.2
%S : 39.8
%G2 : 11.8
G1 Mean : 190
G2 Mean : 362
G1 CV : 10.0
G2 CV : 6.71
% less G1 : 1.45
% greater G2 : 5.38

T24 MDA- Control
Sample 1

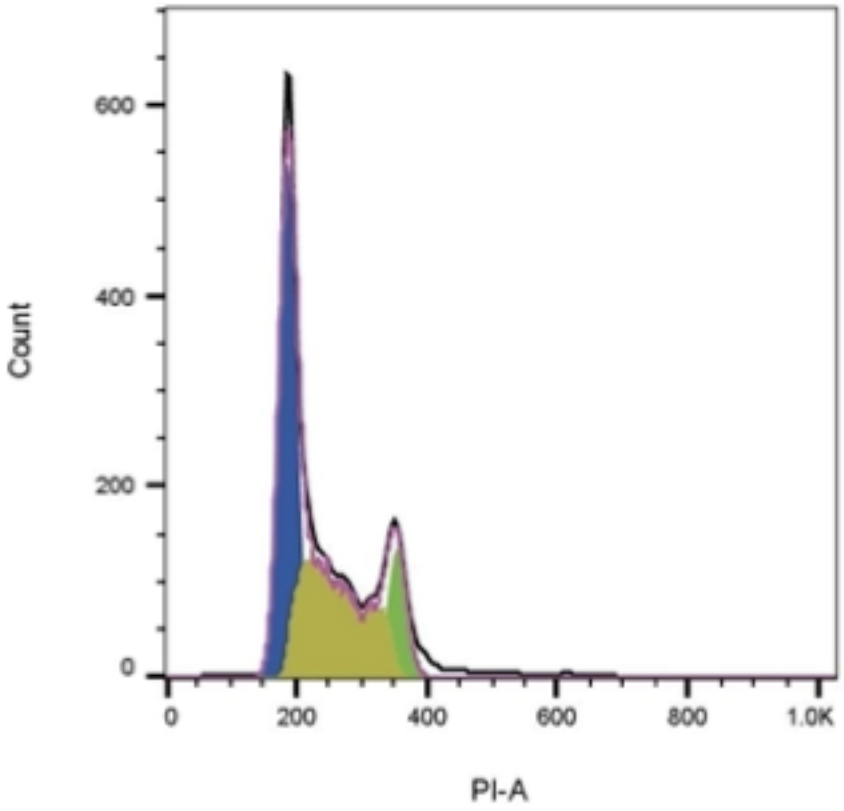

T24_MDA C 2.fcs
Cell Cycle
10920

RMSD : 4.54
%G1 : 46.9
%S : 39.2
%G2 : 12.4
G1 Mean : 189
G2 Mean : 357
G1 CV : 10.0
G2 CV : 5.56
% less G1 : -2.55
% greater G2 : 5.91

T24 MDA- Control
Sample 2

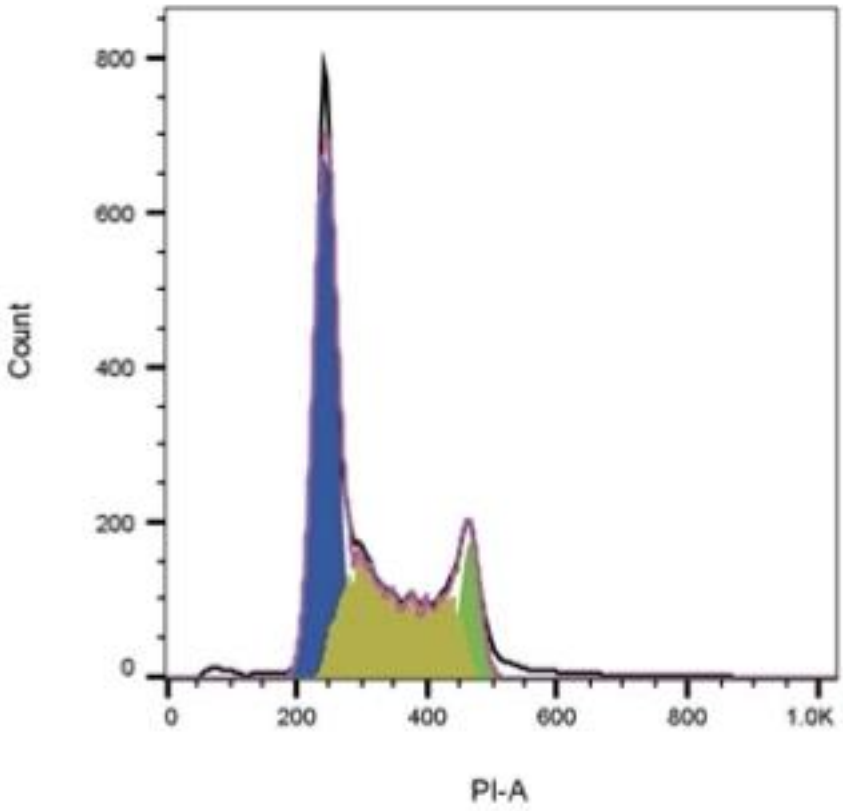

T24_MDA C.fcs
Cell Cycle
16164

RMSD : 7.25
%G1 : 49.1
%S : 39.0
%G2 : 10.9
G1 Mean : 245
G2 Mean : 468
G1 CV : 10.0
G2 CV : 4.45
% less G1 : -2.47
% greater G2 : 5.50

T24 MDA- Compound #1 Sample 1

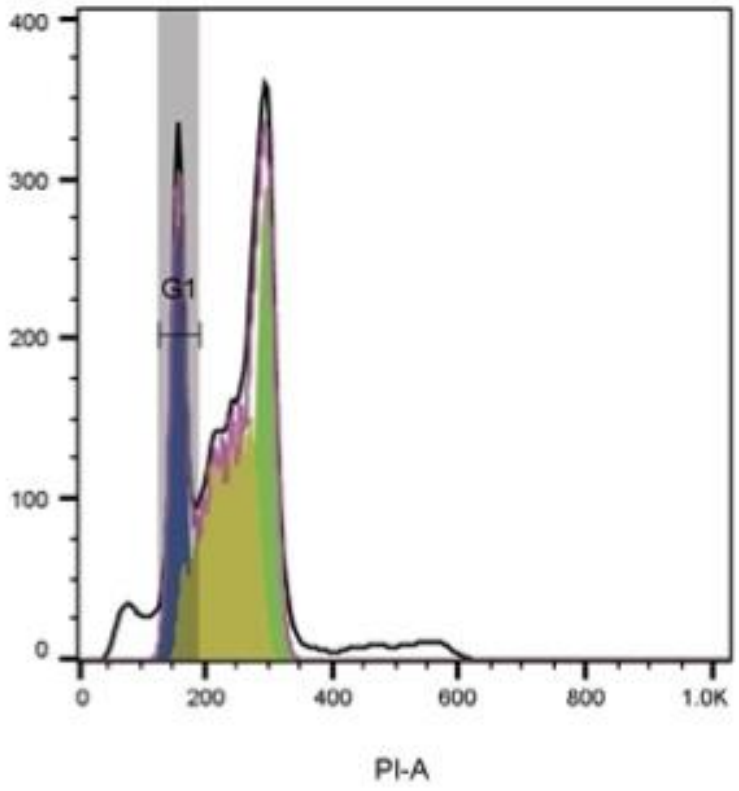

T24_MDA1 2.fcs
Cell Cycle
10780

RMSD : 3.84
%G1 : 21.0
%S : 40.8
%G2 : 28.2
G1 Mean : 158
G2 Mean : 299
G1 CV : 10.0
G2 CV : 6.55
% less G1 : 4.36
% greater G2 : 6.68

T24 MDA- Compound #2
Sample 1

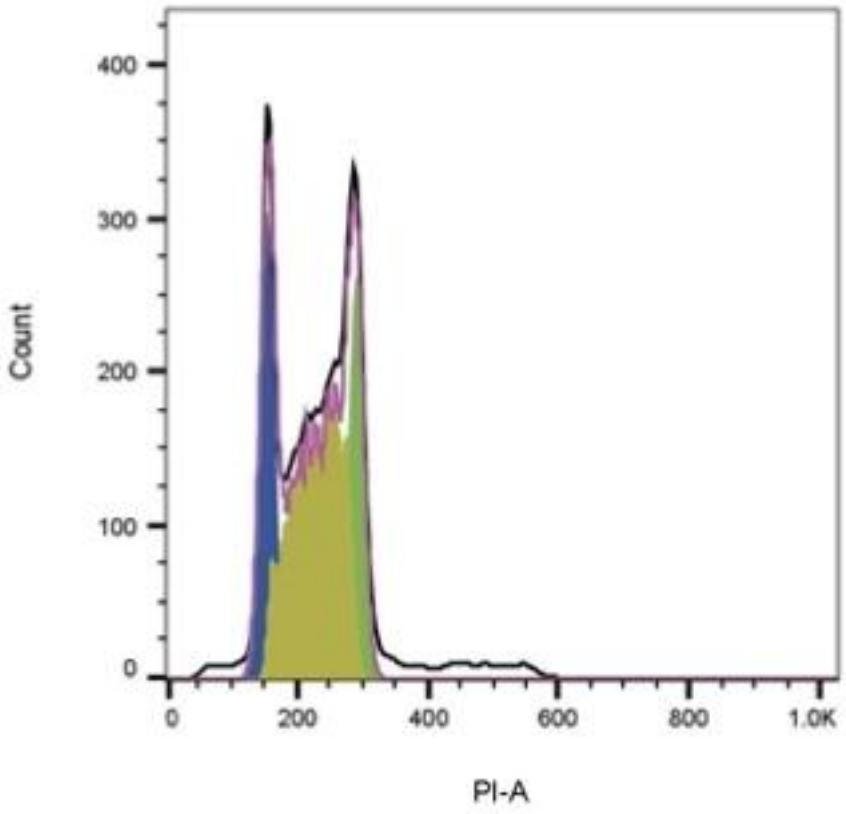

T24_MDA2 1.fcs
Cell Cycle
10457

RMSD : 3.61
%G1 : 23.3
%S : 51.0
%G2 : 20.6
G1 Mean : 155
G2 Mean : 293
G1 CV : 10.0
G2 CV : 5.44
% less G1 : 0.18
% greater G2 : 6.91

T24 MDA- Compound #1
Sample 2

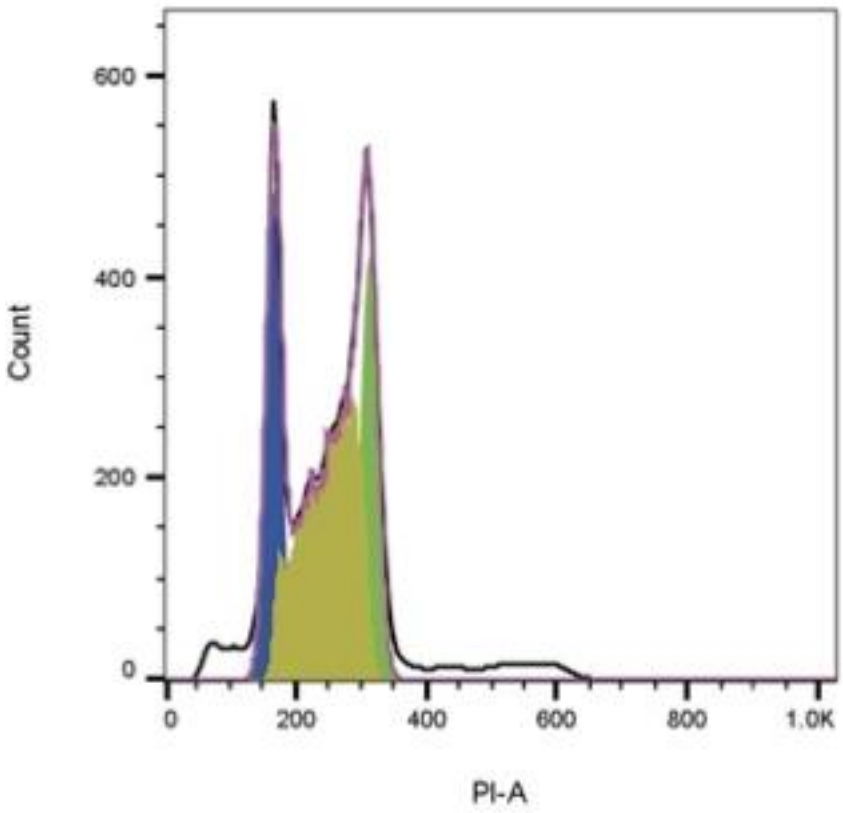

T24_MDA1.fcs
Cell Cycle
16932

RMSD : 5.34
%G1 : 22.9
%S : 46.2
%G2 : 21.8
G1 Mean : 167
G2 Mean : 315
G1 CV : 10.0
G2 CV : 5.80
% less G1 : 3.47
% greater G2 : 7.36

T24 MDA- Compound #2
Sample 2

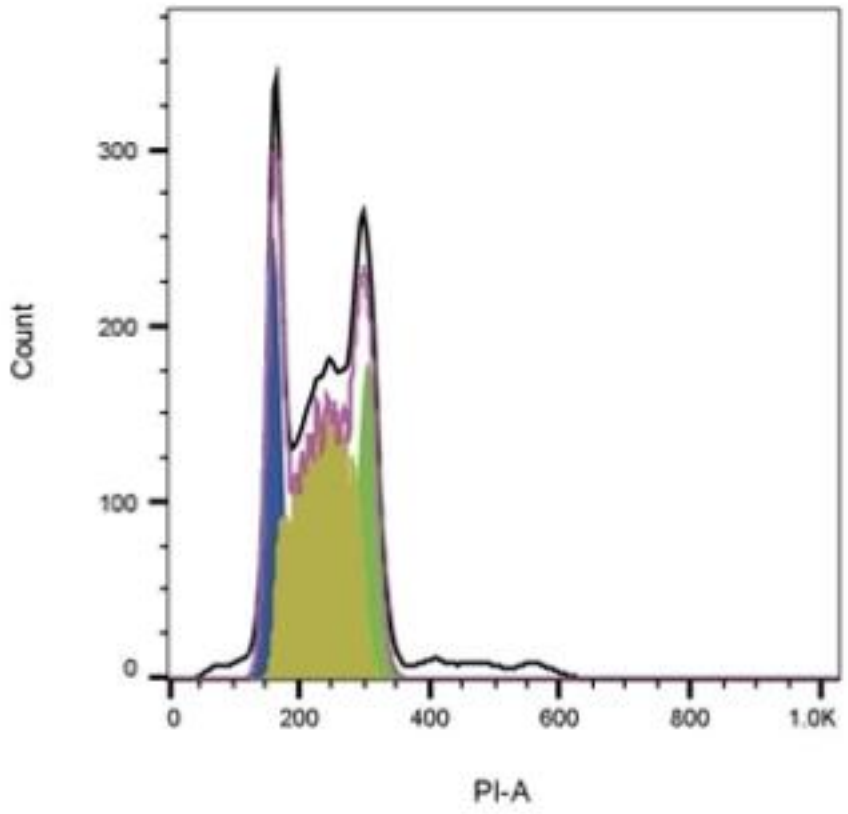

T24_MDA2.fcs
Cell Cycle
10380

RMSD : 2.63
%G1 : 21.6
%S : 51.4
%G2 : 20.9
G1 Mean : 163
G2 Mean : 307
G1 CV : 10.0
G2 CV : 7.15
% less G1 : 1.30
% greater G2 : 6.33

T24 MDA- Compound #3
Sample 1

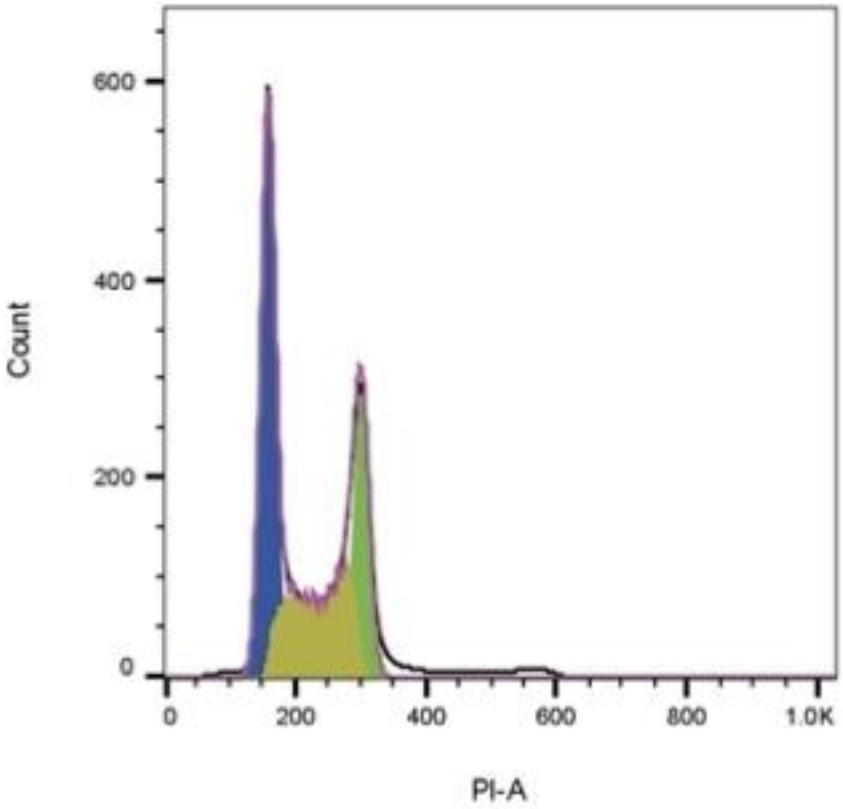

T24_MDA3 2.fcs
Cell Cycle
9499

RMSD : 5.40
%G1 : 44.0
%S : 32.5
%G2 : 22.9
G1 Mean : 160
G2 Mean : 304
G1 CV : 10.0
G2 CV : 5.45
% less G1 : -3.95
% greater G2 : 7.04

T24 MDA- Compound #3
Sample 2

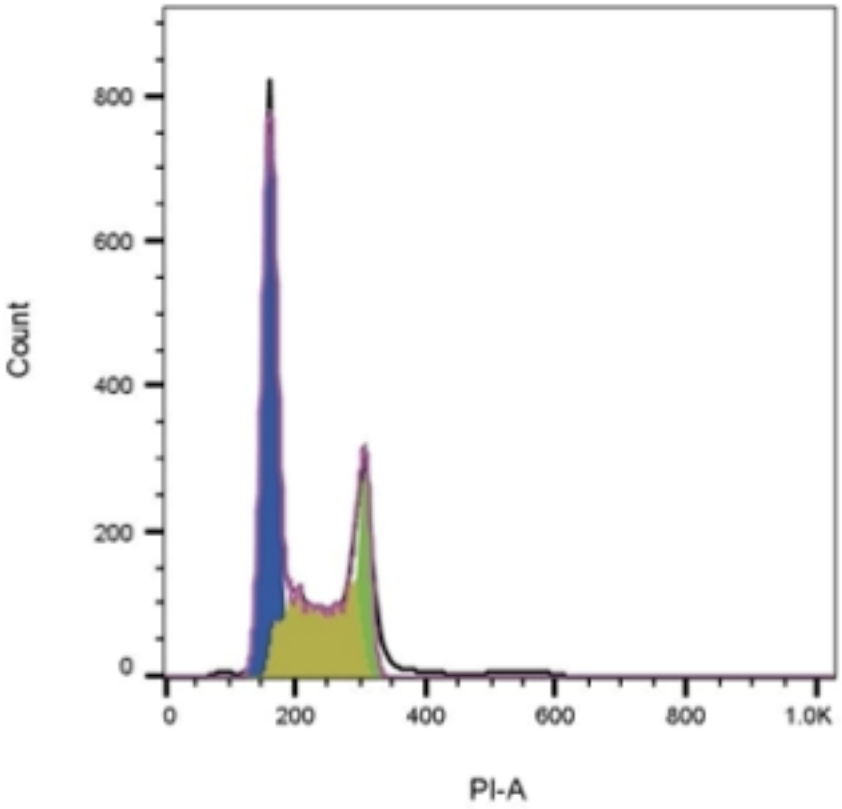

T24_MDA3.fcs
Cell Cycle
11050

RMSD : 8.43
%G1 : 51.7
%S : 33.9
%G2 : 16.8
G1 Mean : 163
G2 Mean : 309
G1 CV : 10.0
G2 CV : 4.51
% less G1 : -6.08
% greater G2 : 7.69

T48 MDA- Control
Sample 1

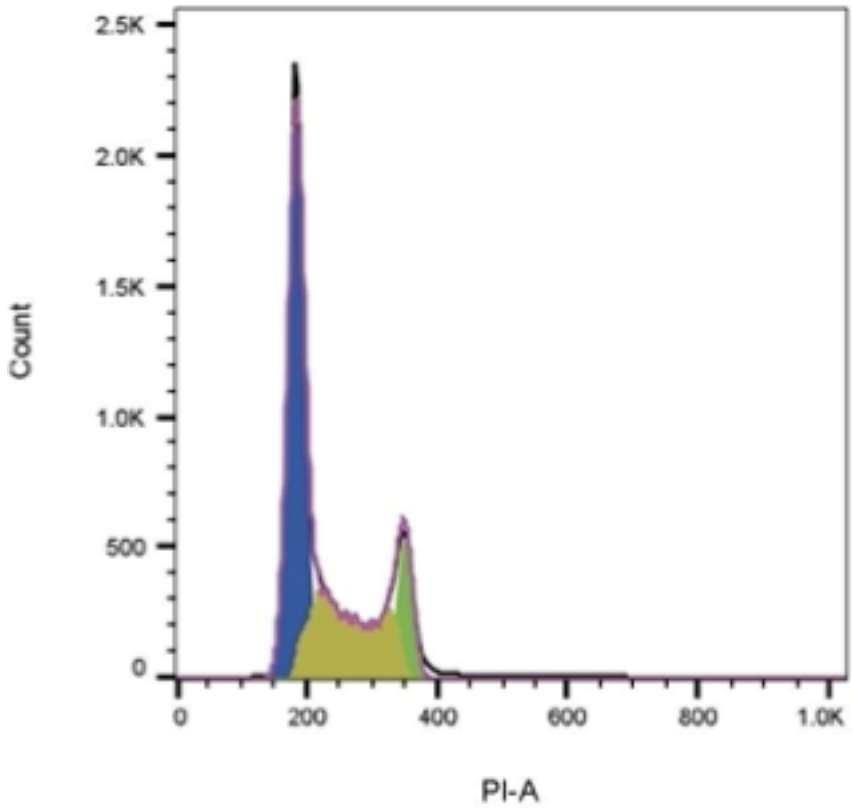

T48_MDA C 2.fcs
Cell Cycle
30510

RMSD : 20.9
%G1 : 58.6
%S : 33.0
%G2 : 13.0
G1 Mean : 185
G2 Mean : 352
G1 CV : 10.0
G2 CV : 4.67
% less G1 : -6.10
% greater G2 : 5.14

T48 MDA- Control
Sample 2

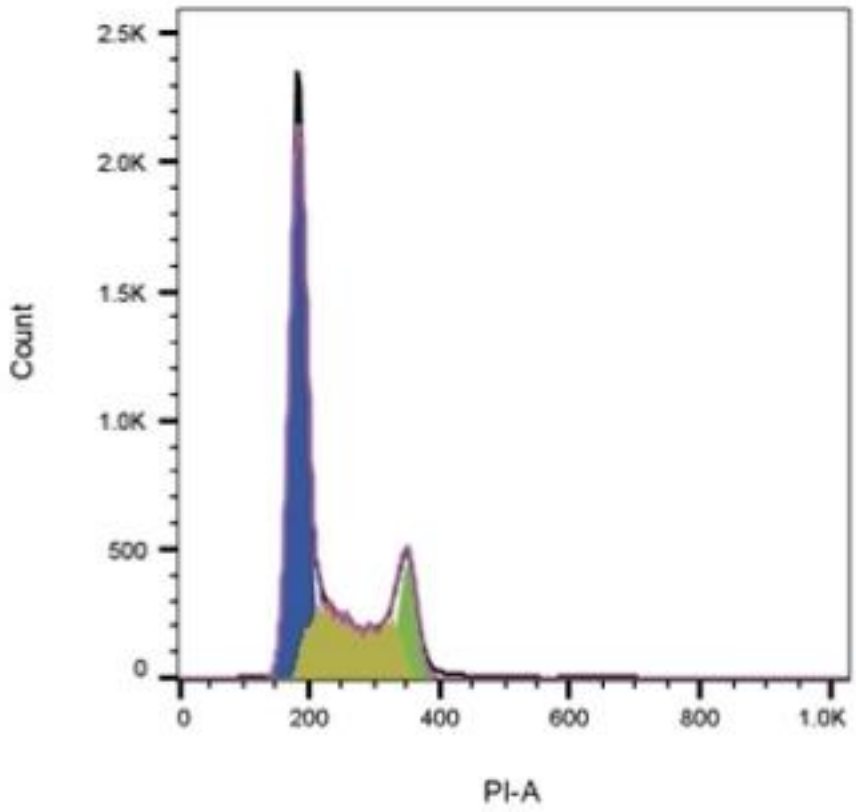

T48_MDA C.fcs
Cell Cycle
30433

RMSD : 18.9
%G1 : 59.7
%S : 31.4
%G2 : 13.1
G1 Mean : 185
G2 Mean : 354
G1 CV : 10.0
G2 CV : 5.35
% less G1 : -4.91
% greater G2 : 4.65

T48 MDA- Compound #1
Sample 1

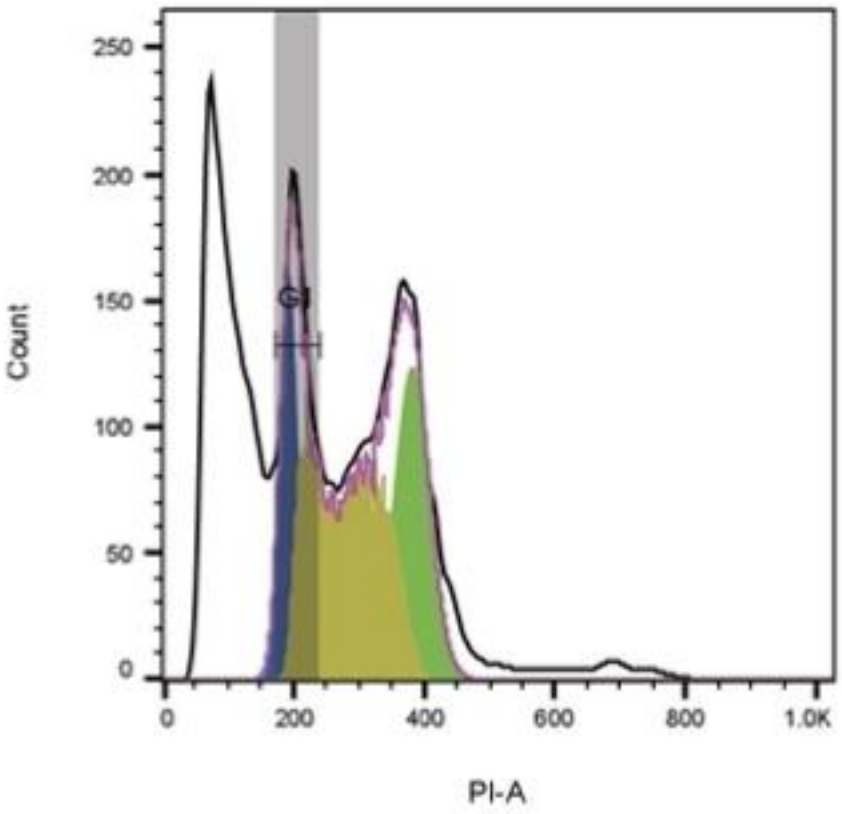

T48_MDA1 2.fcs
Cell Cycle
12783

RMSD : 13.8
%G1 : 12.3
%S : 30.1
%G2 : 18.6
G1 Mean : 194
G2 Mean : 382
G1 CV : 10.0
G2 CV : 10.0
% less G1 : 33.6
% greater G2 : 5.26

T48 MDA- Compound #1
Sample 2

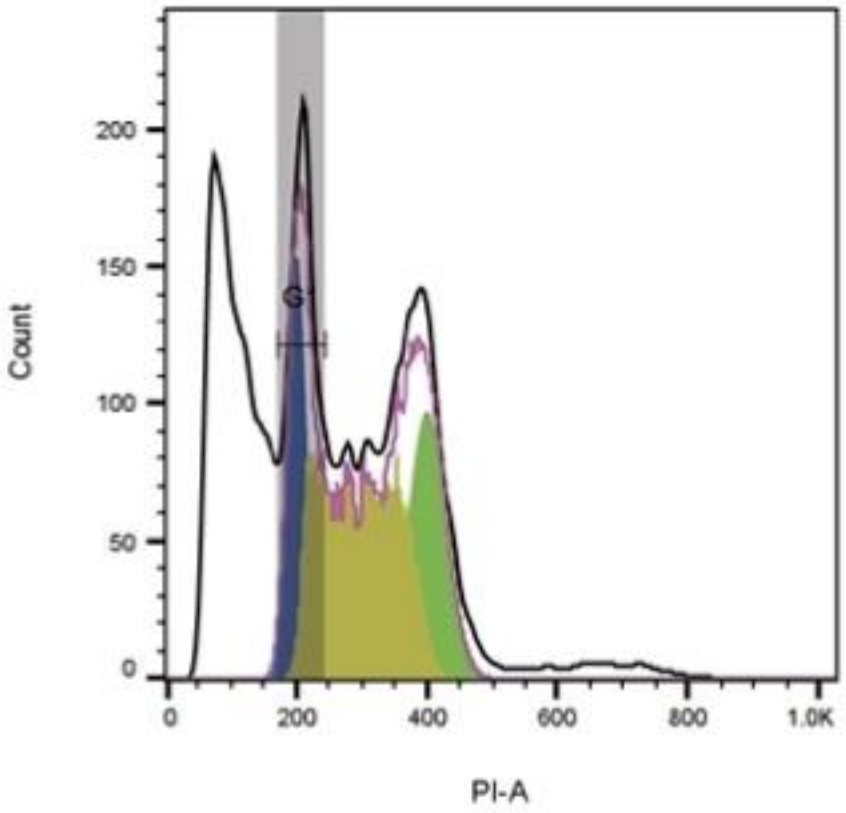

T48_MDA1.fcs
Cell Cycle
12295

RMSD : 12.1
%G1 : 13.8
%S : 32.6
%G2 : 17.3
G1 Mean : 201
G2 Mean : 401
G1 CV : 9.97
G2 CV : 10.0
% less G1 : 32.0
% greater G2 : 4.14

T48 MDA- Compound #2
Sample 1

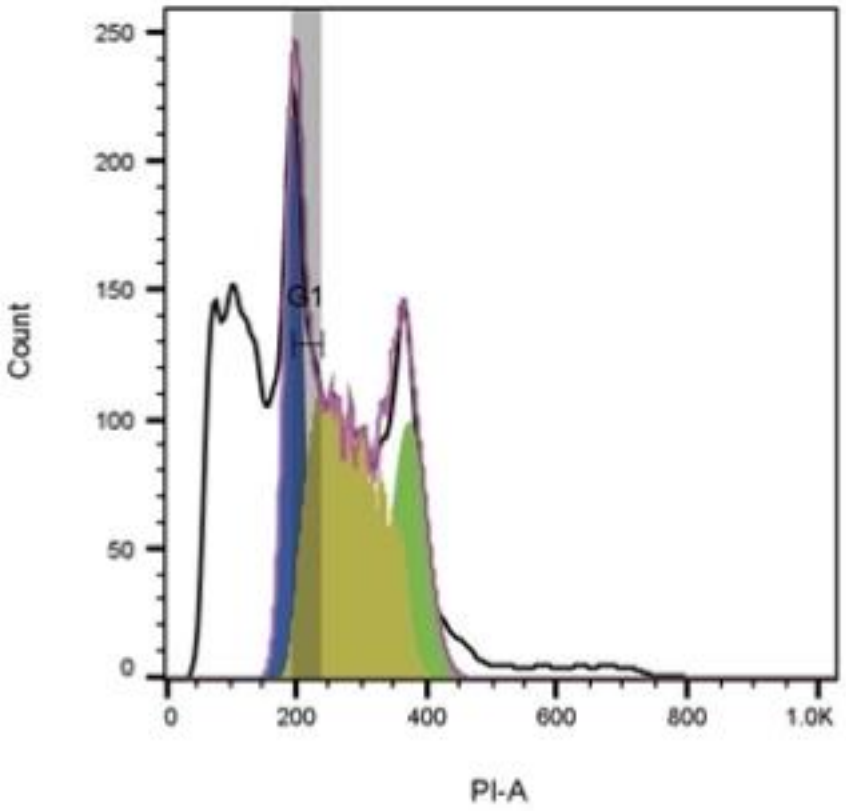

T48_MDA2 1.fcs
Cell Cycle
11897

RMSD : 11.9
%G1 : 16.7
%S : 32.5
%G2 : 14.3
G1 Mean : 198
G2 Mean : 375
G1 CV : 10.0
G2 CV : 10.00
% less G1 : 34.6
% greater G2 : 3.90

T48 MDA- Compound #2
Sample 2

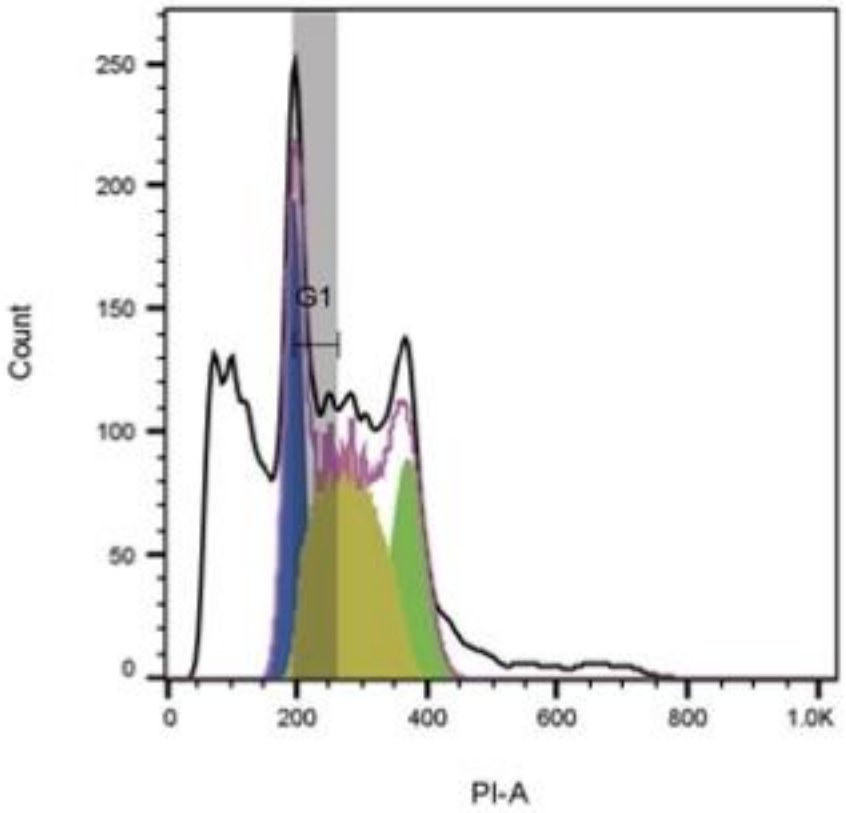

T48_MDA2.fcs
Cell Cycle
11789

RMSD : 10.0
%G1 : 18.7
%S : 33.3
%G2 : 16.0
G1 Mean : 198
G2 Mean : 372
G1 CV : 10.0
G2 CV : 10.0
% less G1 : 27.8
% greater G2 : 5.43

T48 MDA- Compound #3
Sample 1

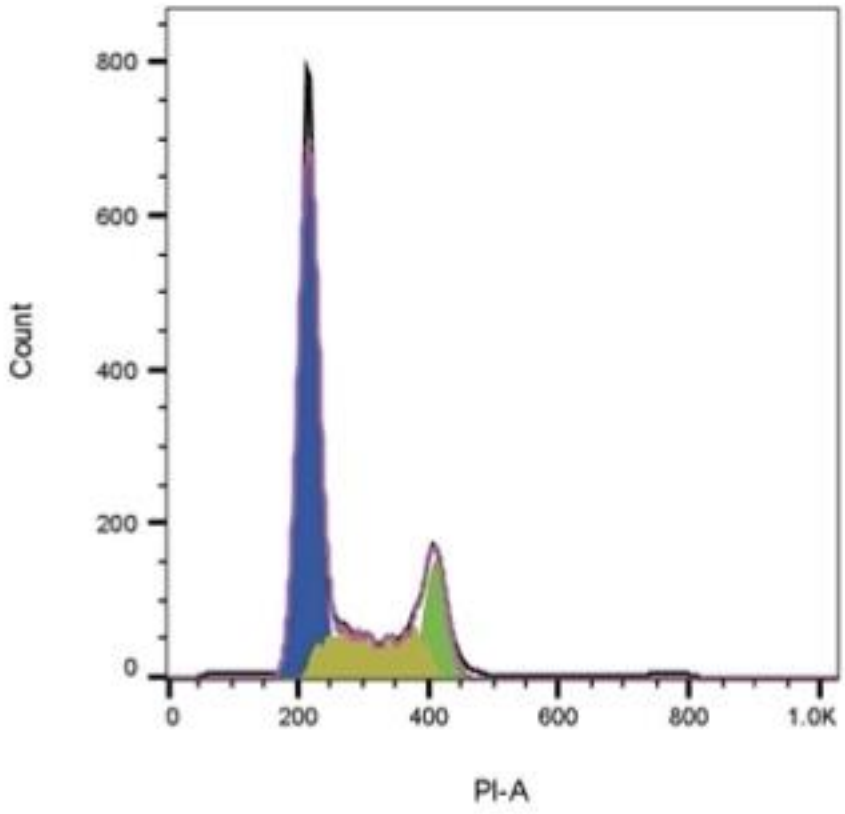

T48_MDA3 2.fcs
Cell Cycle
10831

RMSD : 9.90
%G1 : 66.4
%S : 25.2
%G2 : 16.5
G1 Mean : 217
G2 Mean : 413
G1 CV : 10.0
G2 CV : 5.72
% less G1 : -7.47
% greater G2 : 5.48

T48 MDA- Compound #3
Sample 2

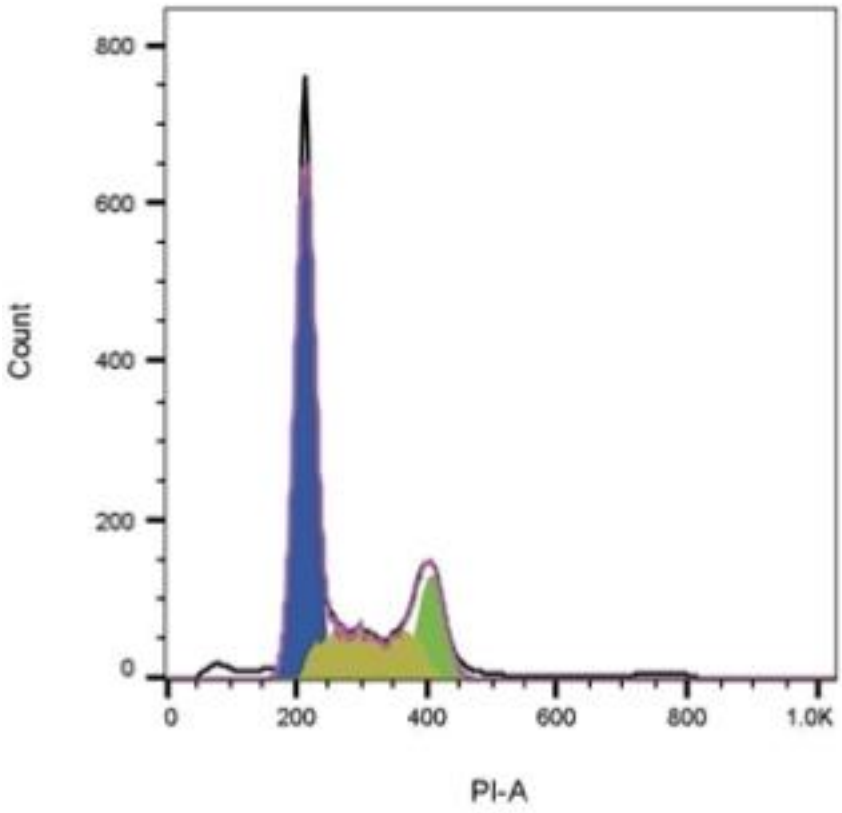

T48_MDA3.fcs
Cell Cycle
11046

RMSD : 7.95
%G1 : 61.0
%S : 24.9
%G2 : 16.2
G1 Mean : 215
G2 Mean : 409
G1 CV : 10.0
G2 CV : 6.79
% less G1 : -2.54
% greater G2 : 5.84

T0 PC3- Sample 1

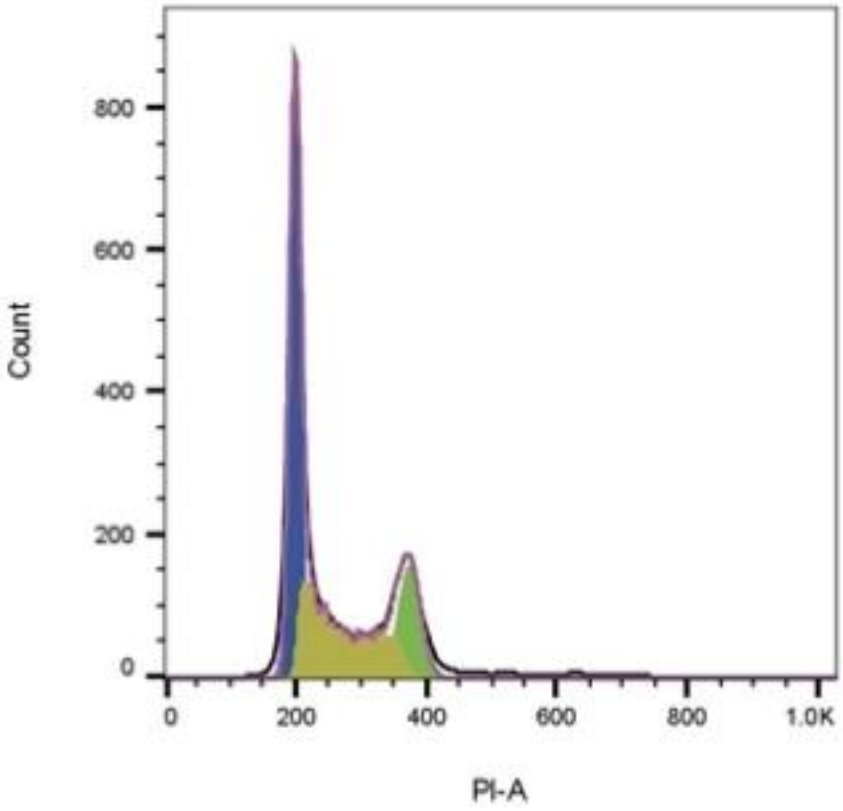

T0_PC3_001.fcs
Cell Cycle
11280

RMSD : 3.14
%G1 : 43.1
%S : 31.7
%G2 : 16.1
G1 Mean : 200
G2 Mean : 375
G1 CV : 6.02
G2 CV : 6.34
% less G1 : 2.99
% greater G2 : 6.65

T0 PC3- Sample 2

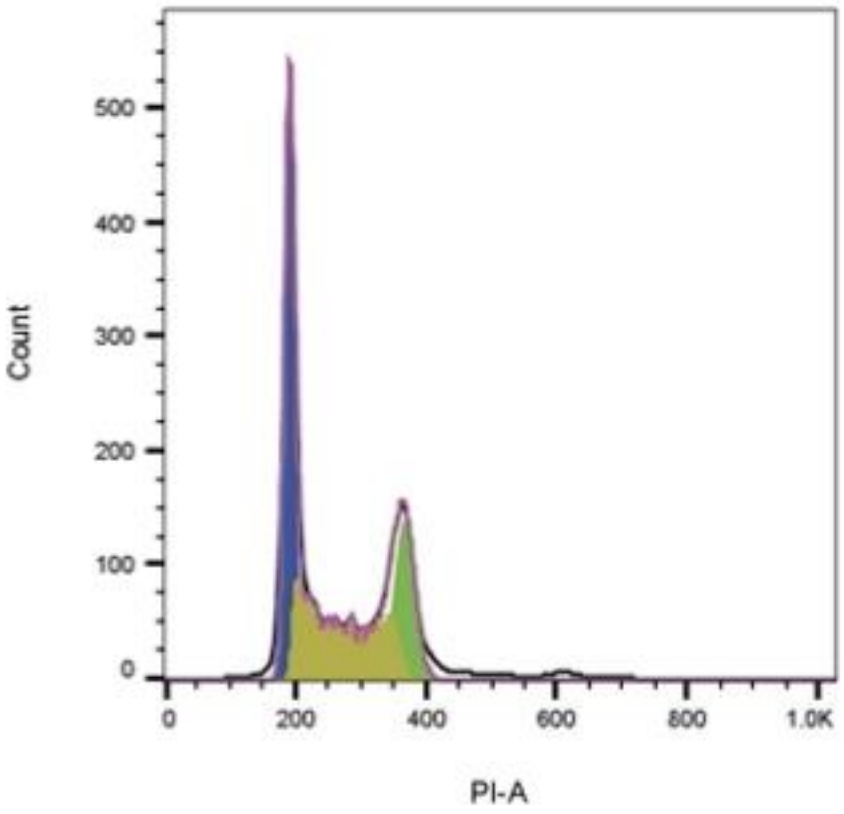

T0_PC3_002.fcs
Cell Cycle
7277

RMSD : 2.66
%G1 : 35.6
%S : 35.2
%G2 : 20.4
G1 Mean : 192
G2 Mean : 369
G1 CV : 5.43
G2 CV : 6.05
% less G1 : 2.34
% greater G2 : 7.14

T24 PC3- Control Sample 1

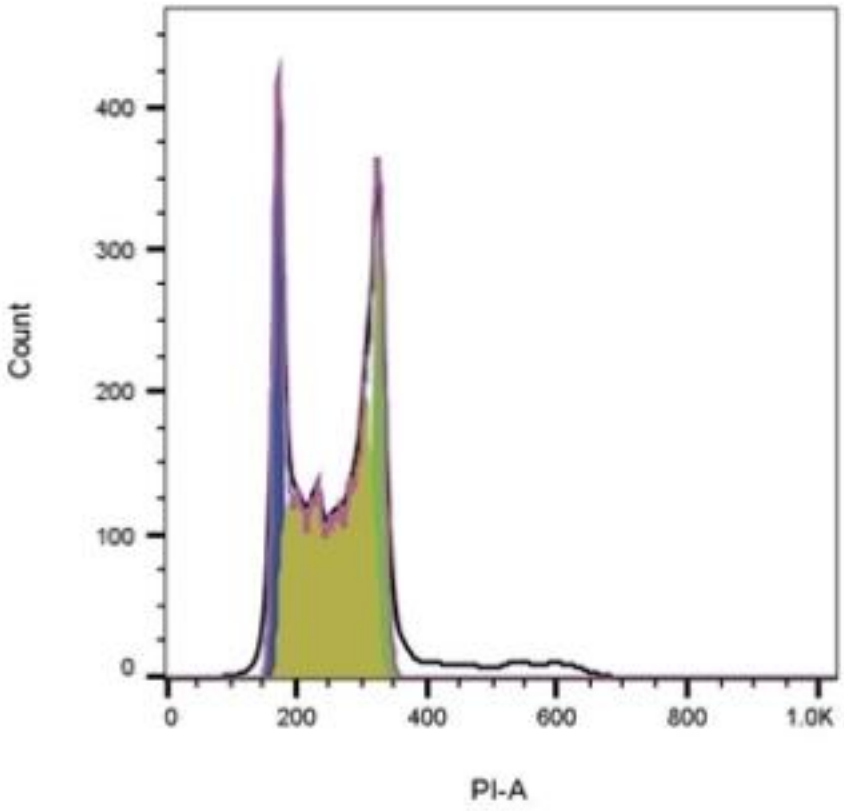

T24_PC3 C 2.fcs
Cell Cycle
10335

RMSD : 3.26
%G1 : 17.8
%S : 51.3
%G2 : 18.9
G1 Mean : 173
G2 Mean : 329
G1 CV : 5.66
G2 CV : 3.85
% less G1 : 2.04
% greater G2 : 10.0

T24 PC3- Control Sample 2

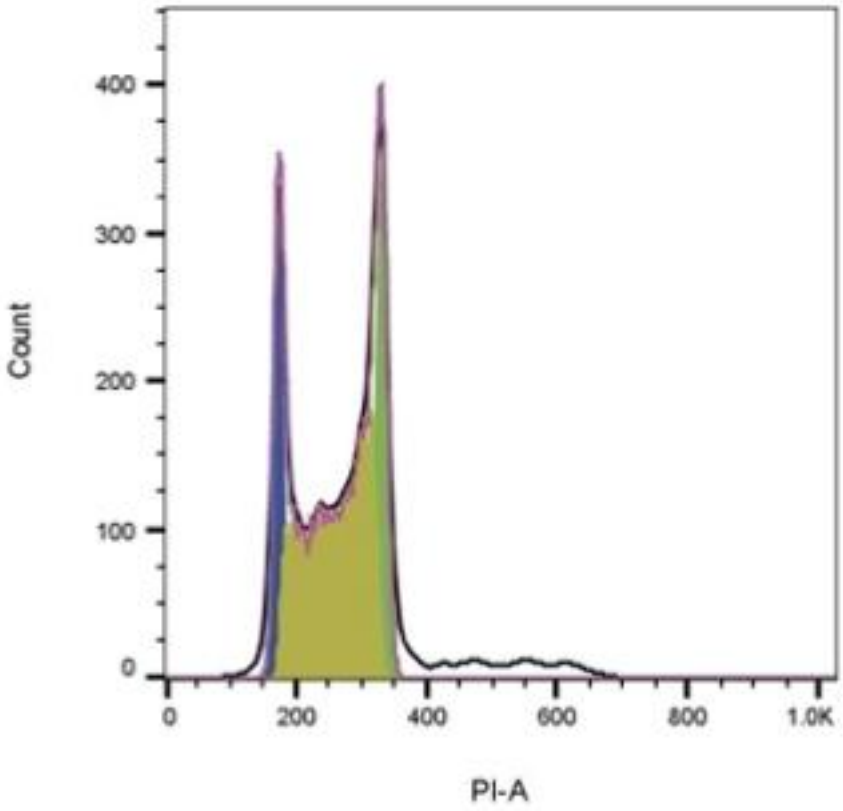

T24_PC3 C 3.fcs
Cell Cycle
10073

RMSD : 3.20
%G1 : 16.6
%S : 50.4
%G2 : 20.7
G1 Mean : 174
G2 Mean : 332
G1 CV : 6.15
G2 CV : 3.62
% less G1 : 1.84
% greater G2 : 10.6

T24 PC3- Control Sample 3

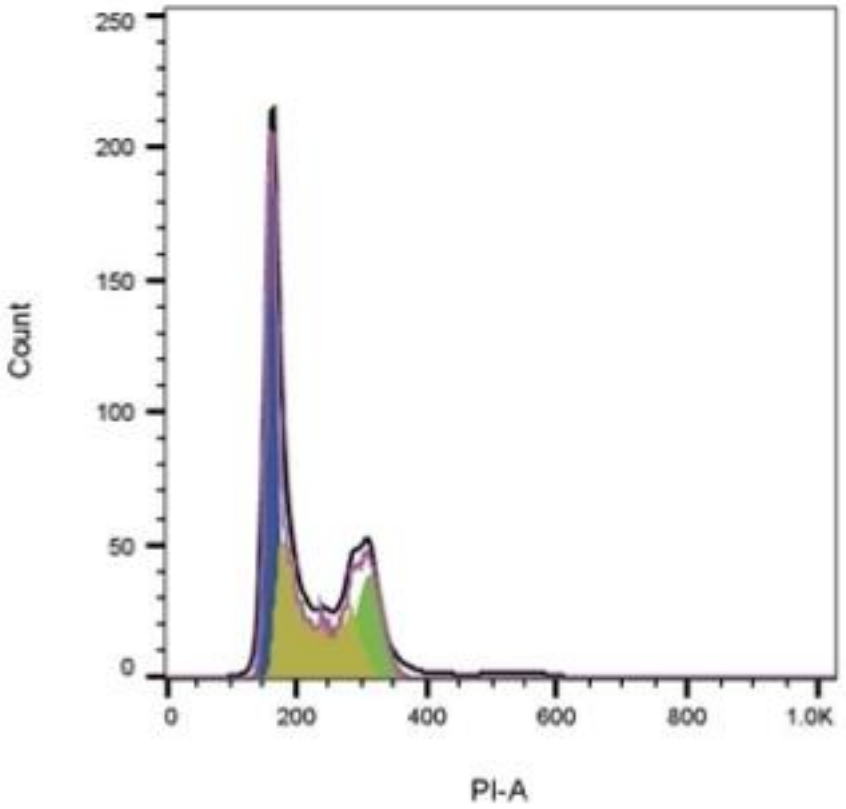

T24_PC3 C.fcs
Cell Cycle
3333

RMSD : 1.41
%G1 : 38.5
%S : 37.8
%G2 : 17.9
G1 Mean : 164
G2 Mean : 314
G1 CV : 7.14
G2 CV : 8.81
% less G1 : 1.61
% greater G2 : 4.38

T24 PC3-compound #1
Sample 1

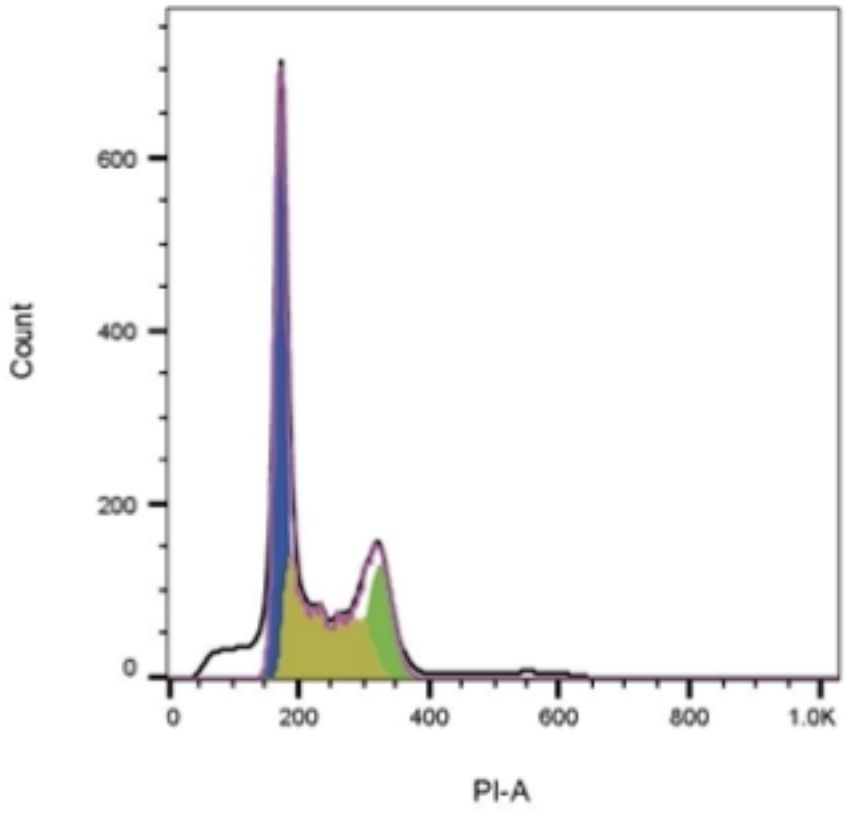

T24_PC3 1 2.fcs
Cell Cycle
10552

RMSD : 4.32
%G1 : 38.0
%S : 30.7
%G2 : 16.7
G1 Mean : 174
G2 Mean : 327
G1 CV : 6.85
G2 CV : 8.34
% less G1 : 9.95
% greater G2 : 5.13

T24 PC3-compound #1
Sample 2

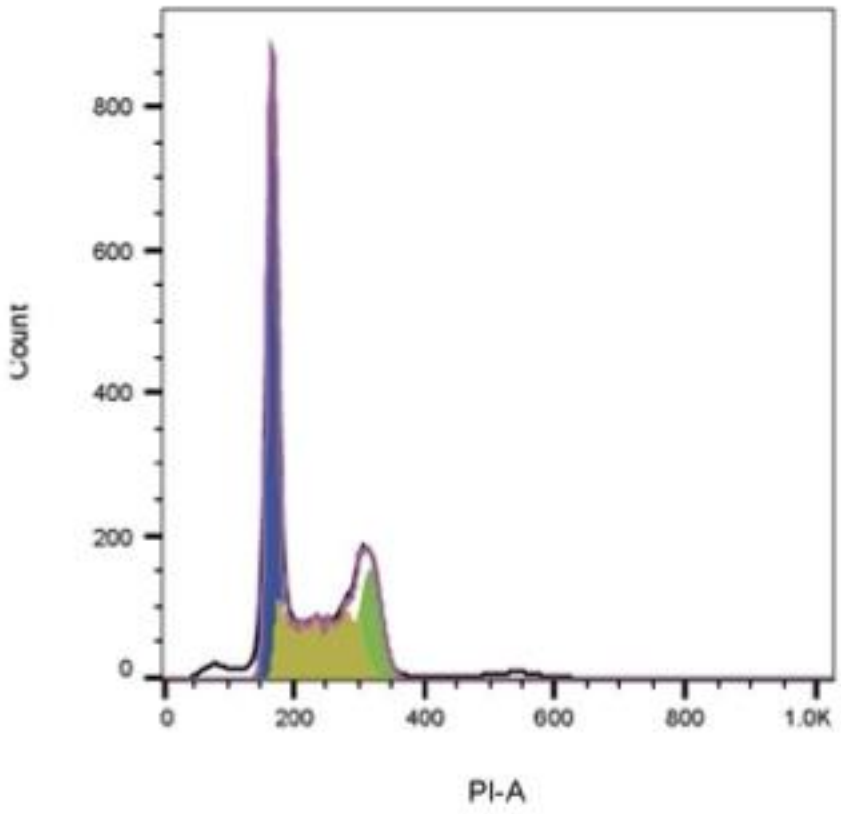

T24_PC3 1.fcs
Cell Cycle
10526

RMSD : 3.49
%G1 : 42.2
%S : 32.1
%G2 : 16.8
G1 Mean : 168
G2 Mean : 319
G1 CV : 6.27
G2 CV : 7.28
% less G1 : 5.01
% greater G2 : 4.64

T24 PC3-compound #2
Sample 1

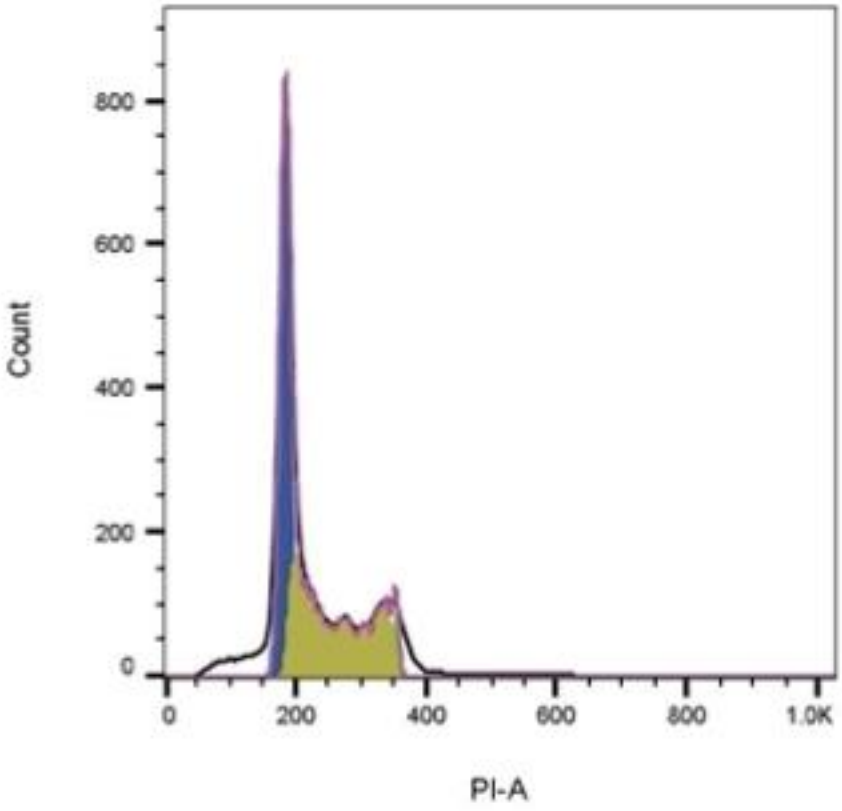

T24_PC3 2 2.fcs
Cell Cycle
10604

RMSD : 4.50
%G1 : 41.3
%S : 40.3
%G2 : 2.93
G1 Mean : 185
G2 Mean : 355
G1 CV : 6.17
G2 CV : 1.84
% less G1 : 8.62
% greater G2 : 6.87

T24 PC3-compound #2
Sample 2

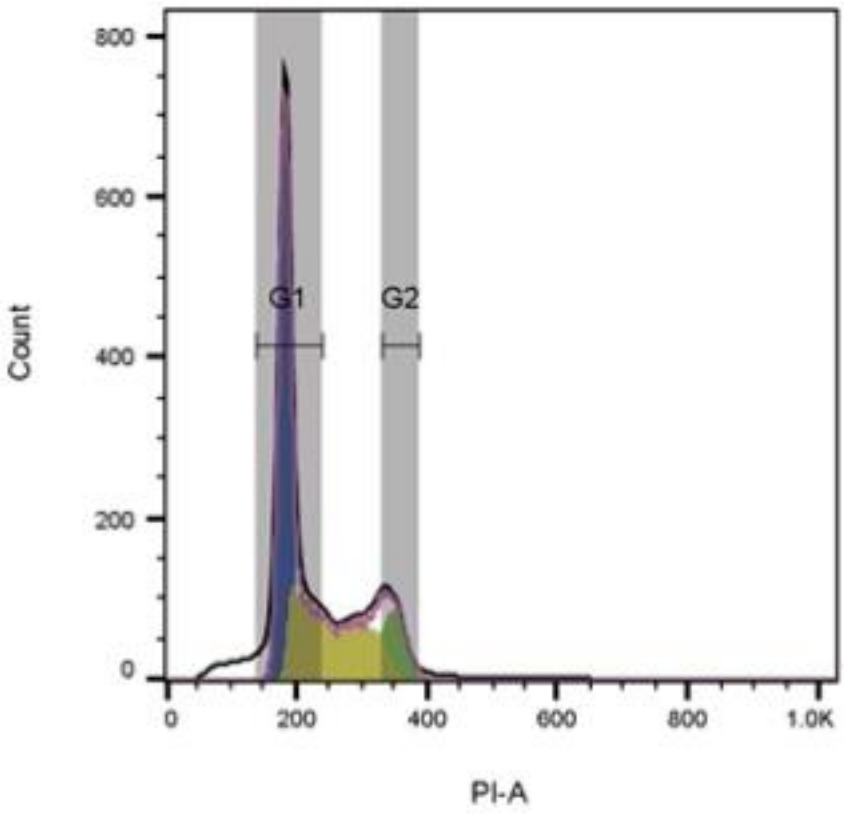

T24_PC3 2.fcs
Cell Cycle
10371

RMSD : 3.86
%G1 : 43.2
%S : 34.6
%G2 : 11.7
G1 Mean : 184
G2 Mean : 350
G1 CV : 6.65
G2 CV : 7.78
% less G1 : 7.55
% greater G2 : 3.40

T24 PC3-compound #3
Sample 1

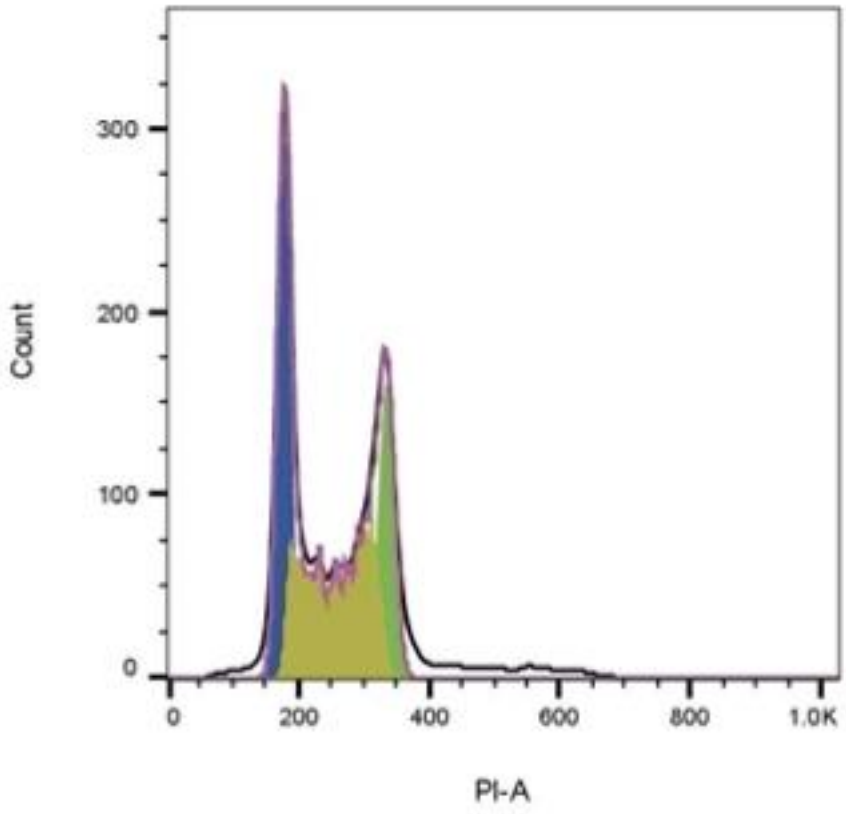

T24_PC3 3 2.fcs
Cell Cycle
6921

RMSD : 2.08
%G1 : 30.0
%S : 39.5
%G2 : 19.3
G1 Mean : 179
G2 Mean : 337
G1 CV : 7.88
G2 CV : 5.03
% less G1 : 2.29
% greater G2 : 9.00

T24 PC3-compound #3
Sample 2

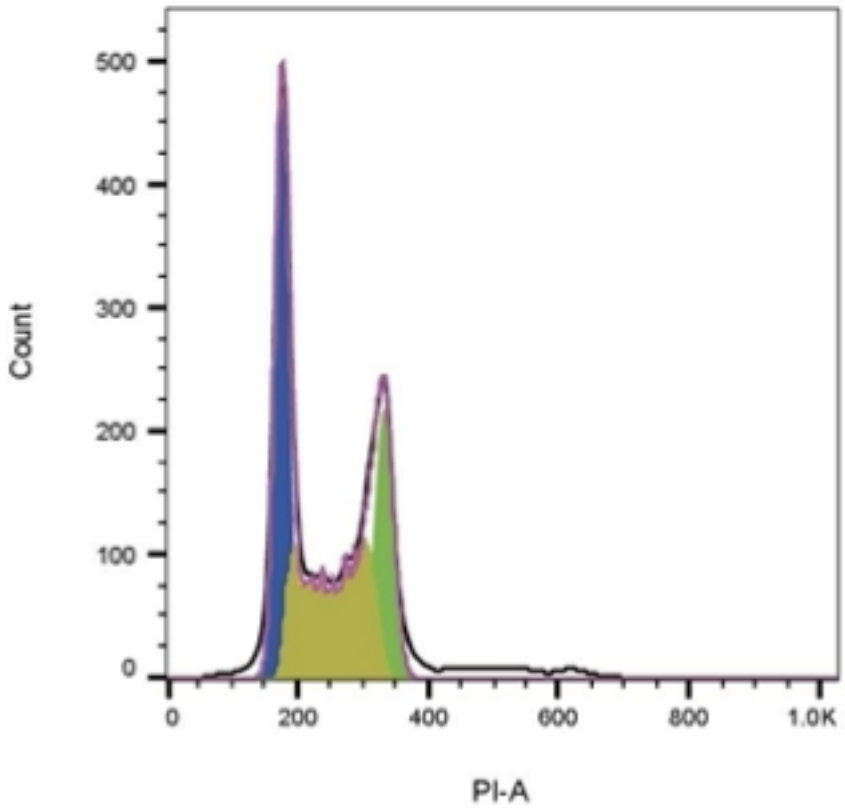

T24_PC3 3.fcs
Cell Cycle
10143

RMSD : 2.87
%G1 : 33.8
%S : 35.7
%G2 : 20.8
G1 Mean : 177
G2 Mean : 335
G1 CV : 8.41
G2 CV : 5.88
% less G1 : 2.48
% greater G2 : 7.63

T48 PC3- Control Sample 1

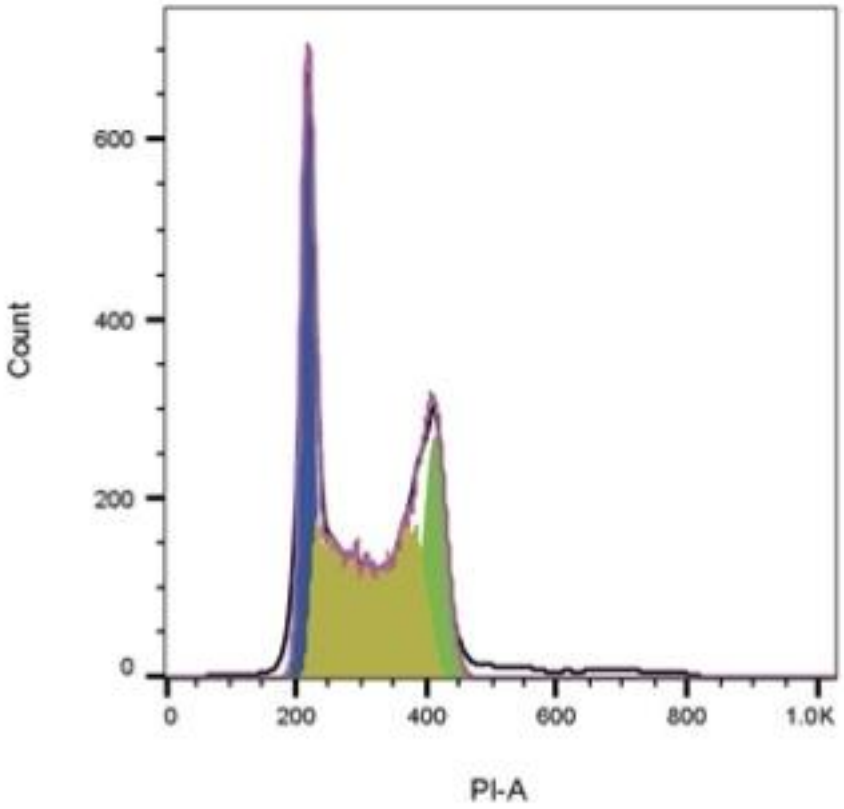

T48_PC3 C 2.fcs
Cell Cycle
15618

RMSD : 3.91
%G1 : 26.3
%S : 44.9
%G2 : 19.3
G1 Mean : 219
G2 Mean : 415
G1 CV : 6.09
G2 CV : 5.81
% less G1 : 3.04
% greater G2 : 6.38

T48 PC3- Control Sample 2

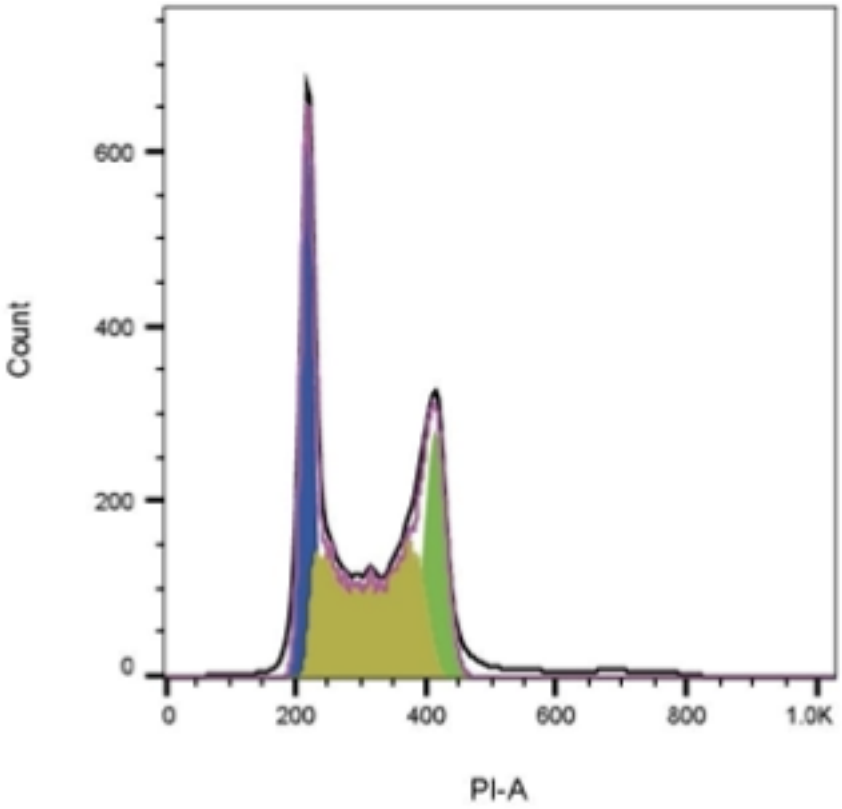

T48_PC3 C 3.fcs
Cell Cycle
15477

RMSD : 3.84
%G1 : 27.3
%S : 42.9
%G2 : 20.9
G1 Mean : 220
G2 Mean : 416
G1 CV : 6.21
G2 CV : 5.47
% less G1 : 2.56
% greater G2 : 6.30

T48 PC3- Control Sample 3

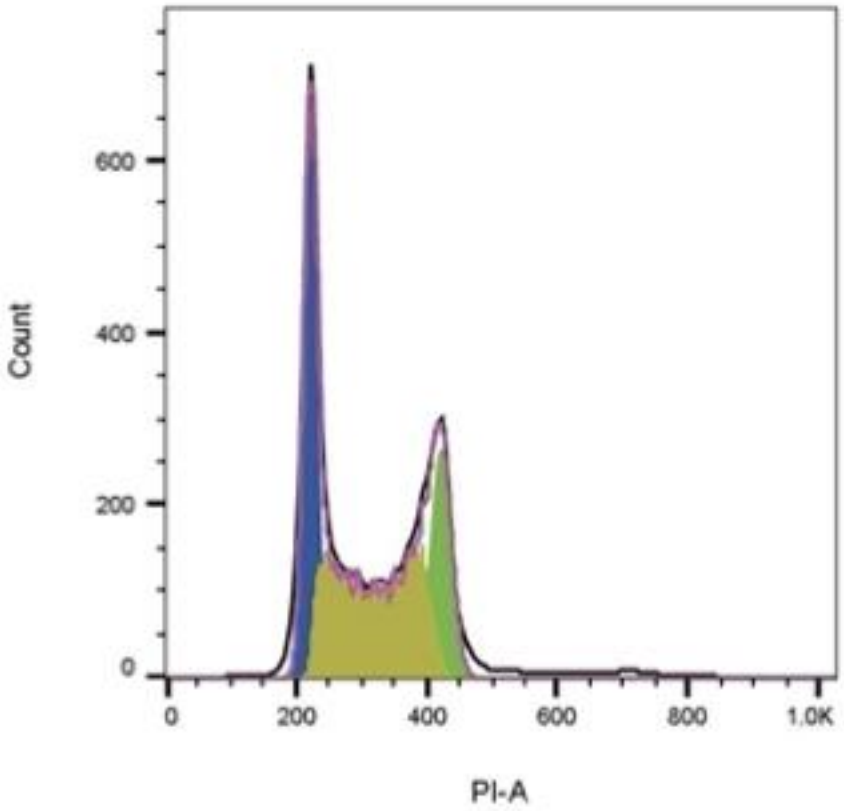

T48_PC3 C.fcs
Cell Cycle
15262

RMSD : 4.08
%G1 : 30.7
%S : 41.9
%G2 : 19.3
G1 Mean : 222
G2 Mean : 423
G1 CV : 6.46
G2 CV : 5.28
% less G1 : 2.80
% greater G2 : 5.68

T48 PC3- Compound #1
Sample 1

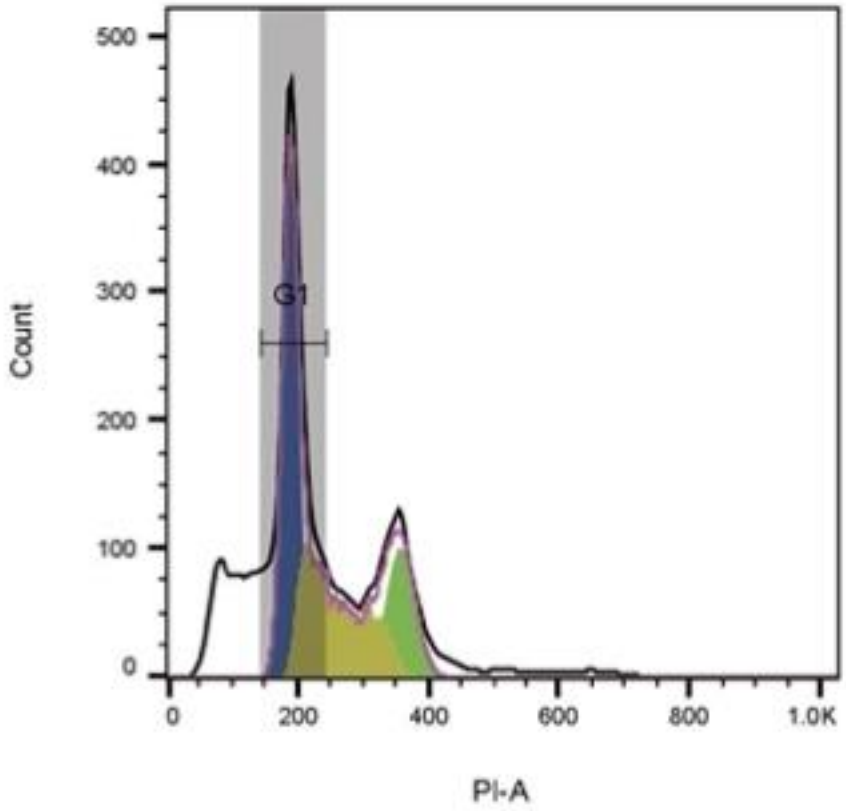

T48_PC3 1 2.fcs
Cell Cycle
11013

RMSD : 7.34
%G1 : 31.9
%S : 27.1
%G2 : 14.7
G1 Mean : 190
G2 Mean : 359
G1 CV : 8.63
G2 CV : 8.42
% less G1 : 20.2
% greater G2 : 5.53

T48 PC3- Compound #1
Sample 2

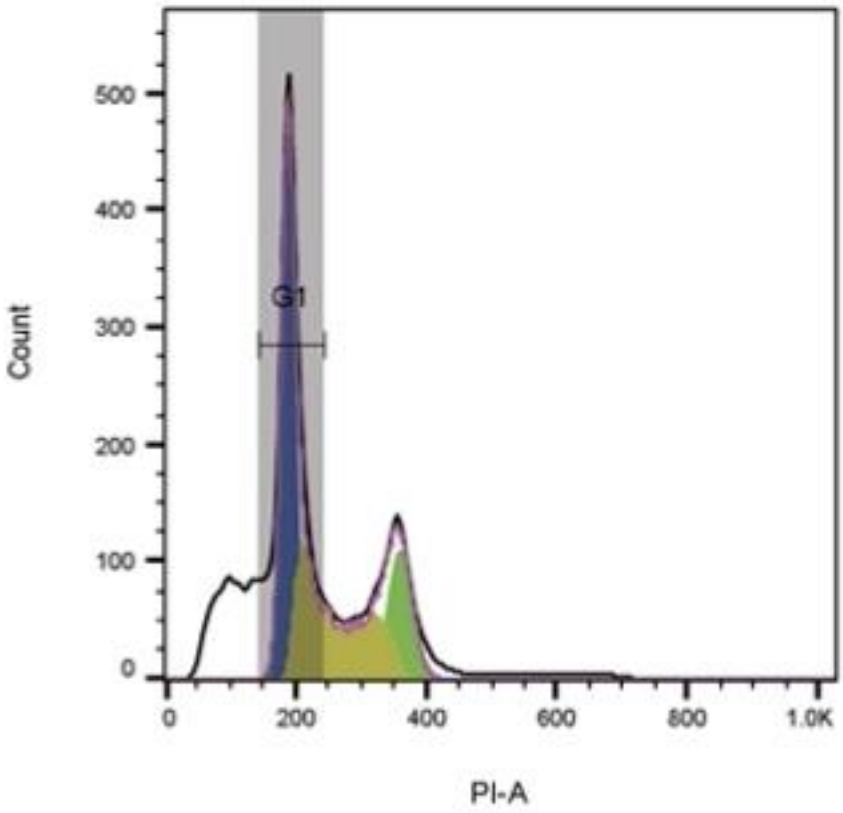

T48_PC3 1.fcs
Cell Cycle
10883

RMSD : 7.37
%G1 : 32.8
%S : 26.9
%G2 : 13.8
G1 Mean : 190
G2 Mean : 361
G1 CV : 7.82
G2 CV : 7.39
% less G1 : 21.0
% greater G2 : 5.41

T48 PC3- Compound #2
Sample 1

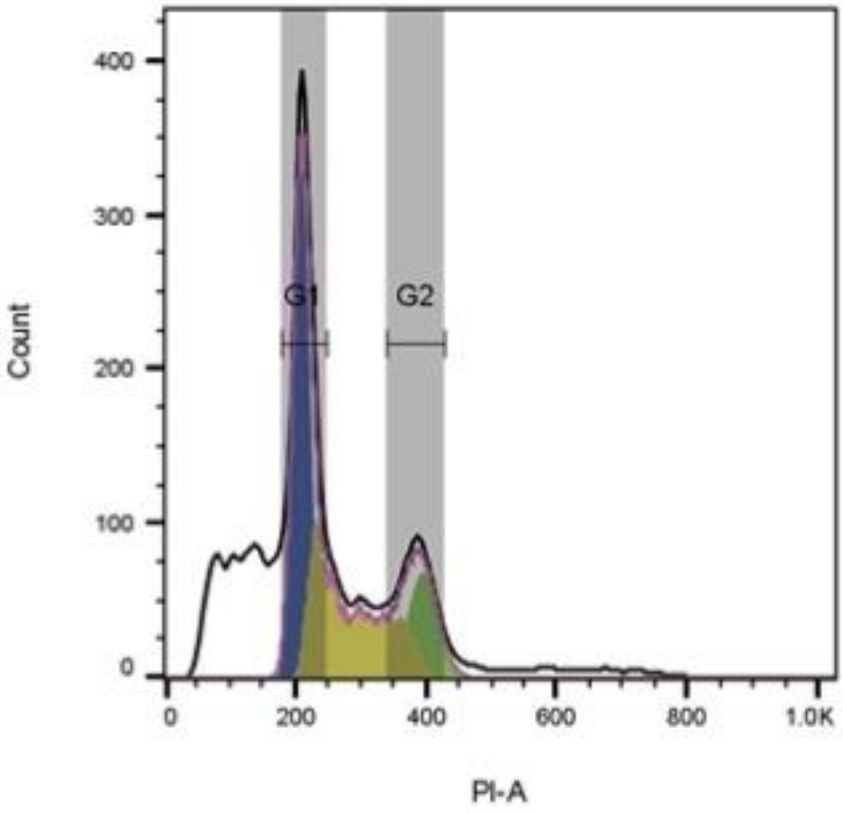

T48_PC3 2 2.fcs
Cell Cycle
10100

RMSD : 7.62
%G1 : 30.9
%S : 27.1
%G2 : 11.4
G1 Mean : 210
G2 Mean : 397
G1 CV : 8.35
G2 CV : 8.01
% less G1 : 25.4
% greater G2 : 5.32

T48 PC3- Compound #2
Sample 2

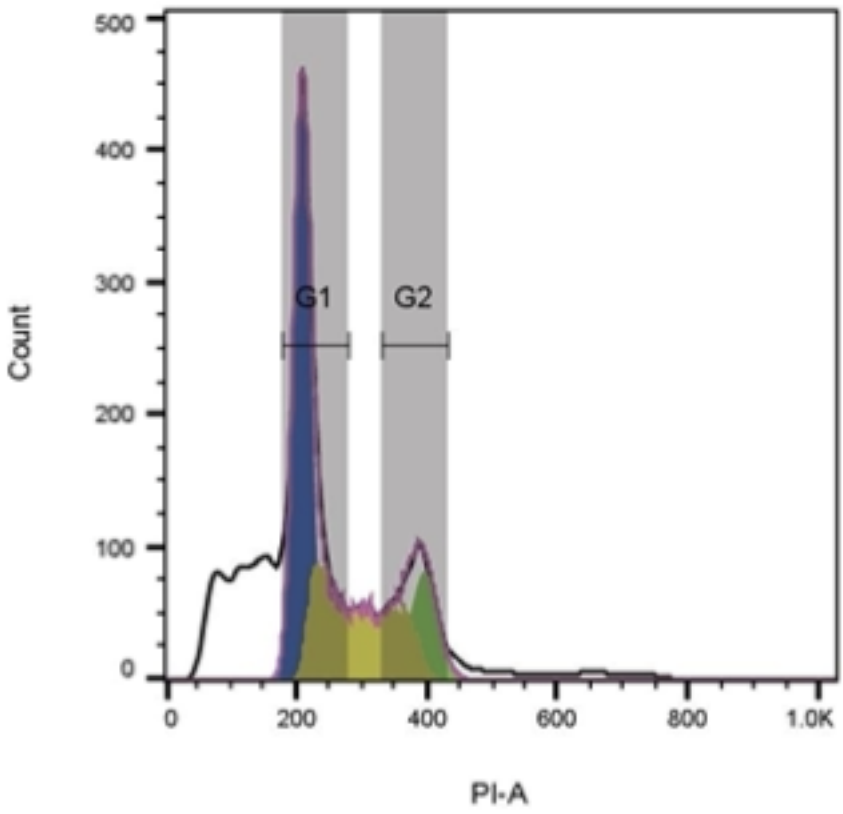

T48_PC3 2.fcs
Cell Cycle
10922

RMSD : 8.08
%G1 : 34.5
%S : 25.8
%G2 : 10.0
G1 Mean : 210
G2 Mean : 398
G1 CV : 8.58
G2 CV : 7.26
% less G1 : 24.7
% greater G2 : 4.93

T48 PC3- Compound #3
Sample 1

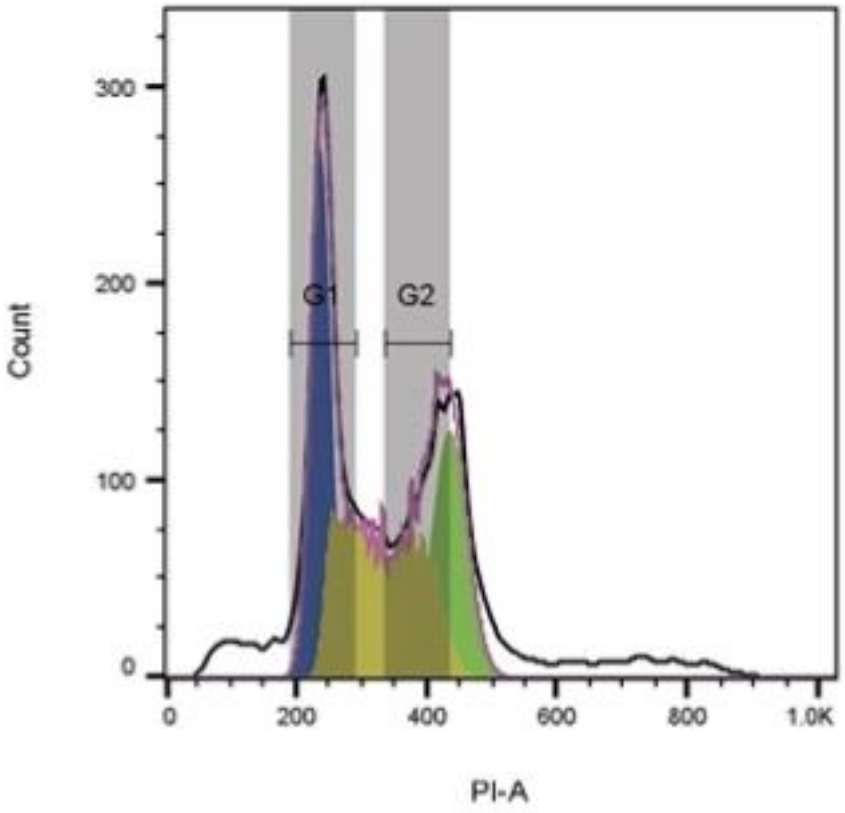

T48_PC3 3 2.fcs
Cell Cycle
10501

RMSD : 3.76
%G1 : 27.1
%S : 35.9
%G2 : 21.7
G1 Mean : 239
G2 Mean : 437
G1 CV : 9.12
G2 CV : 8.52
% less G1 : 6.78
% greater G2 : 11.0

T48 PC3- Compound #3
Sample 2

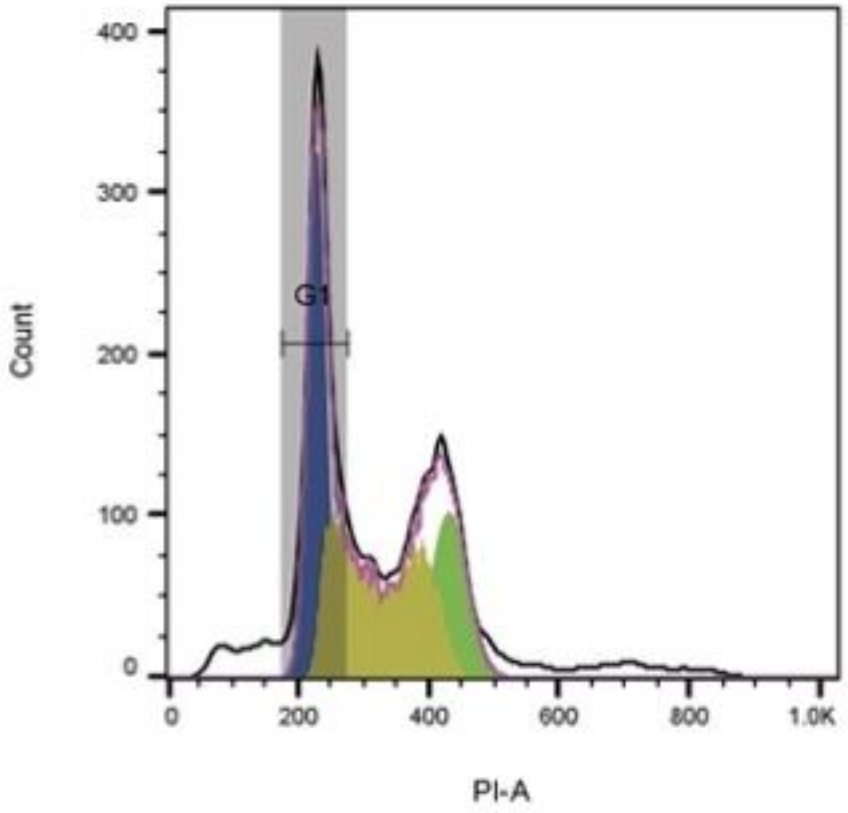

T48_PC3 3.fcs
Cell Cycle
10872

RMSD : 3.47
%G1 : 30.2
%S : 38.0
%G2 : 18.6
G1 Mean : 229
G2 Mean : 432
G1 CV : 8.53
G2 CV : 8.94
% less G1 : 7.03
% greater G2 : 7.03